

For Reference

NOT TO BE TAKEN FROM THIS ROOM

Ex libris
UNIVERSITATIS
ALBERTAENSIS



THE UNIVERSITY OF ALBERTA

RELEASE FORM

NAME OF AUTHOR MOHAMMED ZAHEERUDDIN
TITLE OF THESIS COMPUTER SIMULATION OF DIRECT GAIN
 PASSIVE HOUSE
DEGREE FOR WHICH THESIS WAS PRESENTED MASTER OF SCIENCE
YEAR THIS DEGREE GRANTED FALL 1980

Permission is hereby granted to THE UNIVERSITY OF ALBERTA LIBRARY to reproduce single copies of this thesis and to lend or sell such copies for private, scholarly or scientific research purposes only.

The author reserves other publication rights, and neither the thesis nor extensive extracts from it may be printed or otherwise reproduced without the author's written permission. 11

THE UNIVERSITY OF ALBERTA

COMPUTER SIMULATION OF DIRECT GAIN PASSIVE HOUSE

by



MOHAMMED ZAHEERUDDIN

A THESIS

SUBMITTED TO THE FACULTY OF GRADUATE STUDIES AND RESEARCH
IN PARTIAL FULFILMENT OF THE REQUIREMENTS FOR THE DEGREE
OF MASTER OF SCIENCE

DEPARTMENT OF MECHANICAL ENGINEERING

EDMONTON, ALBERTA

FALL 1980

THE UNIVERSITY OF ALBERTA
FACULTY OF GRADUATE STUDIES AND RESEARCH

The undersigned certify that they have read, and recommend to the Faculty of Graduate Studies and Research, for acceptance, a thesis entitled COMPUTER SIMULATION OF DIRECT GAIN PASSIVE HOUSE submitted by MOHAMMED ZAHEERUDDIN in partial fulfilment of the requirements for the degree of MASTER OF SCIENCE.

ABSTRACT

An interactive computer program to predict the thermal performance of any real house was developed. An improved method of calculating the solar heat gain through single, double, or triple glazing windows was incorporated in the model. The winter solar gains can be maximized by sloping the windows. Two different techniques of reducing summer overheating were studied. Either heat absorbing glass windows or architectural projections such as overhangs may be used.

Two important considerations in modelling the behaviour of a house with thermal mass wall are : the optimum thickness of the thermal mass wall and the effect of the number of nodes on the overall accuracy of the annual heating load calculations. It was found that thermal mass in the form of 5 inch thick masonry wall exposed on both sides to room air or masonry in the form of 2.5 inch thick surfacings on the interior walls was most efficient. In modelling the dynamics of the thermal mass wall by finite difference calculations, division of mass wall into 1/2 inch thick layers ensures the accuracy of the annual heating load calculations within 0.3% of the calculations carried out with twice the number of nodes in the same thickness of mass wall.

Sizing of the windows depending on the time constant of the house can be studied from the general design curves. The applicability of the design curves irrespective of the

weather data and the internal heat load schedule was demonstrated. Two important parameters, the SIG factor and the AHLR factor, along with the time constant, fully describe the thermal design.

The SIG factor gives a quantitative assessment of the heat potential available from solar and the fluctuating component of internal load that occur during the day. The AHLR factor is an output parameter which describes how much auxiliary heat is required in the house.

The economics of the passive design features (insulation level of the house, window shutter system and the thermal capacity in the house) were examined by employing the life cycle cost analysis.

ACKNOWLEDGEMENTS

The author wishes to express his sincere appreciation to the following persons and organizations.

Dr. R.R.Gilpin for his supervision,encouragement, and assistance in all stages of this investigation.

The Department of Energy, Mines and Resources (Conservation and Renewable Energy Branch) and The Department of Mechanical Engineering for financial assistance in the form of research assistantship and teaching assistantship.

Fellow graduate students for their discussion on various aspects of this thesis.

To my wife, Afroz for her excellent typing of this thesis.

Table of Contents

Chapter	Page
1. INTRODUCTION	1
2. THE PHYSICAL MODEL	6
2.1 Introduction	6
2.2 Physical Model	7
2.2.1 The Thermal Enclosure	7
2.2.2 The Window - Shutter System	12
2.2.3 The Thermal Mass	16
2.3 Meteorological Data	17
3. THE DIRECT GAIN WINDOW MODEL	18
3.1 Introduction	18
3.2 Calculation of TAR for a Single Glazing	19
3.3 Equations for TAR for Triple Glazing Window due to Direct Radiation	26
3.4 Applicability of TAR Equations of Triple Glazing Window to Single and Double Glazing Windows	32
3.5 Calculation of TAR for the Heat Absorbing Glass due to Direct Radiation	34
3.6 Calculation of TAR due to Diffuse Radiation	37
3.7 Total Radiation on a Tilted Surface	40
3.8 Equations for Sunlit Fraction of Window due to Direct and Diffuse Radiation	46
3.9 Solar Heat Gain Calculation	50
4. THE THERMAL MODEL OF HOUSE	53
4.1 Introduction	53
4.2 Heat Loss through the Exterior Enclosure Elements	53
4.3 Dynamics of the Thermal Mass	58

4.4 Infiltration Heat Loss	64
4.5 The Energy Balance	64
5. THE COMPUTER PROGRAM	71
6. SIMULATION RESULTS AND DISCUSSION	81
6.1 Introduction	81
6.2 Transmittance of Window Glass as a Function of Angle of Incidence	81
6.3 Effect of Solid Overhang on the Summer Solar Gain ..	84
6.4 Optimal Thickness of Mass Wall	87
6.5 Optimum Number of Nodes	87
6.6 Design Curves for the Houses Modelled	92
6.7 The General Design Curves	97
6.8 The Economics of the Passive Design Features	104
7. CONCLUSIONS AND RECOMMENDATIONS	115
7.1 Conclusions	115
7.2 Recommendations	116
REFERENCES	117
APPENDIX A-1	
Conversion Table	123
APPENDIX A-2	
Calculation of Heat Loss Coefficient (U) of House	124
APPENDIX A-3	
Calculation of Time Constant of House	125
APPENDIX A-4	
Sample Computer Run	126

LIST OF TABLES

Page

1	Design specifications of the houses modelled	88
2	Approximate cost estimates, the savings, as a function of insulation level of the house	107
3	Approximate cost estimates and the calculated savings, as a function of window shutter area.	109
4	Assumed cost estimates and the calculated savings, as a function of thermal mass area.	112

LIST OF FIGURES

	Page
2.1 Schematic of a house illustrating the design components.	8
2.2 The definition of the house orientation angle . .	10
2.3 Internal heat load schedule	11
2.4 The geometry of a sloping window and roof overhang.	13
2.5 Manual shutter operating schedule	15
3.1 Multiple reflections of direct solar radiation from a single sheet of glass.	21
3.2 Multiple reflections of direct solar radiation from a triple glazing window.	28
3.3 Geometry of diffuse radiation on a vertical window.	38
3.4 Radiation on a horizontal and tilted surface. . .	45
3.5 Shading of a sloping window from direct solar radiation by a solid overhang	48
4.1 Schematic of a house illustrating the heat gains and the heat losses	54
4.2 A schematic illustration of the energy fluxes to and from the room air temperature.	55
4.3 Nodal-point arrangement for thermal mass wall . .	60
4.4 Energy balance on Trombe type storage wall. . . .	60
4.5 Flow chart illustrating the solution scheme with no shutters.	68

4.6 Flow chart illustrating the solution scheme
with automatic shutters 69

4.7 Flow chart illustrating the solution scheme
with manual shutters. 70

5.1 Overall flow chart for the main program 72

5.2 Flow chart for subroutine HSDATA. 73

5.3 Flow chart for subroutine HBMDIF. 74

5.4 Flow chart for subroutine HTILT 75

5.5 Flow chart for subroutine GPRDIF. 76

5.6 Flow chart for subroutine GPRDIR. 77

5.7 Flow chart for subroutine SOLHGF. 78

5.8 Flow chart for subroutine QINTER. 79

5.9 Flow chart for subroutine ENRGBL. 80

6.1 Transmittance of window glass as a function of
angle of incidence. 83

6.2 Typical solar heat gain through a double and
triple glass window for the month of January. . . 85

6.3 Effectiveness of a solid overhang in reducing
the summer solar gain 86

6.4 Effect of increasing the thickness of the mass
wall on the yearly heat requirement 89

6.5 Effect of nodal points on the yearly heat
requirement calculations. 90

6.6 Design dimensions of the houses 93

6.7 Effect of south facing window area, the thermal
mass and the insulation level on the yearly
heat requirement of a house 95

6.8 Hours of potential overheating as a function of south facing window area. 96

6.9 A schematic illustration of the energy exchanges through the resistive and capacitive elements of the house 98

6.10 The general design curves103

6.11 The economics of the insulation level of a house106

6.12 The economics of shutter system110

6.13 The economics of thermal mass wall.114

NOMENCLATURE

Notation

Abg	area of below grade walls (Sq.ft)
Ag	basement floor area (Sq.ft)
Ac	area of ceiling (Sq.ft)
Al	lumped storage surface area (Sq.ft)
As	surface area (Sq.ft)
Ast	area of storage wall (Sq.ft)
Awi	area of window (Sq.ft)
Awn	area of north wall (Sq.ft)
Aws	area of south wall (Sq.ft)
Awe	area of east wall (Sq.ft)
Aww	area of west wall (Sq.ft)
AHLR	annual heating load reduction factor (dimensionless)
B _i	reflected component defined by equation 3.3.12
B _j	sum of mutiple reflections defined by equation 3.3.13
C	constant defined by equation 4.5.3 cloud cover index (dimensionless) thermal capacitance (Btu/F°) thermal capacity (Btu/F°)
E	distance between overhang and the top of the window (Ft.) energy stored (Btu)
EAZ	effective azimuth angle
ET	equation of time

F	projection of overhang from wall surface (Ft)
Fb	sunlit fraction due to beam radiation (dimensionless)
Fd	sunlit fraction due to diffuse radiation (dimensionless)
Fcb	coefficient of solar gain due to beam radiation (dimensionless)
Fcd	coefficient of solar gain due to diffuse radiation (dimensionless)
FS	solar heat gain (Btuh/sq.ft)
H	radiation on a horizontal surface (Btuh/sq.ft)
Ho	extraterrestrial radiation (Btuh/sq.ft)
Hb	direct radiation on a horizontal surface (Btuh/sq.ft)
Hd	diffuse radiation on a horizontal surface (Btuh/sq.ft)
Hr	reflected radiation on a horizontal surface (Btuh/sq.ft)
Hdv	diffuse radiation on vertical surface (Btuh/sq.ft)
Hn	total radiation on a surface facing normal to sun (Btuh/sq.ft)
Hw	height of window (Ft)
HDHr	annual heating degree hours (F° -Hr)
HHr	annual heating hours (Hr)
HOA	house orientation angle

Ib	intensity of direct radiation (Btuh/sq.ft)
Id	intensity of diffuse radiation (Btuh/sq.ft)
Io	intensity of direct radiation on the outer surface of glass (Btuh/sq.ft)
Ic	constant component of internal load (Btu)
If	fluctuating component of internal load (Btu)
Isc	solar constant (Btuh/sq.ft)
ISHG	integrated solar heat gain factor (Btu/sq.ft)
K	extinction coefficient of the glass (1/Ft)
KL	product of K and L (dimensionless)
L	thickness of the glass (Ft)
Lw	sloping length of window (Ft)
Ls	local standard time zone
Lg	longitude of the place
M	number of nodes
Ni	fraction of the absorbed radiation transferred to the inside of the building (dimensionless)
Qc	heat loss through ceiling (Btu/hr-sq.ft)
Qwa	heat loss through wall (Btu/sq.ft-hr)
Qwi	heat loss through window (Btu/hr-sq.ft)
Qwn	heat loss through north wall (Btu/hr-sq.ft)
Qws	heat loss through south wall (Btu/hr-sq.ft)
Qwe	heat loss through east wall (Btu/hr-sq.ft)
Qww	heat loss through west wall (Btu/hr-sq.ft)
Qbg	heat loss through below grade walls (Btu/hr-sq.ft)
Qf	heat loss through basement floor (Btu/hr-sq.ft)

Q _{fu}	furnace heat (Btu/hr)
Q _{inf}	heat loss due to infiltration (Btu/hr)
Q _{int}	heat gain due to internal loads (Btu/hr)
Q _{st}	heat stored in mass wall (Btu/hr-sq.ft)
Q _l	heat stored in lumped capacity (Btu/hr-sq.ft)
R _b	ratio of beam radiation on tilted surface to that on the horizontal surface (dimensionless)
R	run the program
	reflected component defined by equation 3.3.1
	air change rate (Ft ³ /hr)
R _j	sum of multiple reflections defined by equation 3.3.3
R _g	resistance of basement floor (Hr-Sq.ft-F ^o /Btu)
R _c	resistance of ceiling (Hr-Sq.ft-F ^o /Btu)
R _{wa}	resistance of wall (Hr-Sq.ft-F ^o /Btu)
R _{st}	resistance of storage wall (Hr-Sq.ft-F ^o /Btu)
R _{bg}	resistance of below grade wall (Hr-Sq.ft-F ^o /Btu)
R _{wn}	resistance of north wall (Hr-Sq.ft-F ^o /Btu)
R _{ws}	resistance of south wall (Hr-Sq.ft-F ^o /Btu)
R _{we}	resistance of east wall (Hr-Sq.ft-F ^o /Btu)
R _{ww}	resistance of west wall (Hr-Sq.ft-F ^o /Btu)
R _{wi}	resistance of window (Hr-Sq.ft-F ^o /Btu)
RC	time constant (Hour)
S	stop the program
	slope (angle)
S _n	solar noon
SAT	sol-air temperature (F ^o)

SATn	sol-air temperature north (F°)
SATs	sol-air temperature south (F°)
SATe	sol-air temperature east (F°)
SATw	sol-air temperature west (F°)
SIG	solar and internal gain factor (dimensionless)
SR,SS	sunrise and sunset angles
SAZ	solar azimuth angle
T	temperature (F°)
T_r	reflected component defined by equation 3.3.2
TestL	lower limit of the heat potential (Btu/hr-sq.ft)
TestH	upper limit of the heat potential (Btu/hr-sq.ft)
Tmin	minimum allowable room temperature (F°)
Tmax	maximum allowable room temperature (F°)
Ta	air temperature (F°)
Tr	room temperature (F°)
Ts	surface temperature (F°)
Tg	ground temperature (F°)
Tl	lumped surface temperature (F°)
Tm	temperature at interior node m (F°)
Tj	sum of mutiple reflections defined by eq.3.3.6
TAR	transmissivity, absorptivity and reflectivity (dimensionless)
U	overall heat transfer coefficient (Btu/Hr-Sq.ft- F°) overall conductance (Btu/Hr-Sq.ft- F°)
U_r	reflected component defined by equation 3.3.11
U_j	sum of mutiple reflections defined by eq. 3.3.12

V	volume (Ft^3)
X	distance (Ft)
a	fraction of radiation available after absorption in the glass (dimensionless)
as	fraction absorbed due to sky diffuse radiation (dimensionless)
c	specific heat (Btu/Lb-F°)
dA	elemental area (Sq.ft)
dEs	energy received on unit surface area (Btu/sq.ft)
dq	energy received in proportion to the solid angle
dw	solid angle
f	function defined by equation 3.5.1
h	heat transfer coefficient ($\text{Btu/Hr-Sq.ft-F}^\circ$)
i	incidence angle
k	conductivity ($\text{Btu-in/Sq.ft-Hr-F}^\circ$)
kg	conductivity of glass ($\text{Btu-in/Sq.ft-Hr-F}^\circ$)
n	day of the year (dimensionless) refractive index (dimensionless)
q	heat flux (Btu/Hr-Sq.ft)
q	heat flux due to convection (Btu/Hr-Sq.ft)
q	heat flux due to conduction (Btu/Hr-Sq.ft)
r	fraction reflected (dimensionless)
rs	fraction reflected due to sky diffuse radiation (dimensionless)
	radius (Ft)
t	time
w	hour angle

Subscripts

1	outer or first glazing
2	middle or second glazing
3	inner or third glazing
12	effective value due to two glazings 1 and 2
123	effective value due to three glazings 1, 2 and 3
M	last node
T	tilted surface
l	referring to lumped capacity

Greek Symbols

θ	latitude of the location
λ	wave length (micron)
δ	declination
α	absorptivity (dimensionless)
α_b	absorptivity due to beam component (dimensionless)
α_d	absorptivity due to diffuse component (dimensionless)
$\alpha_{1\text{ of }3}$	absorptivity of first glazing of a triple glazing window (dimensionless)
$\alpha_{2\text{ of }3}$	absorptivity of second glazing of a triple glazing window (dimensionless)
$\alpha_{3\text{ of }3}$	absorptivity of third glazing of a triple glazing window (dimensionless)

α_{123}	effective absorptivity of a triple glazing window (dimensionless)
α	thermal diffusivity (Sq.ft/Hr)
θ_i	incident angle
θ_r	refraction angle
θ_z	zenith angle
β	altitude of the sun
	atmospheric back scatterence (dimensionless)
Δ	delta
ρ	reflectivity (dimensionless)
	ground / snow cover albedo (dimensionless)
	density (Lb/Ft ³)
τ	transmissivity (dimensionless)
τ_b	transmissivity due to beam component (dimensionless)
τ_d	transmissivity due to diffuse component (dimensionless)
τ_n	transmissivity at normal incidence (dimensionless)
	time constant (hour)

Superscripts

ν	new time step
'	radiation fluxes before multiple reflections in the atmosphere

1. INTRODUCTION

Solar passive heating is one of the most promising alternatives available to reduce house heating requirements. In the context of building heating a definition of passive solar heating system was formulated by the Department of Housing and Urban Development (HUD) which states:

A passive solar energy system is one which uses the building structure as a collector, storage, and transfer mechanism with a minimum amount of mechanical equipment.

Many attempts have been made to define passive solar heating system but none is completely satisfactory because of the wide variety of the forms which such systems can take. The type of design that was studied here is usually called direct gain. That is solar heating occurs directly through the windows of the house and no separate form of solar collector exists.

It will be useful to evolve a concept of an ideal solar passive heating system. An ideal solar passive system can be looked upon as one that requires no auxiliary energy to maintain inside comfort conditions. Based on such an ideal concept, it can be said that a building structure should be so designed that it controls the amount of solar energy reaching the interior masses of the building, directly as sunlight, and transacting all heat exchanges and storage at the building interior masses. In effect such a building would behave like a temperate solar collector. With this

approach part of the external structure must be composed of a transparent insulation (affording visibility), and at the same time the total external structure should act as a sun light modulator. Although the ideal solar passive system may not be achievable in practice one can approach this ideal in a building if the thermal components of the building have been designed as a single entity right from the outset.

Although the solar passive system has advantages of being simple and economic, the calculations involved in the design are relatively sophisticated. This stems from the fact that a complex pattern of heat exchanges take place in and around any real enclosure.

Today's architects and designers are really faced with the problems of determining parameters like: Resistance values of enclosure elements, amount of heat capacity in the structure, the area of window as well as its orientation, and the operational characteristics of window shutters, the design of overhang etc. and eventually they are faced with the problem of determining the annual auxiliary heat requirements for their designs.

It is the purpose of the present work to provide the designers and researchers with an interactive computer program that can accept every possible design variable(s) and can model their design by simulating the dynamic response of the house to temporal variations in radiation fluxes and ambient air temperatures.

Any thermal model is necessarily only an approximation

to the complex heat exchanges taking place in and around any real enclosure. Then the question arises as to how accurately the thermal model predicts the performance of any real enclosure.

The above subject of calculation of energy consumption in residential buildings using simulation techniques has been studied in recent years by Konard and Larsen (1), Zulfikar et.al (2) , Davies (3), Balcomb et al.(4), Mazria and Wessling (5), DOE - 2 "Energy Analysis Program" (6), etc. On the other hand the design and performance of direct gain passive houses using static calculations has been studied by many investigators, Dumont, Besant and Green (7), Jones and Tymura(8), Balcomb and MacFarland (9) etc. The performance of passive test units has been reported by Wheeling et al. (10), Dumont and Besant et al.(11), Chen et.al. (12), Palmiter et al. (13), Balcomb et al.(4), and Jones (14) etc.

However, the above simulation models were either too specific or too complex requiring prohibitively high computer (CPU) time to study the design of passively heated houses.

Gilpin,(15) developed a computer model of a house employing a south facing window and a mass wall. An essential feature of this model is that it is a dynamic model.

The present study is an extension of Gilpin's thermal model of passive house. An improved method of calculating

the solar heat gain was developed. Greater emphasis was placed on two important elements of the passive house namely: the windows and the mass walls.

The logical question then arises as to what is the best combination of the windows and the mass wall for a given floor area that results in the least auxiliary heat requirement for maintaining the inside comfort conditions.

Several alternatives are available. Collector windows could be sloped to maximize the solar heat gain. Triple glazing or heat absorbing glass windows could be used to minimize the summer overheating. Overhangs could be provided on the sloping windows.

Two different techniques of storing heat in the mass wall can be studied. In the first technique the mass wall can be placed inside the house and the heat flow into and out of the wall can be studied as a result of rise or fall in the room temperature. In the second technique the mass wall could be oriented to receive the direct solar heat gain through the window as in the case of Trombe Wall.

In modelling the behaviour of the mass walls, stability and accuracy of the finite difference calculations is important. One is often faced with problems like: What is the optimum thickness of the mass wall for diurnal energy storage? How few nodes could be considered in studying the dynamics of the mass wall without impairing the accuracy?

The present work examines the above alternatives and provides logical solutions to the possibility of minimum

energy for maximum comfort through solar passive design.

It was recognized that not all the designers and architects have access to computing facility. As a result they cannot take full advantages offered by the present interactive computer program. To help such designers, a set of general design curves have been prepared. These design curves are the useful means of estimating the annual energy consumption of any house.

Alternatively parameters like, window and mass wall areas, for minimum auxiliary heat requirement, can also be estimated from the design curves. These design curves could be used irrespective of the weather data and the internal heat load schedule. This is possible with an additional table on the ISHG(Integrated solar heat gain) factors for various locations.

These ideas and the accompanying solutions are presented in chapters 2 through 5. The physical model and the governing equations are discussed in chapters 2 through 4. Chapter 5 presents the flow charts illustrating the solution scheme. Some results like : the transmittance of window glass as a function of angle of incidence, the optimum mass wall thickness for diurnal energy storage, the optimum number of nodes for modelling the dynamics of the mass wall, the general design curves and the economics of the passive design features are presented in chapter 6. This is followed by the conclusions drawn from this study.

2. THE PHYSICAL MODEL

2.1 Introduction

A mathematical model has been developed to enable predictions to be made of the thermal behaviour of any real house. An essential feature of the model is its flexibility in modelling the dynamic behaviour of almost any type of design and construction. Some of the flexibilities offered by the model are:

1. Provision to model solar heat gain from any number of windows (as in the real house) facing north, south, east, or west.
2. Orientation of the house could be varied to study the optimum house orientation angle.
3. Solar heat gain can be maximized by sloping one or all of the windows as desired.
4. Summer overheating can be reduced by judicious design of overhang on the windows.
5. Another useful technique of reducing the overheating can be studied by varying the number of glazings and their KL product. Alternatively, the effectiveness of heat absorbing glass in reducing the overheating can also be studied.
6. The possibility of using automatic shutters which open and close according to the thermostatic control switch exists in the model. Alternatively, shutters which open at sunrise and close at sunset during winter months,

while being left open all through summer months can be examined. The performance of both types of shutters can be compared with the case of no shutters.

7. The model can investigate such possibilities as placement of the thermal mass exterior or interior to the structure. Further the possibility of modelling the Trombe type of storage wall is also included.

A number of such possibilities can be studied from the present thermal model. The theory and the calculations are illustrated as and when they appear in the following chapters.

2.2 Physical Model

2.2.1 The Thermal Enclosure

Figure 2.1 shows the schematic of one of the several house designs the present model can handle. The thermal enclosure 1 is comprised of elements such as north, south, east and west facing walls, above and below grade walls, ceiling and basement floor. The exterior walls of the enclosure are assumed to be of standard construction. The possibility of modelling the heavier construction (such as brick or concrete walls) in place of wood frame construction can also be analysed.

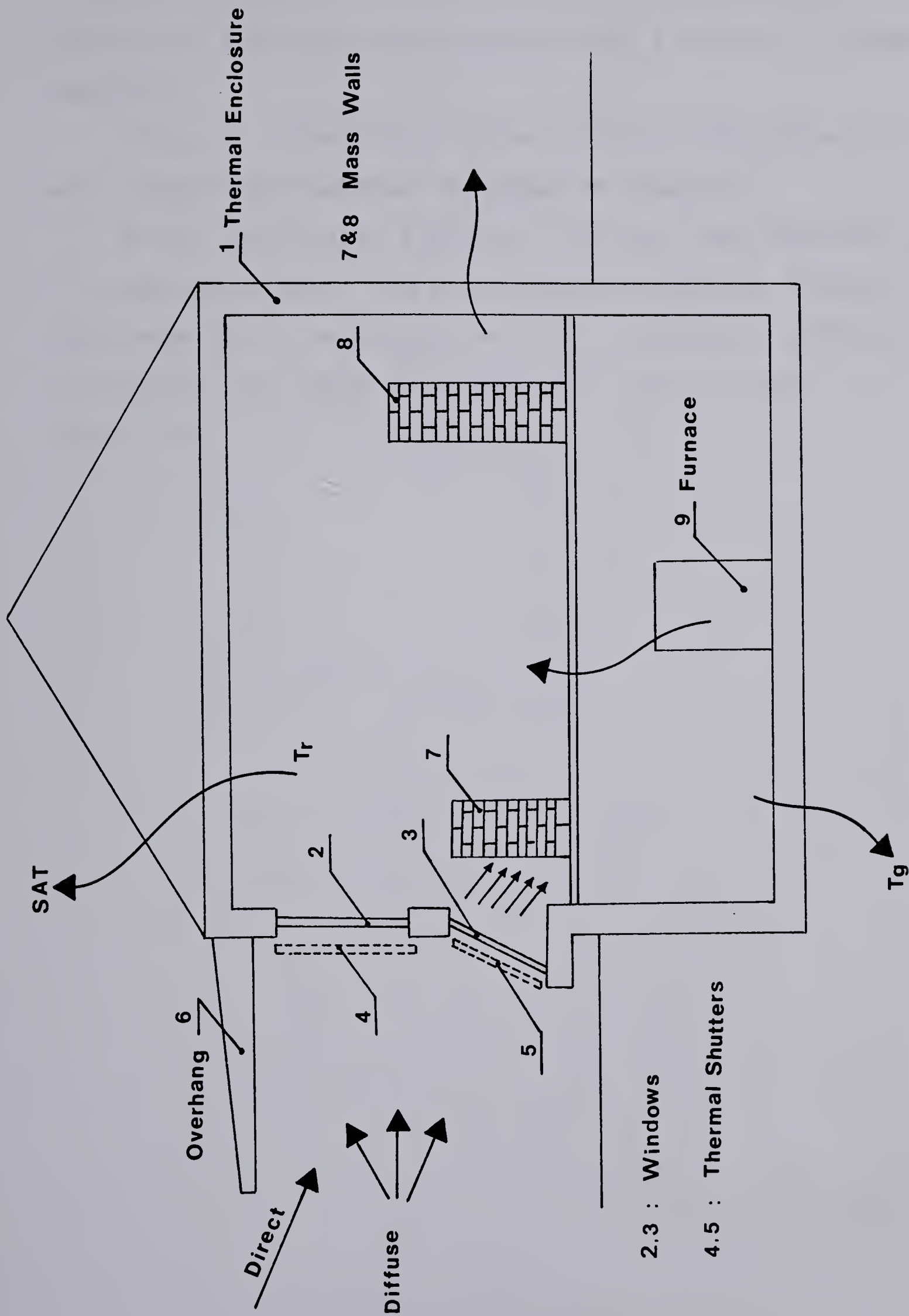


Figure 2.1 Schematic of a house illustrating the design components

A single overhang 6 is an architectural projection for shading the sloping windows against high altitudes of summer radiation.

The whole orientation of the building could be varied with respect to true south as shown in figure 2.2.

Within the thermal enclosure, internal heat gains due to lights, appliances and people were considered. Based on experience and literature survey (2) a reasonable schedule of internal heat gains was worked out. This is shown in figure 2.3.

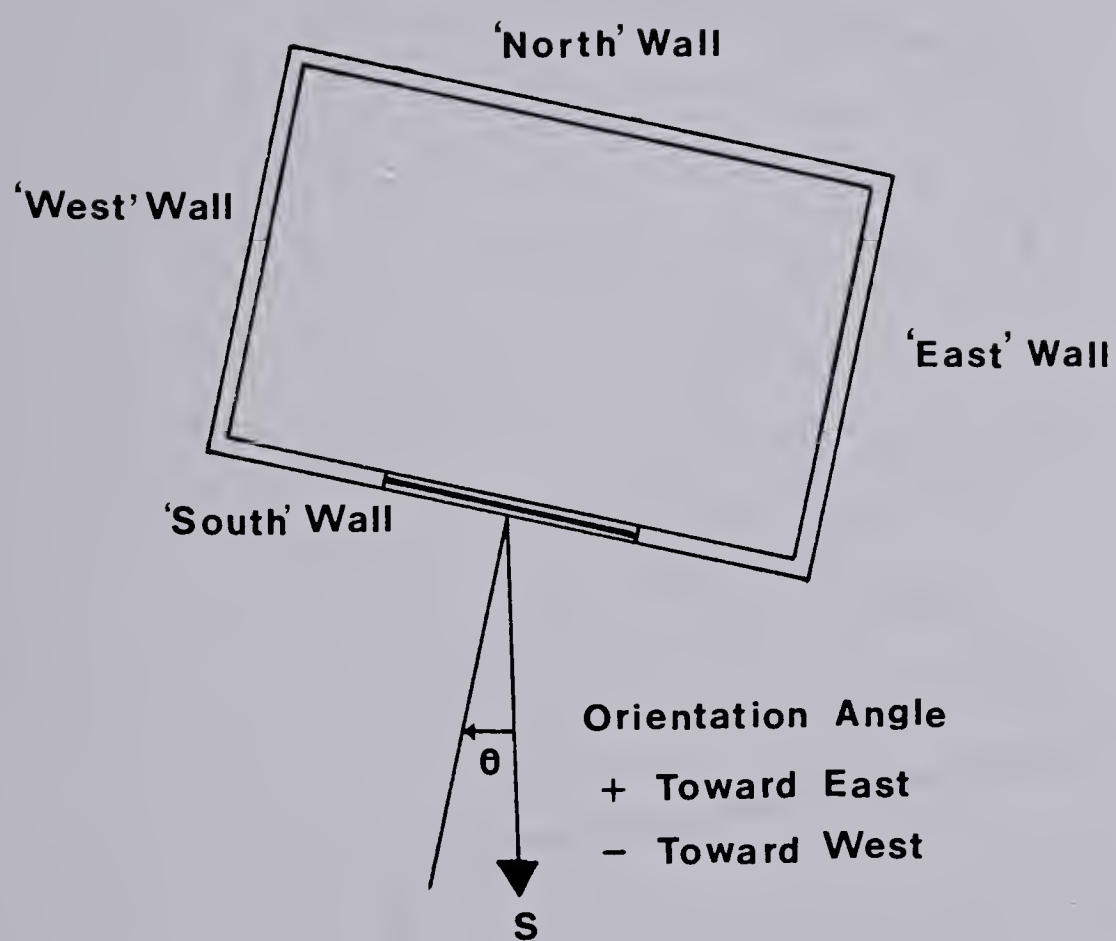


Figure 2.2 The definition of the house orientation angle

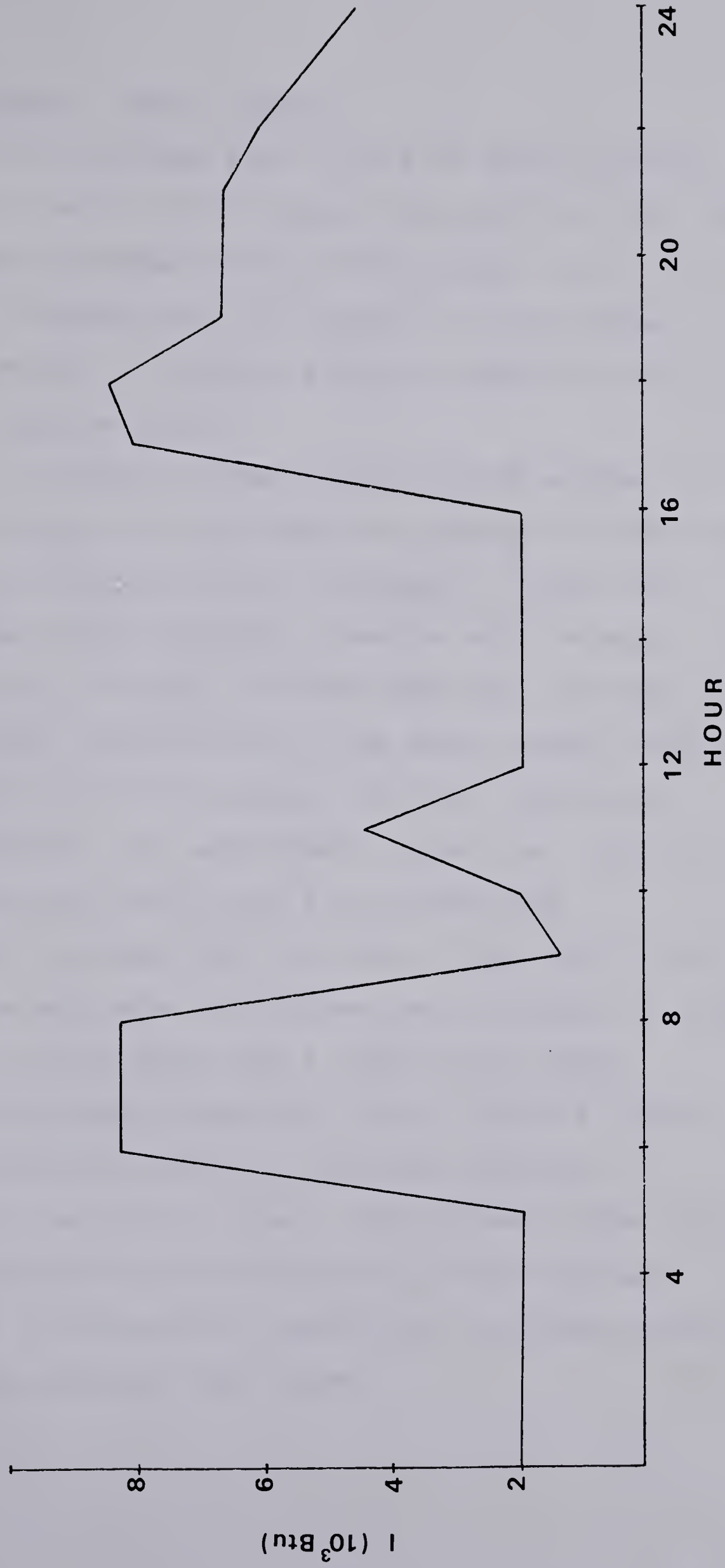


Figure 2.3 Internal heat load schedule

2.2.2 The Window - Shutter System

Most of the problems associated with passive design such as heat loss in winters (apart from contributions like heat loss due to conduction and infiltration), and overheating in summers are attributable to the window element; therefore, its design plays an important part in a direct gain passive system.

Figure 2.4 shows a sloped triple glazing window facing due south. The possibility of partial shading of window can be studied by providing a solid overhang 6. Large south facing windows though desirable from the solar energy collection point of view, introduce two major problems. In the first place, during winters, the large windows could be net losers of heat in the absence of night insulating shutters. Secondly they would admit large solar radiation in summer months which could result in overheating.

In order to prevent the net loss of heat and to control the excessive heat gain, two systems were proposed. In the first case it was assumed that a temperature sensor depending on the room temperature, would transmit signals to a shutter mechanism to open or close the shutters, in proportion to the control signal. The problem of admitting day light irrespective of net loss or gain of heat was incorporated in the model by specifying a minimum opening of shutters during the day light hours.

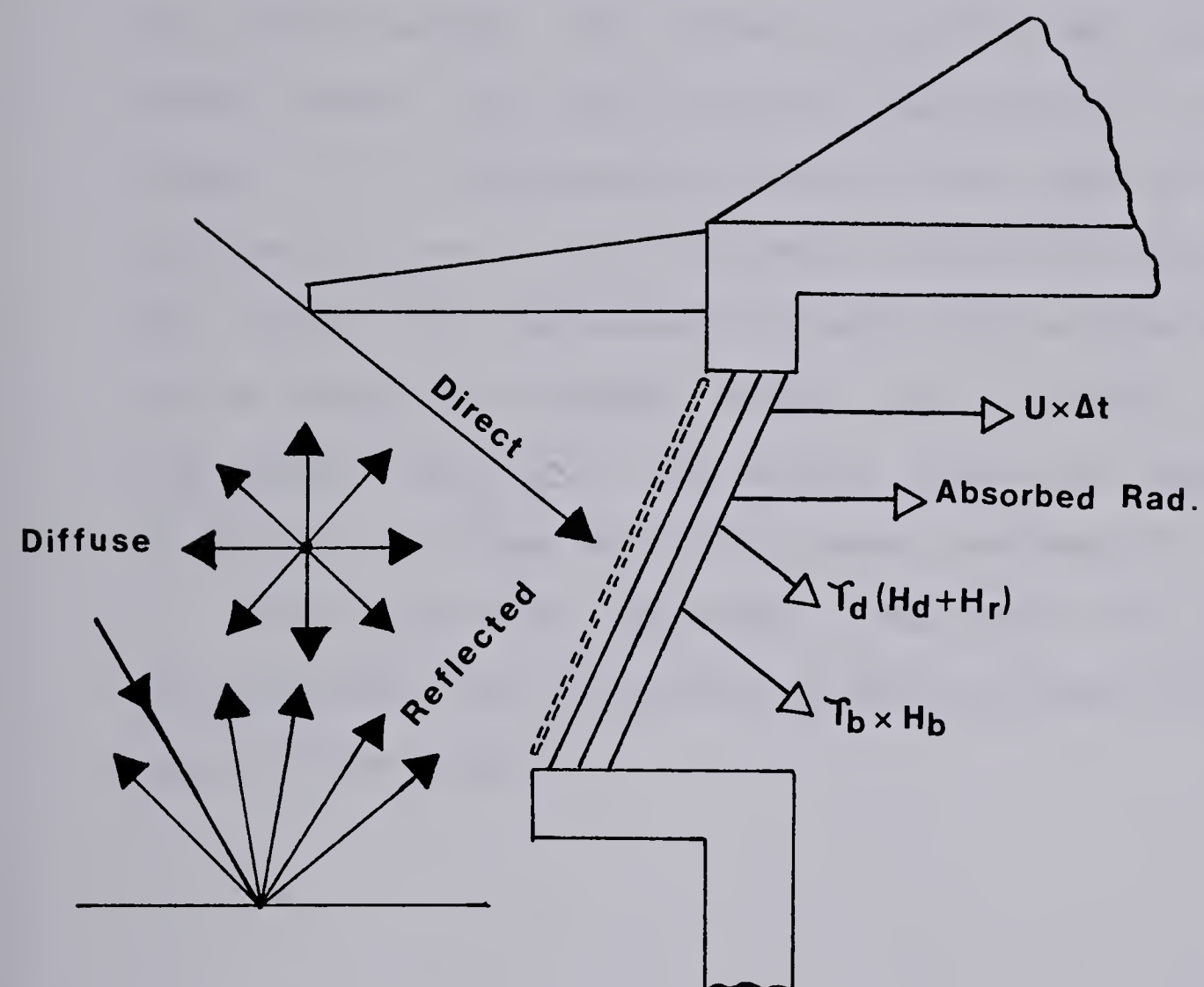


Figure 2.4 The geometry of a sloping window and roof overhang

The above mechanism is somewhat sophisticated and to date no such mechanism has been developed commercially. Another logical and simple shutter routine could be thought of as one that opens at sun rise and closes at sunset during the winter months. The shutters could be left open during summer months. The shutter operating schedule is depicted in figure 2.5. A reasonable assumption that goes with this shutter routine is that the people would do something when the inside room temperature exceeds the maximum value. This can be expected in summer months. It is natural to believe that people would pull the drapes, close the venetian blinds or open the windows when they sense overheating.

Hence provision was made in the model for comparing the performance of the above two shutter systems with that of a case with no shutters.

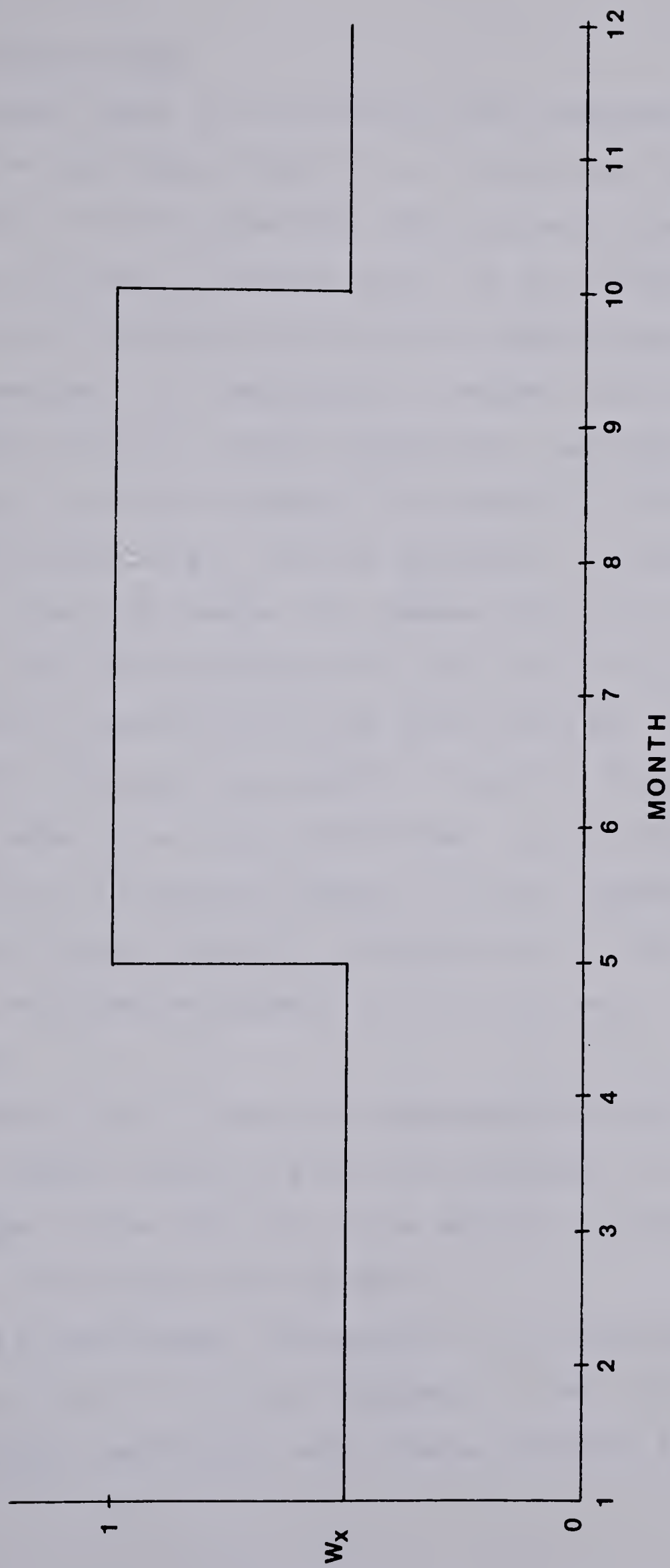


Figure 2.5 Manual shutter operating schedule

2.2.3 The Thermal Mass

The thermal mass in the structure was assumed to occur in one of the two forms. That is the thermal mass could consist either of thin materials such as plaster board or thick materials such as masonry walls. In the thermal model the thin plaster board was treated by a lumped-capacity approach. Because it is reasonable to assume the thin plaster board to be at uniform temperature. Applying the same analogy the thermal capacity introduced by the wood frame construction as well as the furniture in the house is studied by Jones and Tymura (8). However, this has to be approached with caution because not all the wood used in the house directly interacts with the inside room air. The thick masonry walls shown by the elements 7 and 8 in figure 2.1 have to be modelled using a distributed - capacitance approach. This is necessary because a diurnal temperature variation will occur through a thick mass wall. This phenomenon was modelled using a finite difference calculation.

The masonry wall 8 could be considered to exist in one of the two forms. Either as a wall of thickness (t) exposed on both sides to the room air, or as masonry surfacings of thickness ($t/2$) on the interior walls.

In the present model the possibility of studying the Trombe type of wall 7 is also included. Further the effects of distributing the thermal mass between elements 7 and 8

can also be examined.

The thickness of the element 8 in the present study was considered to be 5.0 inch. This is based on the simulation results discussed in section 6.4.

2.3 Meteorological Data

Generally, all the meteorological stations record the hourly insolation level on a horizontal surface, together with ambient air temperature and wind velocity etc. However, for modelling a passive house, the irradiation of vertical or tilted surfaces is desired. In section 3.1.7 an analytical method for estimating the total radiation on a tilted surface is described.

One year's data "comprised of" the hourly radiation on horizontal surface and the corresponding air temperatures were used in the model as weather data.

3. THE DIRECT GAIN WINDOW MODEL

3.1 Introduction

In the development of the thermal model several possibilities of maximizing the winter solar gain and minimizing the summer overheating were considered. As a result, a more sophisticated method of calculating the solar heat gain through a single, double or triple glazing, employing clear glass and (or) heat absorbing glass was developed.

Calculation of solar heat gain through glass has been studied by Yellot (16), Parmelee, and et al. (17), and Stephenson (18). Yellot's study is limited to single glass. Parmelee's experimental investigation is an useful source of comparing the predicted heat gains through double glass. However, this study is limited to double glass.

The solar heat gain factors published by Stephenson (19) and ASHRAE (20) are not based on the real hourly meteorological data. The equations for TAR used in the calculation of solar heat gain factors in Stephenson's method are based on a polynomial function. This method, although simple, is not accurate. Another limitation of the published solar heat gain factors is that they are applicable to a single pane of clear glass, with a fixed vertical geometry.

In the present direct gain window model the solar heat gain was calculated from the real hourly meteorological

data. The model estimates the solar heat gain through single, double or triple glazing windows employing clear glass or heat absorbing glass. It should be recognized that the TAR of clear and heat absorbing glass varies with angle of incidence of the beam radiation. Therefore, the TAR values of glass were calculated at each hour angle. Further the fraction of diffuse radiation transmitted, and absorbed is not the same as that of the direct radiation. Therefore a method of calculating TAR of the glass for diffuse radiation was incorporated in the model.

It is believed that due to the above refinements, the estimated solar heat gain will be relatively accurate.

The solar heat gain is defined as the total instantaneous radiation transmitted through the glass plus the fraction of heat transferred due to radiation absorbed by the glass.

From the definition, it follows that the TAR of a particular glass and the instantaneous radiation incident on the glass should be known before estimating the solar heat gain. This is illustrated in the following sections.

3.2 Calculation of TAR for a Single Glazing

Transmittance of glass is a function of wavelength, angle of incidence of the incoming radiation, the refractive index, and the extinction coefficient of the material.

Hsieh and Su (21) have presented a method of calculating the thermal radiative properties of glass for

wavelengths between 0.3 to 206 micron. Hsieh and Su's study accounts for the effects of longwave radiation and as well as the surface temperature of the glass. Their results show that for a clear glass the refractive index and so its extinction coefficient is wavelength independent in shortwave region but is irregular in the far infrared region. However, for most solar energy applications only the shortwave radiation is considered (22). Therefore the study of Parmelee (23), which neglects the effects of longwave radiation, temperature and dust etc., was employed in the present model.

Figure 3.1 shows a glass of thickness L irradiated by a ray of intensity I . The multiple reflections occurring as a result of I are shown in the figure 3.1., where ' r ' is the fraction reflected and ' a ' is the fraction of radiation available after absorption in the glass. The transmissivity τ is calculated as follows.

The sum of the intensities of the transmitted components is

$$Ia(1-r)^2 + Ia^3r^2(1-r)^2 + Ia^5r^4(1-r)^2 + \dots$$

This is a geometric series and hence by definition the transmissivity can be written as

$$\tau = Ia(1-r)^2 [1 + a^2r^2 + a^4r^4 + \dots] / I$$

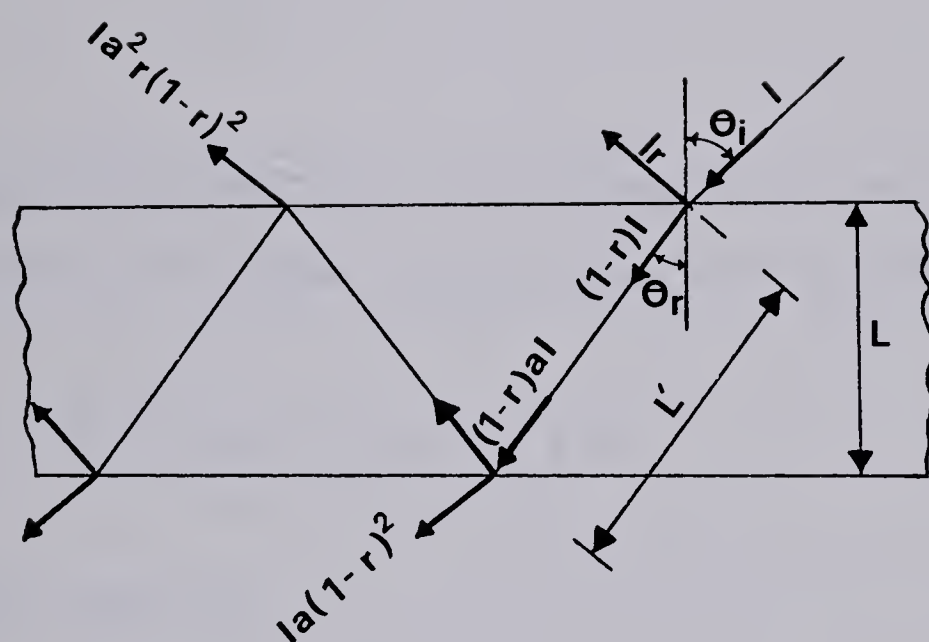


Figure 3.1 Multiple reflections of direct solar radiation from a single sheet of glass

on simplification

$$\tau = a(1-r)^2 / (1-a^2r^2) \quad 3.2.1$$

Similarly the reflectivity ρ is the sum of the intensities of the reflected components divided by the intensity of the incident radiation.

$$\rho = [I_r + I_a^2 r (1-r)^2 + I_a^4 r^3 (1-r)^2 + \dots] / I$$

On simplifying the sum of the geometric series the reflectivity ρ of the single glass can be written as

$$\rho = r + a^2 r (1-r)^2 / (1-a^2 r^2) \quad 3.2.2$$

From the identity

$$\tau + \alpha + \rho = 1$$

$$\alpha = 1 - \tau - \rho$$

Therefore the absorbtivity of the single glass can be written as

$$\alpha = 1 - r - a(1-r)^2 / (1-ar) \quad 3.2.3$$

In the above equations both ' r ' and ' a ' are functions of the angle of incidence of the incoming solar radiation.

The absorption of radiation in a partially transparent medium is described by Bouger's law, which is based on the assumption that the absorbed radiation is proportional to the local intensity in the medium and the distance the radiation travels in the medium. By dividing the sheet of the glass into a number of layers of equal thickness dL , each of which reduces the intensity by dI , that is

$$-dI = I K dL$$

Integrating between limits 0 to L

$$\int_{I_0}^I (dI/I) = -K L$$

$$\text{Log}_e(I/I_0) = -KL$$

$$\frac{I}{I_0} = \frac{e^{-KL}}{e^0} = a$$

Where 'a' is the fraction of the energy available after passage through the glass.

The thickness of the glass L should be modified to account for the refraction or the bending of the ray. The modified L' is therefore given by

$$\text{Cos}\theta_i = L/L'$$

$$L' = L \text{ Sec}\theta_i \text{ or } L/\text{Cos}\theta_i$$

Writing in terms of the incident angle

$$a = e^{\frac{-KL}{\sqrt{1 - \sin^2 \theta_i / n^2}}} \quad 3.2.4$$

The other term 'r' in equation 3.2.1 can be obtained from the Fresnel's equation for the reflection of non polarized radiation. This consists of two components of radiation namely, the perpendicular and the parallel component and is given by,

$$2r = \frac{\sin^2 (\theta_i - \theta_r)}{\sin^2 (\theta_i + \theta_r)} + \frac{\tan^2 (\theta_i - \theta_r)}{\tan^2 (\theta_i + \theta_r)} \quad 3.2.5$$

Where the parallel component is given by

$$r = \frac{\sin^2 (\theta_i - \theta_r)}{\sin^2 (\theta_i + \theta_r)} \quad 3.2.6$$

The perpendicular component is given by

$$r = \frac{\tan^2 (\theta_i - \theta_r)}{\tan^2 (\theta_i + \theta_r)} \quad 3.2.7$$

It should be recognized that the above TAR equations for single sheet of glass are strictly applicable to monochromatic radiation only. For solar radiation applications the average or total values of TAR applicable to entire solar spectrum have to be determined.

Deitz's study reported in reference (22) deals with variation of transmissivity of glass with spectral wavelength. Deitz shows that the glass containing little (0.15% ferrous oxide) has essentially constant transmissivity over entire solar spectrum. However, the transmissivity of heat absorbing glass (0.5% ferrous oxide) varies considerably with wavelength.

Parmelee et al. (17) have made extensive experimental studies on the transmission of solar radiation through window glass. For single sheet of glass (less than 0.15% ferrous oxide) they found generally good agreement between measured and calculated values.

The studies of Dietz and Parmelee suggest that the transmissivity of window glass (also called clear glass) is constant over entire solar spectrum. Therefore this assumption was made in the present study.

For a typical 1/4 inch thick clear glass the transmissivity is of the order of 0.88, the absorptivity of the range of 0.04, the rest 0.08 being the reflectivity.

3.3 Equations for TAR for Triple Glazing Window due to Direct Radiation

In this section a method of calculating the TAR of triple glazed windows is presented. The general recurrence formulae developed for a triple glazed window can be applied to single as well as double glazed windows. It is believed that by applying the same principles a general recurrence relation for a series of 'n' glass pane windows can be developed. This however was not attempted in the present study.

Equations for TAR for double glazed windows are commonly found in the literature, e.g. see Parmelee, (23) Mitalas & Stephenson (24). Equation of transmissivity for 'n' glass covers in the solar collectors has been reported (22). However, the latter case neglects the absorption of the glass and assumes that the TAR of each glazing is the same.

Recently, equations for transmittance of 'n' glass covers, based on net radiation method has been reported by Speigel (25). Wijesundera (26) has extended this method for transmissivity as well as absorptivity of 'n' glass covers. However, at higher incident angles the results obtained from net radiation method are about 4% higher than that obtained by ray accounting technique (26).

The present model for TAR is based on the ray accounting technique. Therefore it is expected to give more accurate results. The model accounts for the absorption of

the glass as well as for the different TAR values for each glazing. There is therefore enough scope in that by changing the TAR of each glazing an effective combination of clear glazings can be designed.

Figure 3.2 shows a ray of direct beam radiation falling on the first glazing. Thereafter the multiple reflections follow. By placing the second glass in the centre the pattern of multiple reflections was studied. Let

τ_1, α_1, ρ_1 represent the TAR of the first glazing

τ_2, α_2, ρ_2 represent the TAR of the second glazing

τ_3, α_3, ρ_3 represent the TAR of the third glazing.

Referring to figure 3.2

Let

$$R_1 = \rho_2 \tau_1 \quad 3.3.1$$

$$T_1 = \tau_1 \tau_2 \quad 3.3.2$$

It is clear from the multiple reflection pattern that

$$R_2 = \rho_1 \rho_2 (R_1) + \rho_3 \tau_1 (T_1)$$

$$T_2 = \rho_1 \tau_2 (R_1) + \rho_2 \rho_3 (T_1)$$

Similarly,

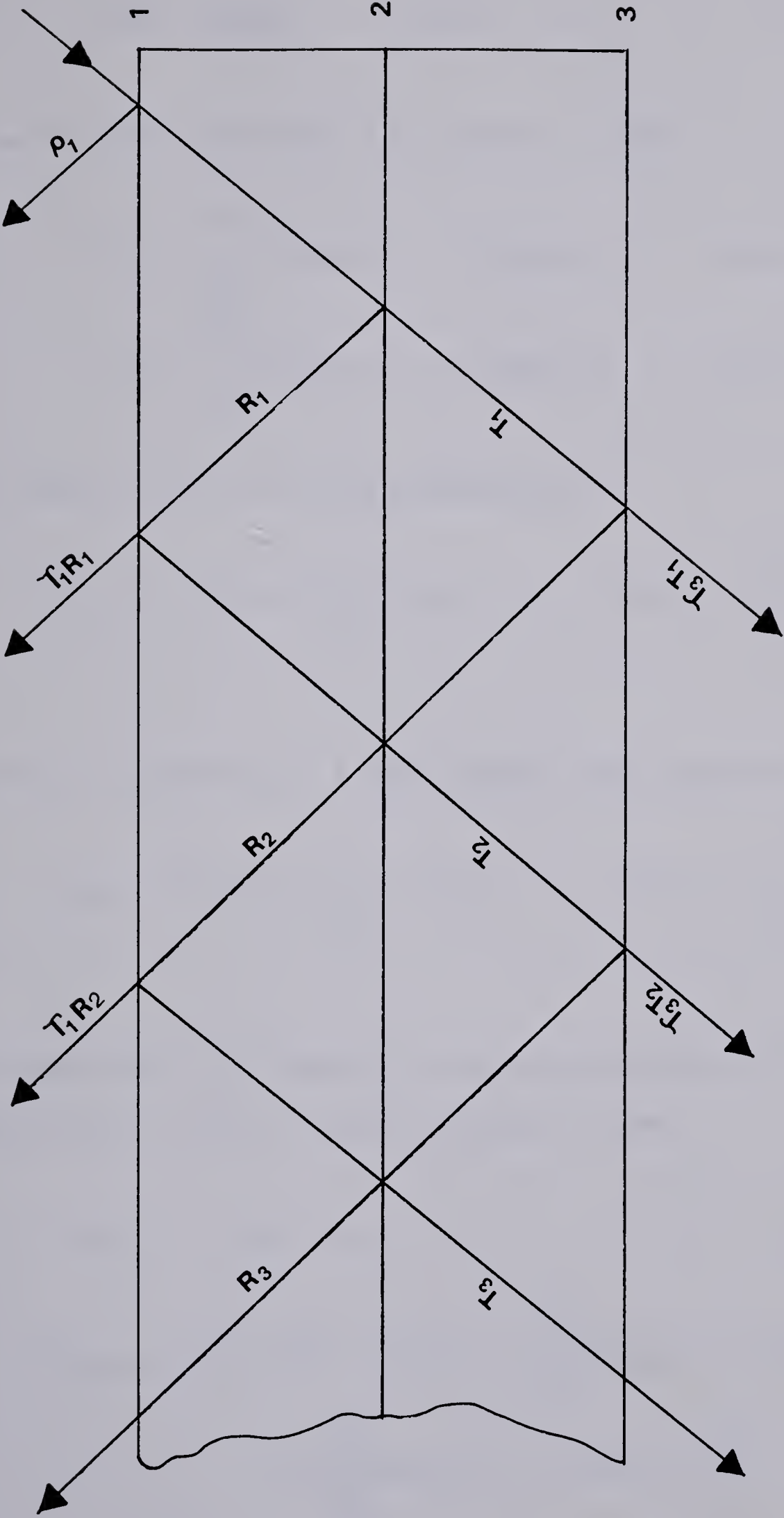


Figure 3.2 Multiple reflections of direct solar radiation from a triple glazing window.

$$R_3 = \rho_1 \rho_2 (R_2) + \rho_3 \tau_2 (T_2)$$

$$T_3 = \rho_1 \tau_2 (R_2) + \rho_2 \rho_3 (T_2)$$

and so on. Writing R and T in general form,

$$R_j = \sum_{j=2}^{\infty} \rho_1 \rho_2 (R_{j-1}) + \rho_3 \tau_2 (T_{j-1}) \quad 3.3.3$$

$$T_j = \sum_{j=2}^{\infty} \rho_1 \tau_2 (R_{j-1}) + \rho_2 \rho_3 (T_{j-1}) \quad 3.3.4$$

Combining all the reflected components,

$$\rho_{123} = \rho_1 + \rho_2 \tau_1^2 + \tau_1 \left[\sum_{j=2}^{\infty} \rho_1 \rho_2 (R_{j-1}) + \rho_3 \tau_2 (T_{j-1}) \right] \quad 3.3.5$$

Similarly, combining all the transmitted components,

$$\tau_{123} = \tau_1 \tau_2 \tau_3 + \tau_3 \left[\sum_{j=2}^{\infty} \rho_1 \tau_2 (R_{j-1}) + \rho_2 \rho_3 (T_{j-1}) \right] \quad 3.3.6$$

From equations 3.3.5 and 3.3.6 we can determine the absorbtivity α_{123} of a triple glazed window.

$$\alpha_{123} = 1 - \rho_{123} - \tau_{123} \quad 3.3.7$$

$$\alpha_{123} = 1 - \left[\rho_1 + \rho_2 \tau_1^2 + \tau_1 \tau_2 \tau_3 + \tau_1 \sum_{j=2}^{\infty} (\rho_1 \rho_2 (R_{j-1}) + \rho_3 \tau_2 (T_{j-1})) \right. \\ \left. + \tau_3 \sum_{j=2}^{\infty} (\rho_1 \tau_2 (R_{j-1}) + \rho_2 \rho_3 (T_{j-1})) \right] \quad 3.3.8$$

However to determine the net heat transfer through the window the absorptivities of the individual glazings, α_{1OF3} , α_{2OF3} , α_{3OF3} , should be known. The procedure of calculating the individual absorptivities of each glazing as an integral part of a triple glazing window is presented below.

To determine the absorptivity of first glazing of a triple glazing window the components of the radiation incident on the first glass should be multiplied by its absorptivity.

Therefore

$$\alpha_{1OF3} = (1 - \rho_1 - \tau_1) \left[1 + \rho_2 \tau_1 + \sum_{j=2}^{\infty} \rho_1 \rho_2 (R_{j-1}) + \rho_3 \tau_2 (T_{j-1}) \right] \quad 3.3.9$$

Similarly absorptivity of the inner glazing is given by

$$\alpha_{3OF3} = (1 - \rho_3 - \tau_3) \left[\tau_1 \tau_2 + \sum_{j=2}^{\infty} \rho_1 \tau_2 (R_{j-1}) + \rho_2 \rho_3 (T_{j-1}) \right] \quad 3.3.10$$

For determining the absorptivity of the middle glass

Let

U_1 be the fraction of the transmitted component from the first glass incident on the middle glass.

B_1 be the fraction of the reflected component from the third glass incident on the middle glass.

That is:

$$U_1 = \rho_1 \rho_2 \tau_1 \quad 3.3.11$$

$$B_1 = \rho_3 \tau_1 \tau_2 \quad 3.3.12$$

From figure 3.2 it follows that

$$U_2 = \rho_1 \rho_2 (U_1) + \rho_1 \tau_2 (B_1) .$$

$$B_2 = \rho_3 \tau_2 (U_1) + \rho_2 \rho_3 (B_1)$$

Similarly,

$$U_3 = \rho_1 \rho_2 (U_2) + \rho_1 \tau_2 (B_2)$$

$$B_3 = \rho_3 \tau_2 (U_2) + \rho_2 \rho_3 (B_2)$$

and so on. Writing U and B in general form,

$$U_j = \sum_{j=2}^{\infty} \rho_1 \rho_2 (U_{j-1}) + \rho_1 \tau_2 (B_{j-1}) \quad 3.3.13$$

$$B_j = \sum_{j=2}^{\infty} \rho_3 \tau_2 (U_{j-1}) + \rho_2 \rho_3 (B_{j-1}) \quad 3.3.14$$

The sum of the intensities of all components incident on the middle glass multiplied by its absorbtivity gives

$$\alpha_{20F3} = (1 - \rho_2 - \tau_2) \left[\tau_1 + \rho_1 \rho_2 \tau_1 + \rho_3 \tau_1 \tau_2 + \sum_{j=2}^{\infty} U_{j-1} (\rho_1 \rho_2 + \rho_3 \tau_2) + B_{j-1} (\rho_2 \rho_3 + \rho_1 \tau_2) \right] \quad 3.3.15$$

3.4 Applicability of TAR Equations of Triple Glazing Window to Single and Double Glazing Windows

The transmissivity, reflectivity, and absorbtivity equations developed in the previous section for a triple glazing window are particularly convenient for use on the digital computers.

The equations are general in nature in the sense that they can be used for calculating the TAR of a single and (or) double glazing windows.

The following analysis demonstrate the applicability of the TAR equations for a double glazing window. The transmissivity equation for a double glazing window can be obtained by substituting $\tau_3=1$ and $\rho_3=0$ in equation 3.3.6

$$\begin{aligned} \tau_{12} &= \tau_1 \tau_2 + 1 \cdot \sum_{j=2}^{\infty} \rho_1 \tau_2 (R_{j-1}) + \rho_{2.0} (T_{j-1}) \\ &= \tau_1 \tau_2 + 1 \cdot \sum_{j=2}^{\infty} (R_{j-1}) \end{aligned}$$

Summing up from $j = 2$ to $j = 3$

$$\tau_{12} = \tau_1 \tau_2 + \rho_1 \rho_2 \tau_1 \tau_2 (1 + \rho_1 \rho_2 + \dots)$$

$$= \tau_1 \tau_2 \left[1 + \rho_1 \rho_2 + \rho_1^2 \rho_2^2 + \dots \right]$$

This is the sum of an infinite series. Hence can be written as

$$\tau_{12} = \tau_1 \tau_2 / (1 - \rho_1 \rho_2) \quad 3.4.1$$

Equation 3.4.1 is the equation for transmissivity of a double glazing window (23).

Similarly as an example the equation 3.3.9 can be reduced to determine the absorptivity of the first glass of a double glazing window.

Substituting $\tau_3 = 1$ and $\rho_3 = 0$ in equation 3.3.9

$$\alpha_{10F2} = (1 - \rho_1 - \tau_1) \left[1 + \rho_2 \tau_1 + \sum_{j=2}^{\infty} R_j \right]$$

Considering three terms of the series and substituting R_1 , R_2 , and R_3

$$= (1 - \rho_1 - \tau_1) [1 + \rho_2 \tau_1 + \rho_1 \rho_2 (\rho_2 \tau_1) + \dots]$$

$$= (1 - \rho_1 - \tau_1) [1 + \rho_2 \tau_1 (1 + \rho_1 \rho_2 + \rho_1^2 \rho_2^2 + \dots)]$$

$$\alpha_{1 \text{ of } 2} = (1 - \rho_1 - \tau_1) [1 - \rho_2 (\rho_1 - \tau_1)] / (1 - \rho_1 \rho_2) \quad 3.4.2$$

This is the equation for absorbtivity of the first glazing of a double glazed window (23).

Hence in general it can be shown that the recurrence equations for TAR of a triple glazing window can be used for double as well as single glazing windows.

To verify the accuracy of the recurrence formulae for different j values a simple arithmetic substitution was carried out. By considering the first two terms in the series the error in the calculated value of transmissivity was observed to be 1.3%. Addition of another term improved the accuracy to within 0.3%. Based on these observations a value of $j = 6$ was considered to be adequate. The TAR values obtained from the recurrence equations are accurate to third decimal place with those reported in the references (23,24).

3.5 Calculation of TAR for the Heat Absorbing Glass due to Direct Radiation

Unlike clear glass (less than 0.15% ferrous oxide), the heat absorbing glass may have 0.5% or more of ferrous oxide which accounts for most of absorption in the glass. The study of Dietz reported in reference (22) shows that the transmissivity of heat absorbing glass varies considerably with wavelength. Hence its effects cannot be neglected.

Therefore the transmittance of heat absorbing glass is a function of the spectral wavelength, the angle of

incidence, and the KL product of the glass. Neglecting the effects of longwave radiation, temperature, dust and dirt, the functional dependence of transmissivity can be written as,

$$\tau = f(\lambda, \theta, K, L) \quad 3.5.1$$

Mitalas (24) suggested a method of calculating the effective transmittance of window glass by dividing the solar spectrum (at air mass 2) into ten bands each containing 10% of solar energy. The present model is based on this technique. The advantage of the present model is that it is possible to combine a single heat absorbing glass in a single or double glazed windows for studying the effective window designs.

Generally the manufacturers provide the monochromatic spectral transmissivity of the glass at normal incidence. This serves as an input to the present model.

The technique of calculating the transmissivity of heat absorbing glass is one of transferring the characteristics from wavelength dependence to KL product dependence, and then integrating these values over the entire spectrum. The calculations involved are illustrated further.

The transmittance of glass at normal incidence was calculated for KL values ranging from 0.01 to 2.0 using equation 3.3.6. A polynomial function of third degree was found to approximate the above results.

$$\tau_n = 0.9047 - 0.8747(KL) + 0.3309(KL)^2 - 0.0512(KL)^3$$

3.5.2

A consideration into the input (monochromatic transmissivity) to the model and the polynomial equation 3.5.2 suggests that by dividing the solar spectrum into equal energy bands, the band transmissivity at normal incidence can be obtained. That is at each band wave lengths, the transmissivity of the glass was obtained by fitting a spline function to the input data.

From the band transmissivities it was possible to calculate the corresponding KL values from the polynomial equation 3.5.2. However, these band transmissivities correspond to normal incidence. From the equation for TAR given in section 3.3, the band transmissivity at any desired angle of incidence can be determined. Therefore a simple average of the band transmissivities gives the spectral or effective transmissivity.

The transmissivity of the heat absorbing glass obtained from the present model is accurate to second decimal point with that reported in reference (24). Typically the transmissivity of heat absorbing glass will be of the order of 0.20 to 0.40 and its absorptivity of the order of 0.60 to 0.80.

3.6 Calculation of TAR due to Diffuse Radiation

In the preceding sections it was shown that the transmissivity of the glass is a function of angle of incidence of direct radiation and the KL product of the glass. It should be recognized that the sky diffuse radiation comes from all parts of the sky.

The transmittance of diffuse radiation is studied by Parmelee (23), Mitalas and Stephenson (24), and Puri (27). Puri's model accounts for isotropy as well as anisotropy of diffuse radiation. Anisotropy of the diffuse radiation introduces further problems. However by assuming the sky diffuse radiation to be isotropic, Parmelee (23) suggested a graphical integration technique to determine the transmissivity of the glass due to diffuse radiation. The present study extends the applicability of the Parmelee's technique for up to triple glazing.

From figure 3.3 the energy received by a vertical window dq is given by

$$dq = I_d dA_1 \cos i dw$$

The solid angle is given by

$$dw = dA_2 / r^2$$

From the geometry of figure 3.3 dA_2 can be written as

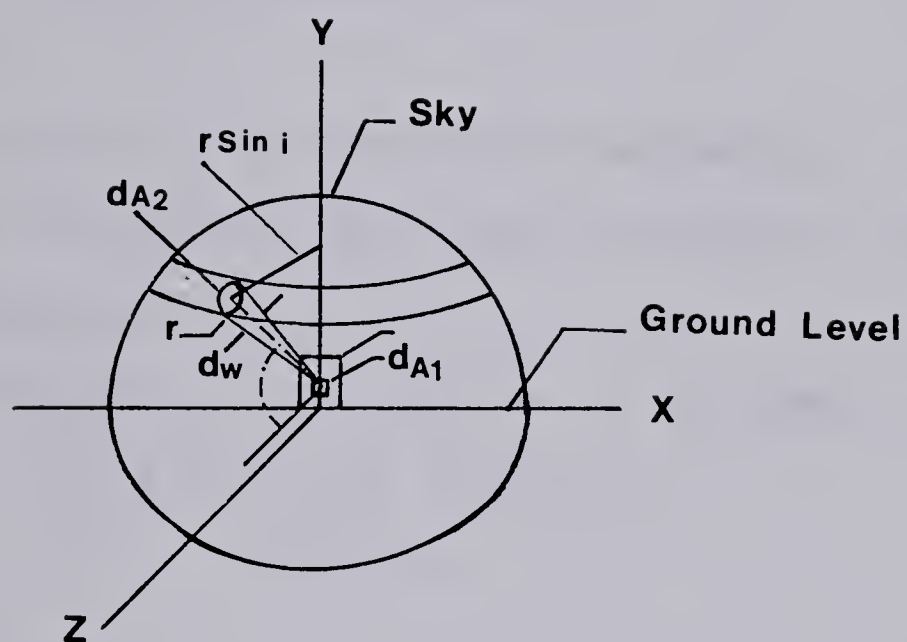


Figure 3.3 Geometry of diffuse radiation on a vertical window.

$$dA_z = \pi(r \sin i) (r di)$$

The unit energy received by the window then becomes

$$dq/dA_1 = dE_s = I_d \cos i \pi (r \sin i) (r di)/r^2$$

$$dE_s = \pi I_d \sin(2i) di$$

The fraction of the radiation reflected r is the sum of the energy reflected at each angle divided by the total incident radiation.

Therefore integrating over quarter of the sky

$$r_s = \frac{\int_0^{\pi/2} 0.5 \pi I_d r(i) \sin(2i) di}{0.5 \pi I_d}$$

$$r_s = \int_0^{\pi/2} r(i) \sin(2i) di \quad 3.6.1$$

Similarly the fraction absorbed due to sky diffuse radiation 'as' can be written as

$$a_s = \int_0^{\pi/2} e^{-KL/\sqrt{1-\sin^2 i/n^2}} [\sin(2i) di] \quad 3.6.2$$

Two separate transmissivities have to be computed (one for parallel and another for perpendicular component of radiation) using the TAR equations derived in section 3.3. A simple average will give the effective transmissivity due to

sky diffuse radiation. The same procedure is applicable for calculating the absorptivity due to sky diffuse radiation.

The diffuse transmissivity computed by the present model is accurate to second decimal place with that reported in reference (23). However, the predicted values are primarily based on the assumption that the sky diffuse radiation is isotropic. The errors introduced due to such an assumption may not be large.

3.7 Total Radiation on a Tilted Surface

The present model utilizes the hourly insolation on the horizontal surfaces. But in the thermal model the irradiation of vertical and (or) tilted surfaces is required. Several authors have developed analytical models to estimate the total radiation on a tilted surface.

Liu and Jordan's model (28) is perhaps the simplest. It assumes that the sky diffuse radiation is isotropic and introduces a view factor to account for the tilted surfaces. Parmelee (29), and Threlkeld's (30) experimental investigation suggests the non-isotropic nature of the diffuse radiation. Puri (31) has developed a model considering the diffuse radiation to be partly isotropic and partly non-isotropic.

Several other researchers have studied the relationship between the diffuse and total radiation. Among them Ruth and Chant (32), Pereira and Rabl (33), and Hay (34) have

proposed corrections to Liu and Jordan's model. Wesely and Lipschutz (35) have reported a method of estimating hourly average diffuse and direct radiation under scattered clouds. Nicholas and Child (36) have published the solar radiation charts. All the above studies are primarily concerned with shortwave radiation. However, Cole (37) suggests the errors involved in neglecting the longwave radiation effects. The study of Dave (38) shows the errors involved in isotropic distribution approximations.

Therefore estimation of total radiation on tilted surfaces is a matter of continuous research. From the literature survey, a combination of the above methods was adopted for the present study.

The magnitude of diffuse radiation estimated by Liu and Jordan's method for a tilted surface is somewhat underestimated (34). It was observed that for a vertical surface, the H_{dt} calculated by Liu and Jordan's method was 12-15% less than that obtained by Threlkeld's method. The difference was consistent. Due to this fact the diffuse radiation on a tilted surface calculated by Liu and Jordan's method was multiplied by a factor of 1.12.

There is no justification to this approach, but it is believed that introduction of factor like 1.12 is never likely to overestimate the diffuse radiation component.

Derived Solar Angles

For a particular surface orientation, the sun's incidence angle θ , altitude β , azimuth angle SAZ , can be derived

from three basic angles: namely, latitude(θ), hour angle (w) and declination (δ).

$$\delta = 23.45 \sin [360(284 + n / 365)] \quad 3.7.8$$

where n is the day of the year.

The hour angle w is given by .

$$w = (12.0 - S_n) \times 15.0 \quad \text{degrees} \quad 3.7.2$$

where

$$S_n = ET - 1/15 (L_s - L_g) + 12.0$$

The Sun's altitude β , solar azimuth SAZ, effective azimuth EAZ and the incident angle θ were calculated using the following equations.

$$\sin \beta = \cos \theta \cos w \cos \delta + \sin \theta \sin \delta \quad 3.7.3$$

$$\sin (\text{SAZ}) = \cos \delta \sin w / \cos \beta \quad 3.7.4$$

$$\text{EAZ} = \text{SAZ} \pm \text{HOA} \quad 3.7.5$$

$$\cos \theta = \cos \beta \cos (\text{EAZ}) \cos S + \sin \beta \sin S \quad 3.7.6$$

Neglecting longwave radiation the total radiation on a tilted surface is therefore

$$H_T = H_{b_T} + H_{d_T} + H_{r_T} \quad 3.7.7$$

Hay (34) showed that the total radiation H on a horizontal surface can be split into beam and diffuse components with the following ratios:

$$\frac{H'}{H_o} = \frac{H (1 - \rho\beta)}{H_o} \quad 3.7.8$$

where

$$\beta = 0.6C + (1-C) (0.25)$$

and

$$\begin{aligned} H_d' / H' = & 1.0408 - 0.7016 (H' / H_o) - 4.4329 (H' / H_o)^2 \\ & + 6.5059 (H' / H_o)^3 - 2.2752 (H' / H_o)^5 \end{aligned} \quad 3.7.9$$

$$\frac{H_d'}{H'} = \frac{H_d - H}{H(1 - \rho\beta)} \quad 3.7.10$$

From the above equation H_d on a horizontal surface was calculated.

Therefore

$$H_b = H - H_d \quad 3.7.11$$

The extraterrestrial radiation H_o was calculated by using the equation

$$H_o = I_{sc} [1 + 0.033 \cos (360n/365)] \sin \beta \quad 3.7.12$$

The magnitude of beam radiation on the tilted surface was estimated as follows.

From figure 3.4 R_b can be written as,

$$R_b = \cos \theta / \cos \theta_z$$

OR

$$R_b = \cos \theta / \sin \beta$$

Therefore

$$H_{b_T} = H_b (R_b) \quad 3.7.13$$

From Liu and Jordan's (28) model

$$H_{d_T} = H_d (1 + \cos S / 2) \quad 3.7.14$$

and

$$H_{r_T} = H_r (1 - \cos S / 2) \quad 3.7.15$$

therefore

$$H_T = H_b (R_b) + H_d (1 + \cos S/2) + H_r (1 - \cos S/2) \quad 3.7.16$$

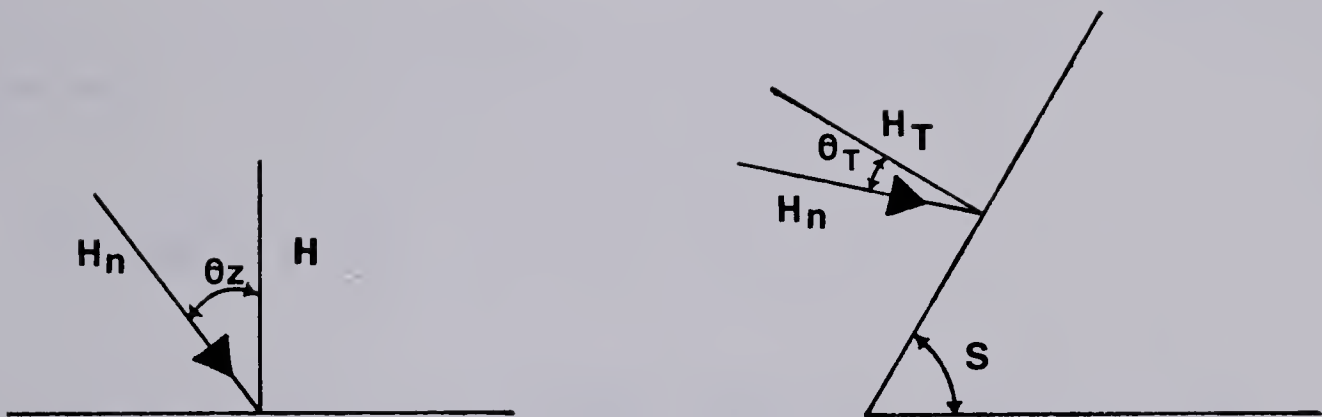


Figure 3.4 Radiation on a horizontal and tilted surface.

For a vertical surface Threlkeld's function for estimating H_{dv} was employed

Threlkeld showed that for $\cos\theta > -0.2$

$$H_{dv}/H_d = 0.55 + 0.437 (\cos\theta + 0.313 \cos^2\theta)$$

3.7.17

otherwise

$$H_{dv}/H_d = 0.45$$

For surfaces which are tilted, the total radiation was estimated using Liu & Jordan's equation but with a correction factor of 1.12

$$H_T = H_b (R_b) + 1.12 H_d (1 + \cos S/2) + H_p (1 - \cos S/2)$$

3.7.18

3.8 Equations for Sunlit Fraction of Window due to Direct and Diffuse Radiation

An obvious, but important problem in solar heat gain calculations, is determining the sunlit fraction of a surface.

A typical problem arises when architectural projections like solid overhangs are to be designed. Monthly average solar radiation on a shaded surface is studied by Utzinger and Klein (39). For the present study a general case as

shown in figure 3.5 was considered. The sunlit fraction (of the window) due to direct radiation was calculated at each hour angle from the geometry of the overhang and the sun's position in the sky.

Similarly, the overhang partially shades the diffuse radiation. Applying the same analogy another equation for sunlit fraction due to diffuse radiation was developed. The applicability of these equations to a more familiar geometry like a vertical window is demonstrated.

From figure 3.5 it follows that,

$$\frac{X}{\sin \beta} = \frac{F}{\sin(\beta + S)}$$

The sunlit fraction due to beam radiation is the ratio of the net sunlit area to the total area of the surface.

Therefore

$$F_b = \frac{X}{H_w / \sin(S)} \quad 3.8.1$$

Where

$$X = F \sin \beta / \cos \beta \quad \text{for a vertical surface.}$$

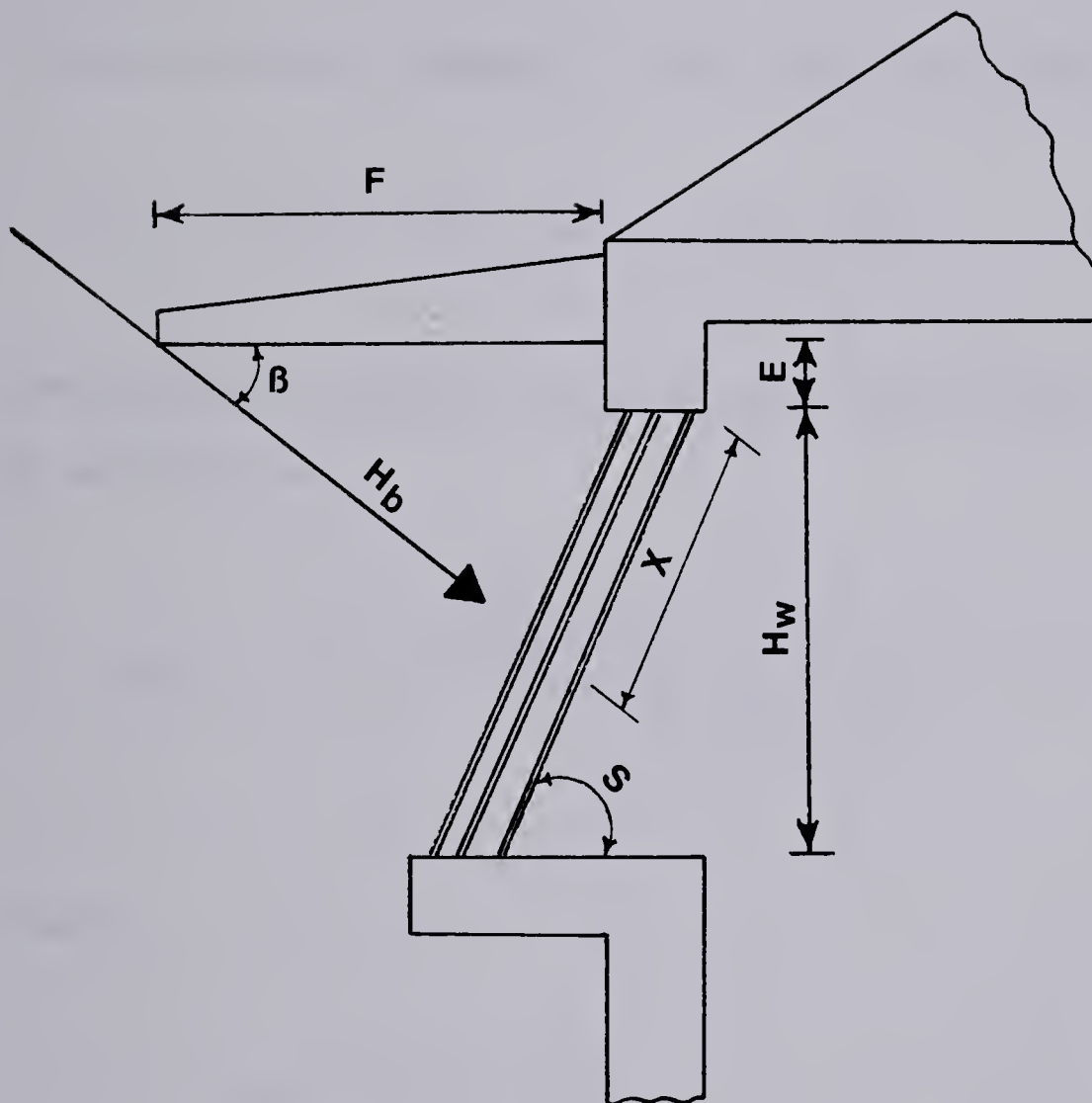


Figure 3.5 Shading of a sloping window from direct solar radiation by a solid overhang

The general equation for F_b is

$$F_b = \frac{F \sin \beta}{\sin(\beta + S)} - \frac{E}{\sin S} \bigg/ (Hw / \sin S) \quad 3.8.2$$

For a vertical window $S = 90^\circ$, and therefore F_b reduces to

$$F_b = [(F) \tan \beta - E] / Hw \quad 3.8.3$$

Similarly the sunlit fraction due to diffuse radiation can be written as

$$F_d = 1 - \left(1 - \frac{\sqrt{(Lw \sin S + E)^2 + F^2} - F}{Lw \sin S + E} \right) \quad 3.8.4$$

Where

$$Lw \sin(S) = Hw$$

For a vertical window and with no overhang ($S = 90^\circ$, $F = 0$)

$$F_d = 1 - \left(1 - \frac{\sqrt{Lw^2}}{Lw} \right) = 1 \quad 3.8.5$$

3.9 Solar Heat Gain Calculation

By definition solar heat gain is the sum of the radiation transmitted and the inward flow of heat transferred due to radiation absorbed by the glass.

$$\begin{array}{rcl} \text{Solar heat} & & \text{Radiation transmitted} \\ \text{gain} & = & \text{through the glass} \quad + \quad \text{Inward flow of the} \\ & & \text{absorbed radiation} \end{array}$$

In general for a triple glazing window

$$FS = H_b \tau (\tau_b + N_i \alpha_b) + H_d \tau (\tau_d + N_i \alpha_d) \quad 3.9.1$$

Where N_i is the fraction of the absorbed radiation transferred to the inside of building .

For the direct beam component, we can write

$$\begin{aligned} FS_b = H_b \tau (\tau_b) + N_{io} (\alpha_{bo} I_o) + N_{im} (\alpha_{bm} I_m) \\ + N_{ii} (\alpha_{bi} I_i) \end{aligned} \quad 3.9.2$$

Rewriting in a simplified form

$$FS_b = F_{cb} (H_b \tau) \quad 3.9.3$$

Where

$$F_{cb} = \tau_b + U \alpha_{bo} / h_o + U (1/h_o + 1/h_1) \alpha_{bm} \\ + U (1/h_o + 1/h_1 + 1/h_2) \alpha_{bi} \quad 3.9.4$$

And U is the overall heat transfer coefficient of the window given by

$$U = \frac{1}{1/h_o + 1/h_1 + 1/h_2 + 1/h_i + L_o/k_{go} + L_m/k_{gm} + L_i/k_{gi}} \quad 3.9.5$$

In which

h is the overall heat transfer coefficient

L is the thickness of the glass

Kg conductivity of the glass

In the above equations the following characters denote:

- 1 first air space
- 2 second air space
- o outer glass
- m middle glass
- i inside glass

Similarly the solar heat gain due to diffuse radiation can be written as

$$F_{Sd} = F_{cd} (H_d \tau) \quad 3.9.6$$

Where

$$F_{cd} = \tau_d + U \propto d_o / h_o + U (1/h_o + 1/h_1) \propto d_m \\ + U (1/h_o + 1/h_1 + 1/h_2) \propto d_i \quad 3.9.7$$

Total solar heat gain is given by

$$F_S = F_{Sb} + F_{Sd} \quad 3.9.8$$

4. THE THERMAL MODEL OF HOUSE

4.1 Introduction

The problem of energy balance of a house is one of balancing the various heat gains and heat losses taking place in and around the house. In figure 4.1 the heat gains and the heat losses through the various elements of the house are shown.

To study the transient behaviour of a house, the effects of different thermal elements of the house were compounded. The problem then reduced to one of solving transient heat equation expressing an energy balance in the house.

Knowledge of conductances of the different elements together with heat sources and ambient air temperatures are sufficient to solve these equations. The procedure is illustrated in the sections to follow.

4.2 Heat Loss through the Exterior Enclosure Elements

Gilpin 1977 (40) employed the technique of classifying the elements of the thermal enclosure into two types, resistive and capacitive. Employing the same technique of classifying the enclosure elements, a thermal net work of energy fluxes, figure 4.2, of a house was constructed. Each of these exterior element see's a different temperature. This temperature is characterized by the orientation of the element and is commonly referred to as SOL-AIR temperature.

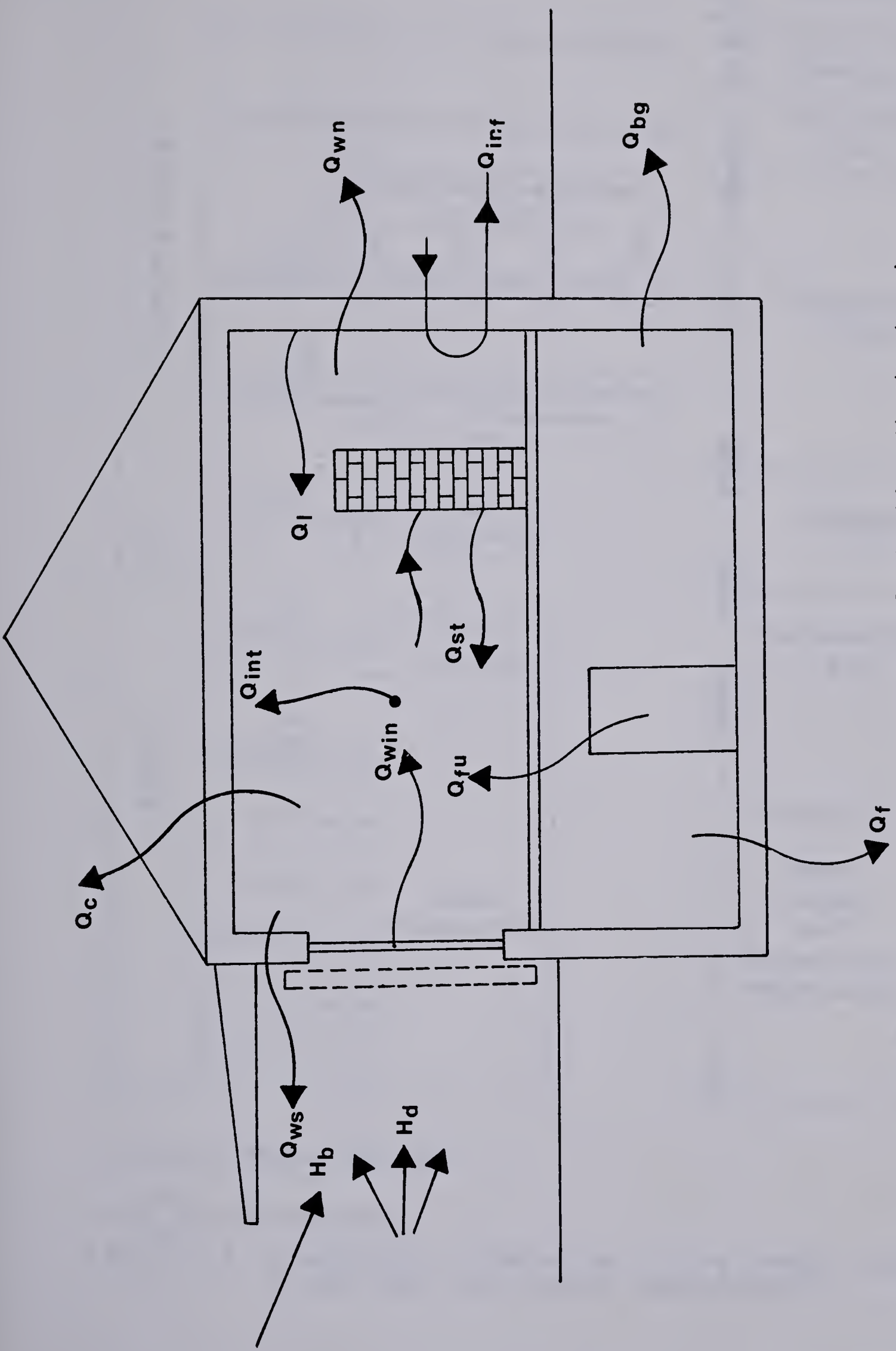


Figure 4.1 Schematic of a house illustrating the heat gains and the heat losses.

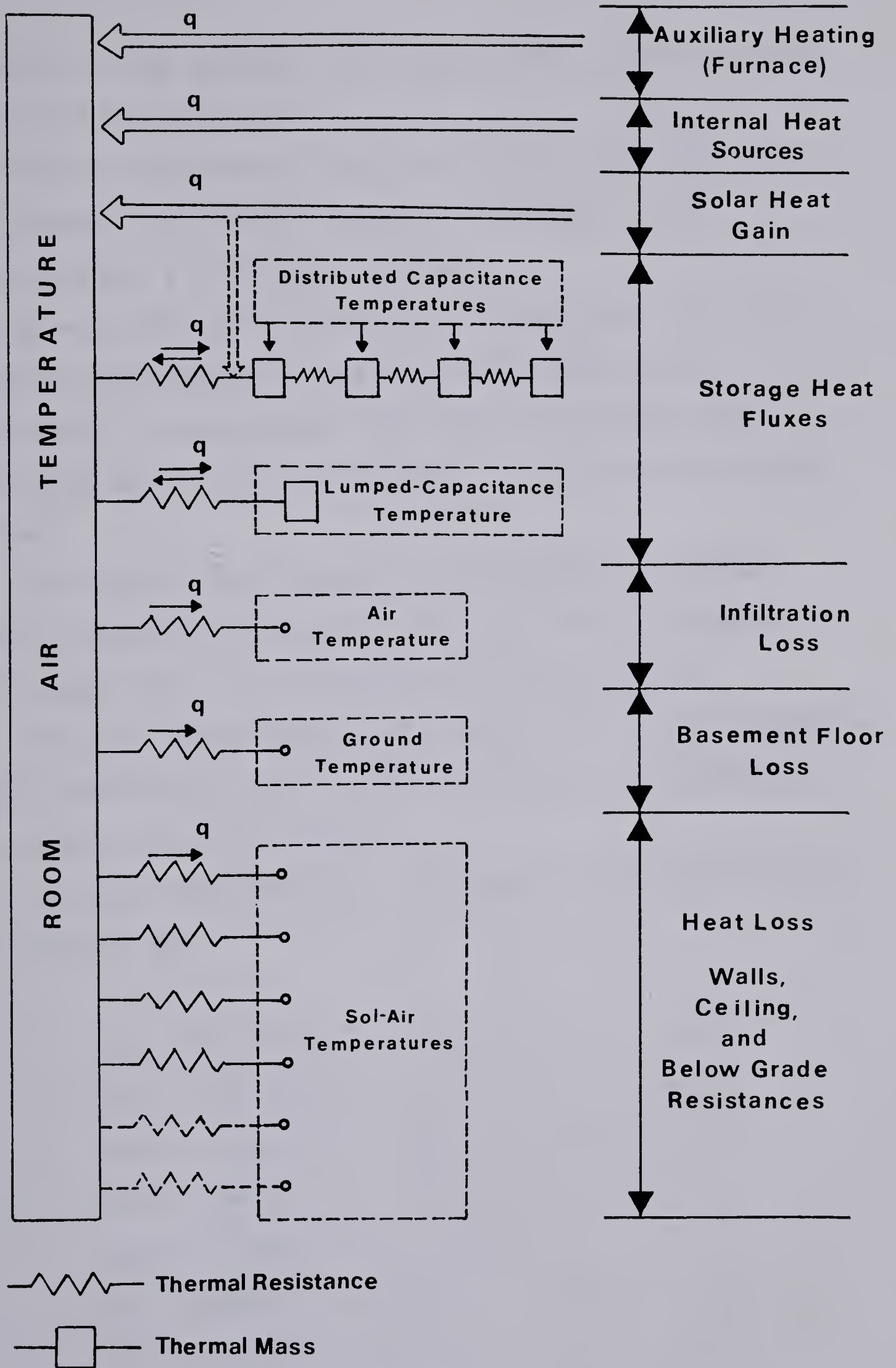


Figure 4.2 A schematic illustration of the energy fluxes to and from the room air temperature.

Therefore it was assumed that a North wall would lose heat to SAT (North) and so on.

The roof and the ceiling resistances were combined. It was assumed that the ceiling would lose heat to SAT calculated for a horizontal surface.

By employing the technique of Boileau and Latta (41), the heat loss through the below grade elements was calculated. It was assumed that the below grade elements would lose heat to SAT calculated for a horizontal ground surface.

For calculating the heat loss through the basement floor a reasonable assumption was made that the basement floor loses heat to an average ground temperature.

The wood frame type of wall construction was treated as purely resistive in nature and the capacity introduced by the plaster board was lumped.

The heat loss equations, through each of the elements were written as

$$Q_{wn} = A_{wn}/R_{wn} (T_r - SAT_n) \quad 4.2.1$$

$$Q_{ws} = A_{ws}/R_{ws} (T_r - SAT_s) \quad 4.2.2$$

$$Q_{we} = A_{we}/R_{we} (T_r - SAT_e) \quad 4.2.3$$

$$Q_{ww} = A_{ww}/R_{ww} (T_r - SAT_w) \quad 4.2.4$$

$$Q_{bg} = \sum A_{bg}/R_{bg} (T_r - SAT_c) \quad 4.2.5$$

$$Q_c = A_c/R_c (T_r - SAT_c) \quad 4.2.6$$

$$Q_f = A_f/R_f (T_r - T_g) \quad 4.2.7$$

The net heat gain through the window is the sum of the solar heat gain and the heat loss or gain through the window due to indoor, outdoor temperature difference.

$$Q_{wi} = F_s + A_{wi}/R_{wi} (T_r - T_a) \quad 4.2.8$$

The lumped capacity was treated by equating the convection heat loss from the body to the decrease in the internal energy of the body. Thus

$$hA_L (T_L - T_r) = - c\rho V (dT/dt)$$

Rearranging

$$dT/dt = -hA_L / c\rho V (T_L - T_r) \quad 4.2.9$$

The term $c\rho V/hA_L$ is called the time constant of the lumped capacitance. This was calculated from the properties of the plaster board. The heat transfer coefficient in equation 4.2.9 accounts for heat transfer due to convection as well as radiation.

The time derivative was approximated employing Euler's method.

$$T_L^{v+1} = T_L^v + dT/dt|_v \Delta t$$

Hence

$$\frac{T_L^{v+1} - T_L^v}{\Delta t} = - \frac{h A_L}{\rho c V} (T_L^v - T_r^v)$$

Denoting $\rho c V / h A_L$ by RC and Δt by dt the equation for temperature T^{v+1} at some later point in time t^{v+1} becomes

$$T_L^{v+1} = T_L^v + dt/RC (T_L^v - T_r^v) \quad 4.2.10$$

4.3 Dynamics of the Thermal Mass

The thick mass walls were treated with a distributive capacitance approach. The effect of storage was included in the model to examine the diurnal swings of temperature. It should be realised that because of the capacitive nature of the thick mass wall the temperature and the heat flow into the mass wall are not in phase. All temperatures lag behind the heat inputs.

To model the dynamics of the mass wall a finite difference calculation was used. The mass wall was divided into 1/2 inch thick layers and the temperatures at the nodal points were recalculated for each time step. To ensure stability and accuracy, a time step of 3 minutes was required for the finite difference calculations. The differential equation together with the boundary conditions and the finite difference solution scheme are presented

below:

The transient behaviour of a finite thickness of slab such as the mass wall in this case can be studied by the one dimensional transient, parabolic heat conduction equation:

$$\frac{\partial T}{\partial t} = \alpha \frac{\partial^2 T}{\partial x^2} \quad 4.3.1$$

Subject to boundary conditions

$$dT/dt = 0 \quad \text{at } x = L/2 \quad 4.3.2$$

$$T = T_r \quad \text{at } x = 0 \quad 4.3.3$$

and the initial condition

$$T = T_{min} \quad \text{at } t = 0 \quad 4.3.4$$

Where $\alpha = k/\rho c$ is the thermal diffusivity of the material. One half of the mass wall was considered due to symmetry of the problem.

Dividing the mass wall into M layers of thickness Δx as shown in figure 4.3 an energy balance for each of the nodes was written.

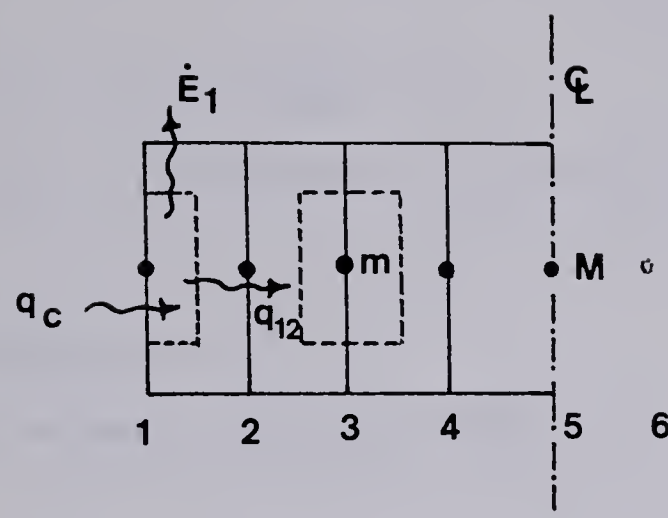


Figure 4.3 Nodal-point arrangement for thermal mass wall.

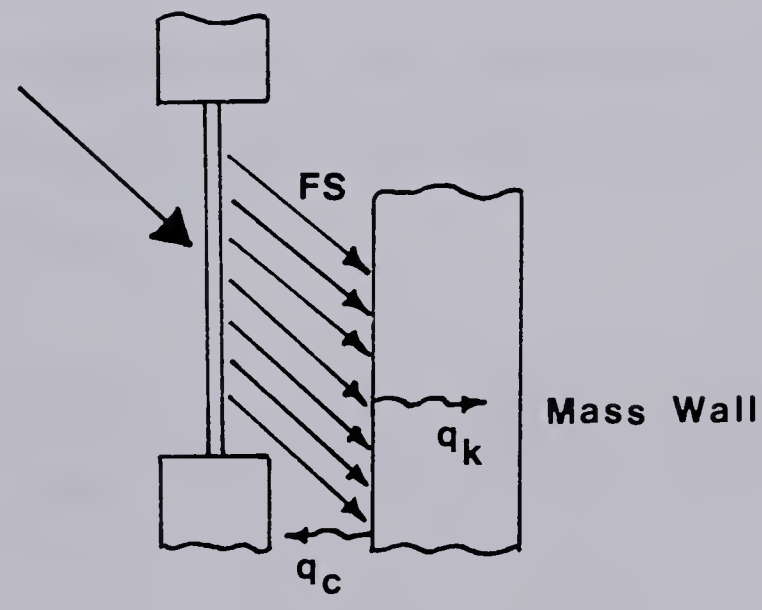


Figure 4.4 Energy balance on Trombe type storage wall

This gives a set of finite difference equations.

Let Δt = time step in t
 Δx = thickness of each layer.

For first node $m = 1$:

The energy balance may be written as

$$q = q_{1,2} + \dot{E}_1$$

writing in terms of rate equations

$$h A_s (T_r - T_1) = \frac{kA}{\Delta x} (T_1 - T_2) + \rho c A \frac{\Delta x}{2} \frac{dT_1}{dt}$$

Applying Euler's method for approximating the time derivative and rearranging, the temperature T_1 at a new time step can be written as

$$T_1^{y+1} = T_1^y + \frac{2h\Delta t}{\rho c \Delta x} (T_r^y - T_1^y) - \frac{2k\Delta t}{\rho c \Delta x^2} (T_1^y - T_2^y) \quad 4.3.5$$

For nodes $m = 2$ to $M - 1$:

For the central nodes, using the mathematical formulation of finite difference equation in space coordinates, the equation for temperature distribution can be written as

$$\frac{dT_m}{dt} = \propto \frac{(T_{m-1} - 2T_m + T_{m+1}))}{\Delta x^2}$$

Forming an explicit equation for T_m to move ahead in time:

$$T_m^{y+1} = \frac{k \Delta t}{\rho C \Delta x^2} (T_{m-1}^y - 2T_m^y + T_{m+1}^y) \quad 4.3.6$$

For last node $m = M$:

The boundary condition $dT/dx = 0$ can be written in terms of difference equation as

$$\frac{T_{M+1} - T_{M-1}}{(2 \Delta x)} = 0$$

$$T_{M+1} = T_{M-1} \quad 4.3.7$$

Hence equations 4.3.5 through 4.3.7 can be solved simultaneously to determine the surface temperature of the storage wall.

In modelling the Trombe type of storage wall, the procedure essentially remains the same. One of the boundary condition now has to be modified to the fact that the storage wall is oriented to receive the solar heat gain.

From figure 4.4 the energy balance can be written as

$$FS - q_c - q_k + E = 0 \quad 4.3.8$$

Writing in terms of rate equations

$$h A_s (T_s - T_r) = -\frac{kA}{\Delta x} (T_1 - T_2) - \rho c A \frac{\Delta x}{2} \frac{dT_s}{dt} + FS$$

Approximating the time derivative and rearranging

$$T_s^{y+1} = T_s^y - \frac{2h\Delta t}{\rho c \Delta x} (T_s^y - T_r^y) - \frac{2k\Delta t}{\rho c \Delta x^2} (T_1^y - T_2^y) + \frac{2 FS \Delta t}{\rho c A \Delta x} \quad 4.3.9$$

To study the dynamics of the Trombe type of storage wall the equation 4.3.9 together with equations 4.3.6 and 4.3.7 have to be solved simultaneously moving ahead in time.

It can be seen that the heat flows, into and (or) out of the mass wall at each time step. This means that the temperatures and the heat balance calculations are to be recalculated at each time step.

4.4 Infiltration Heat Loss

A great deal of uncertainty exists in handling the infiltration heat loss term. To date, there is no reliable data which can be employed with confidence in the simulation studies. Konard's (1) model for calculating the infiltration rate is too complex. For instance Konard assumes for a limited building configurations a leakage opening represented by several equally spaced holes, and the mass flow through the holes is computed. The accuracy of this model is yet to be established. A simple and yet reasonably accurate method of modelling the infiltration heat loss have to be investigated.

However, for the present study a simple approach was employed in that a fixed number of air changes per hour were assumed to occur. The average air change rates measured by Dale et al. (42) on the experimental solar test modules built at The University of Alberta, were used. This air change rate is based on the total volume of the house that is including the below grade volume. The heat loss due to an air change rate of R is given by

$$Q_{inf} = \rho c V R (T_r - T_a) \quad 4.4.1$$

4.5 The Energy Balance

Thus far the heat gains, the heat losses and the storages occurring in the model have been described. It is a matter of interest to balance the gains and the losses along

with the storages. The parameters of interest are the room temperature and the yearly auxiliary heat requirement of the house. The yearly auxiliary heat is the sum of the furnace heat at each fractional time step to keep the house at a minimum temperature of 65°F. The upper limit of room temperature was set at 75°F. Temperatures beyond the maximum limit were recorded as hours of overheating. Figure 4.2 is a schematic illustration of the energy fluxes to and from the room air temperature.

The energy balance equation can be written as

$$\begin{aligned}
 Q_{wi} + Q_{int} + Q_{fu} + (Q_{st} + Q_{st} + Q) - Q_{wa} \\
 - Q_c - Q_{inf} - Q_{bg} - Q_f = 0
 \end{aligned}
 \quad 4.5.1$$

Expanding the above terms

$$\begin{aligned}
 Q_{wi} + Q_{int} + Q_{fu} + \frac{A_{st}}{R_{st}} (T_{st} - T_r) - \frac{A_{wa}}{R_{wa}} (T_r - SAT) \\
 - \frac{A_{wi}}{R_{wi}} (T_r - T_a) - \frac{A_c}{R_c} (T_r - SAT_c) \\
 - \rho_c V R (T_r - T_a) - \frac{A_g}{R_g} (T_r - T_g) = 0
 \end{aligned}$$

4.5.2

Rewriting

$$\begin{aligned}
 Q_{wi} + Q_{int} + Q_{fu} + & \left(\frac{A_{st}}{R_{st}} T_{st} + \frac{A_{wa}}{R_{wa}} SAT \right. \\
 & + \frac{A_c}{R_c} SAT_c + \frac{A_g}{R_g} T_g \left. \right) \\
 & + \left(\rho_{cVR} + \frac{A_{wi}}{R_{wi}} \right) T_a = C_3(T_r)
 \end{aligned}$$

4.5.3

$$\text{Let } C_3 = \left(\frac{A_{st}}{R_{st}} T_{st} + \frac{A_{wa}}{R_{wa}} SAT + \frac{A_c}{R_c} SAT_c + \frac{A_g}{R_g} T_g \right)$$

$$+ \left(\rho_{cVR} + \frac{A_{wi}}{R_{wi}} \right) T_a$$

and

$$C_2 = \left(\frac{A_{st}}{R_{st}} + \frac{A_{wa}}{R_{wa}} + \frac{A_{wi}}{R_{wi}} + \frac{A_c}{R_c} + \rho_{cVR} + \frac{A_g}{R_g} \right) \quad 4.5.4$$

Rearranging equation 4.5.5

$$T_r = \frac{Q_{wi} + Q_{int} + Q_{fu} + C_3}{C_2} \quad 4.5.5$$

The model handles three possibilities concerning the window shutter system. Therefore the calculation of the yearly auxiliary heat requirement differs in each case. The solution scheme is illustrated in the flow charts 4.5 through 4.7. A complete thermal analysis from the model would include month by month analysis for one year, together with yearly totals. As an illustration a sample computer print out for the month of January is shown in Appendix A-4.

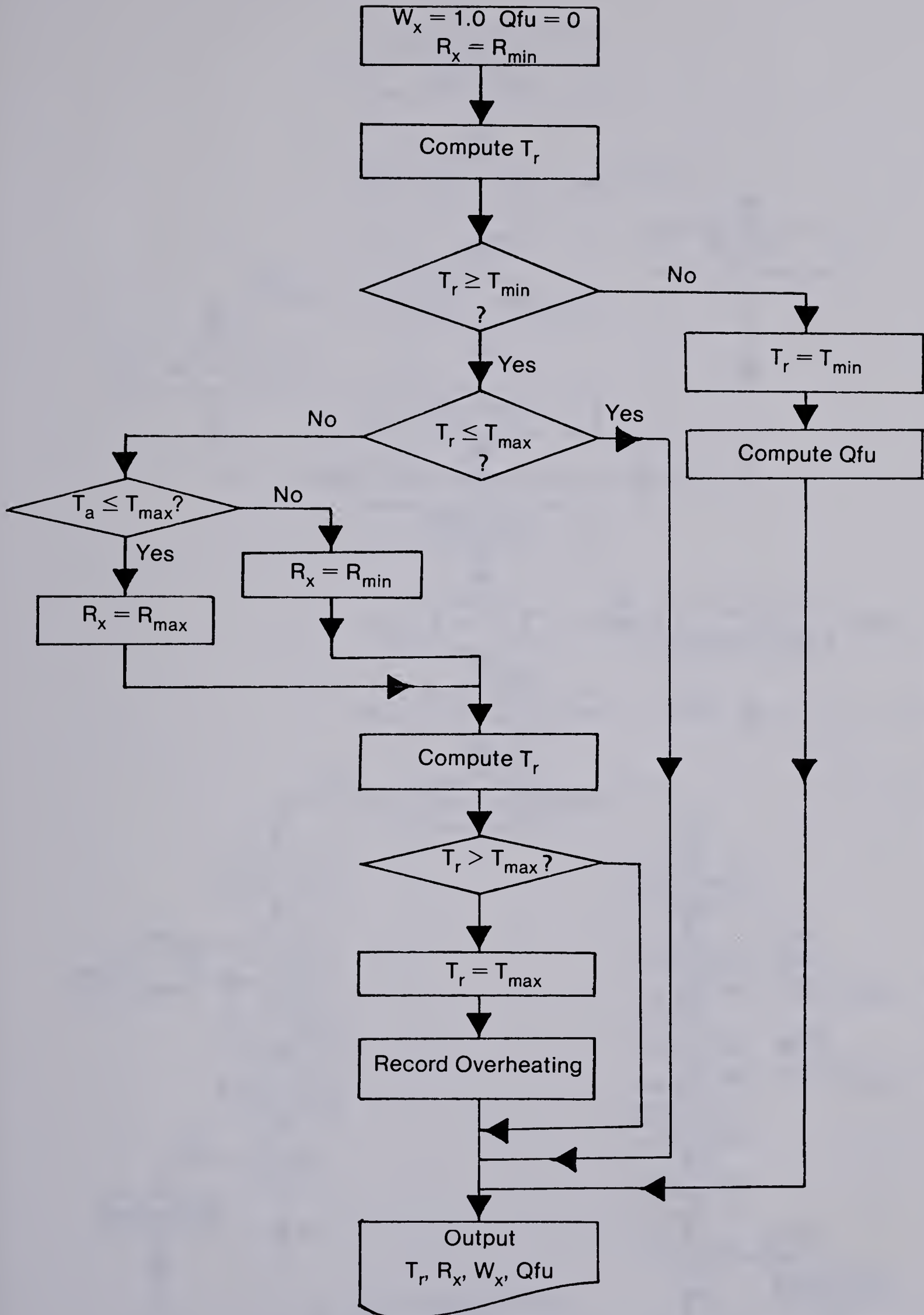


Figure 4.5 Flow chart illustrating the solution scheme with no shutters.

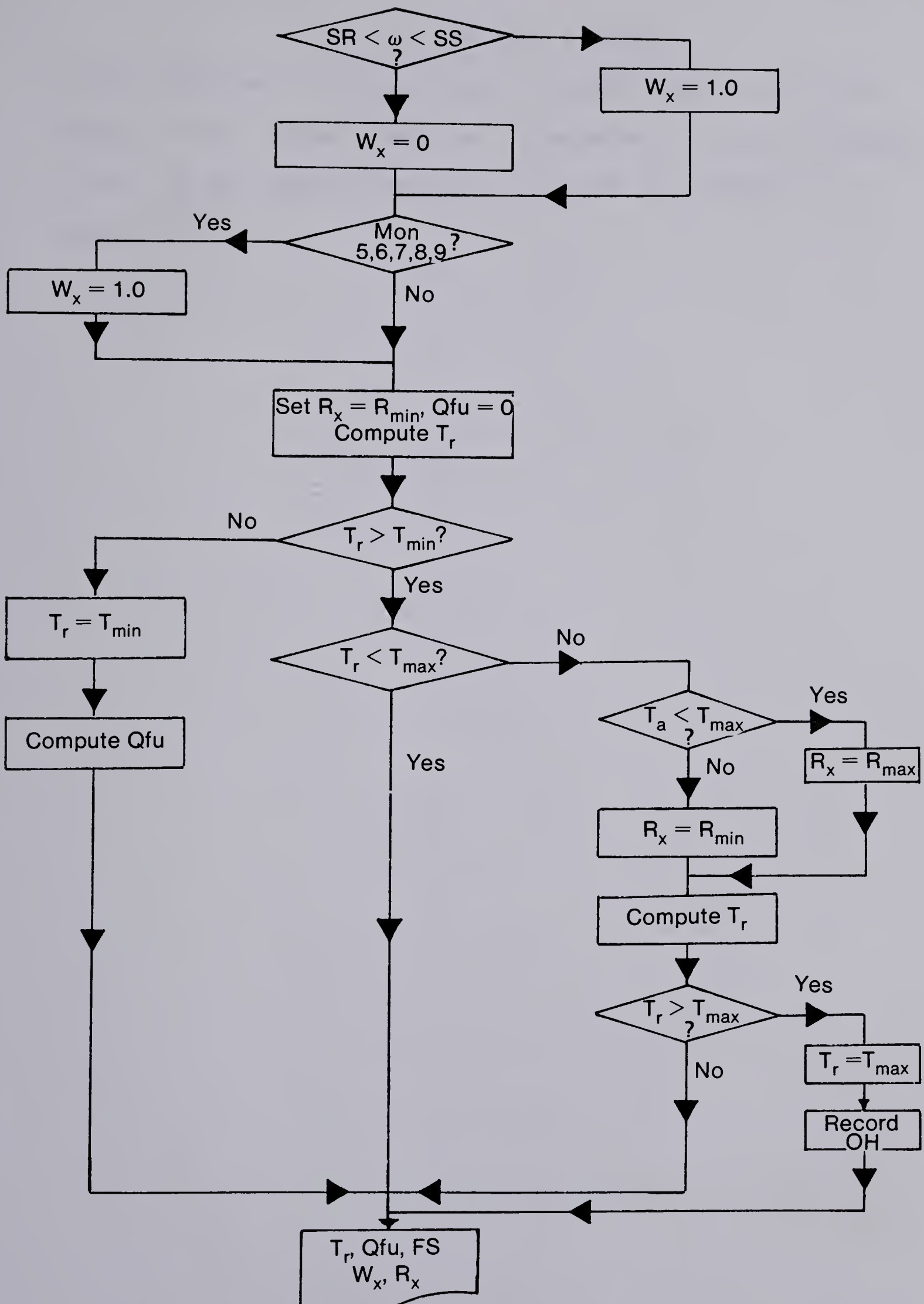


Figure 4.7 Flow chart illustrating the solution scheme with manual shutters.

5. THE COMPUTER PROGRAM

In this section the flow charts illustrating the solution scheme of the thermal model are presented. The main program as well as the subroutines are depicted in figures 5.1 through 5.9

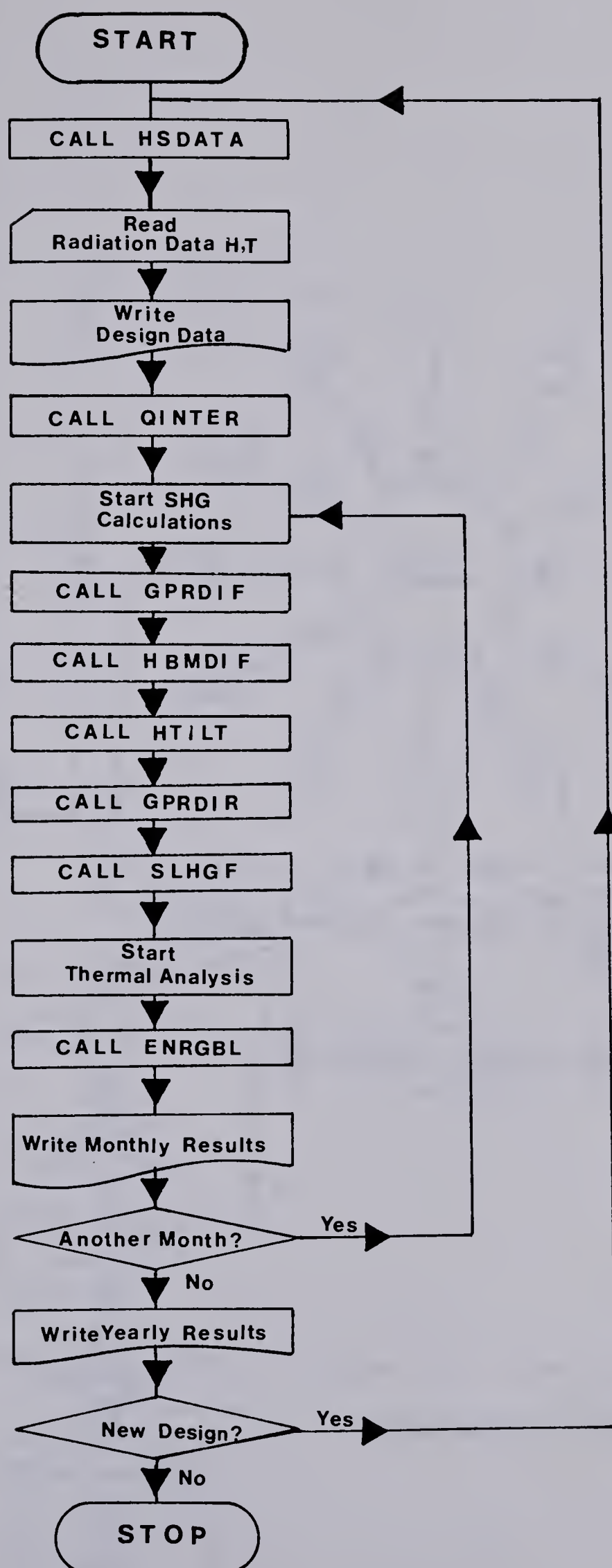


Figure 5.1 Overall flow chart for the main program.

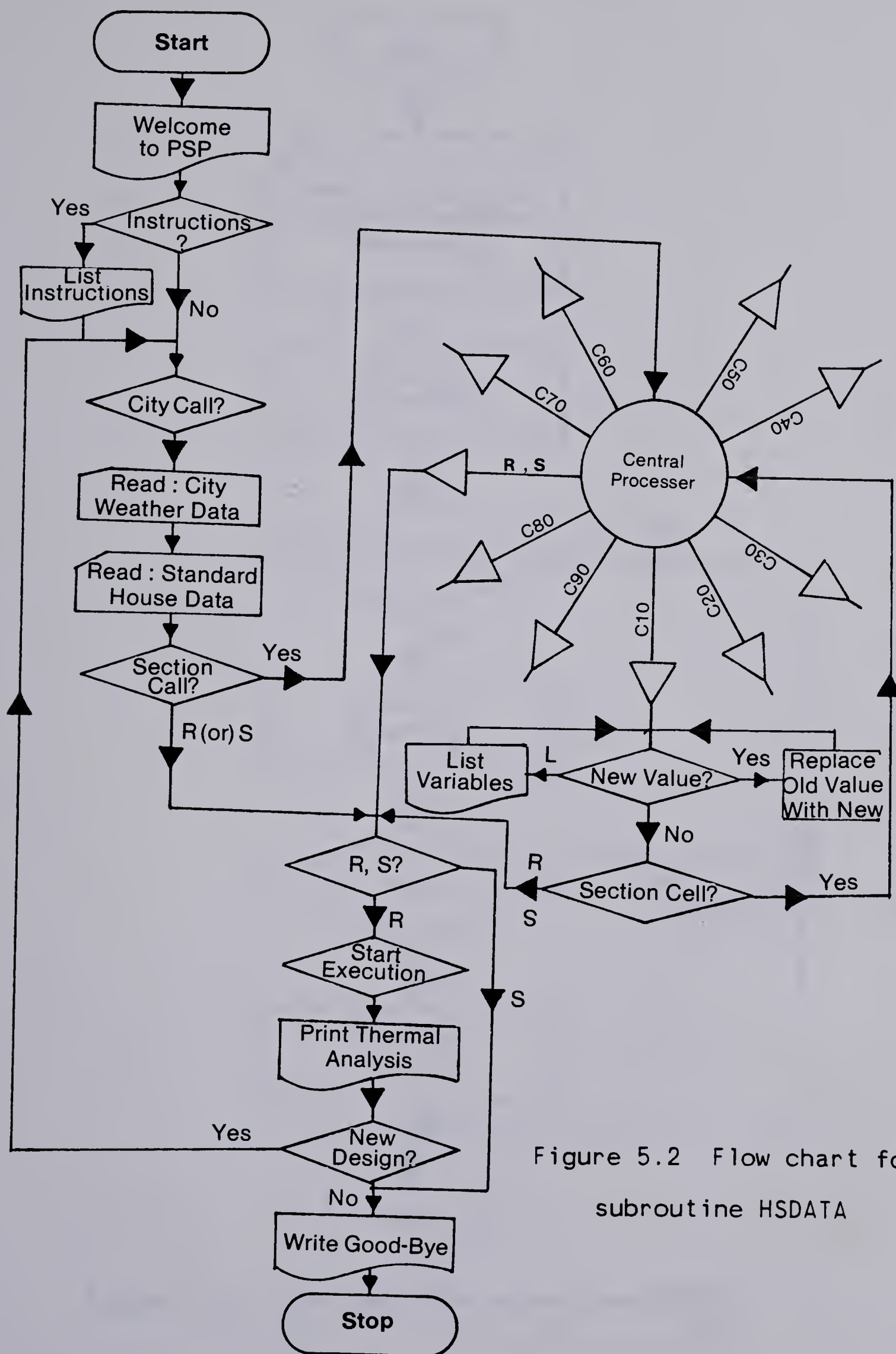


Figure 5.2 Flow chart for
subroutine HSDATA

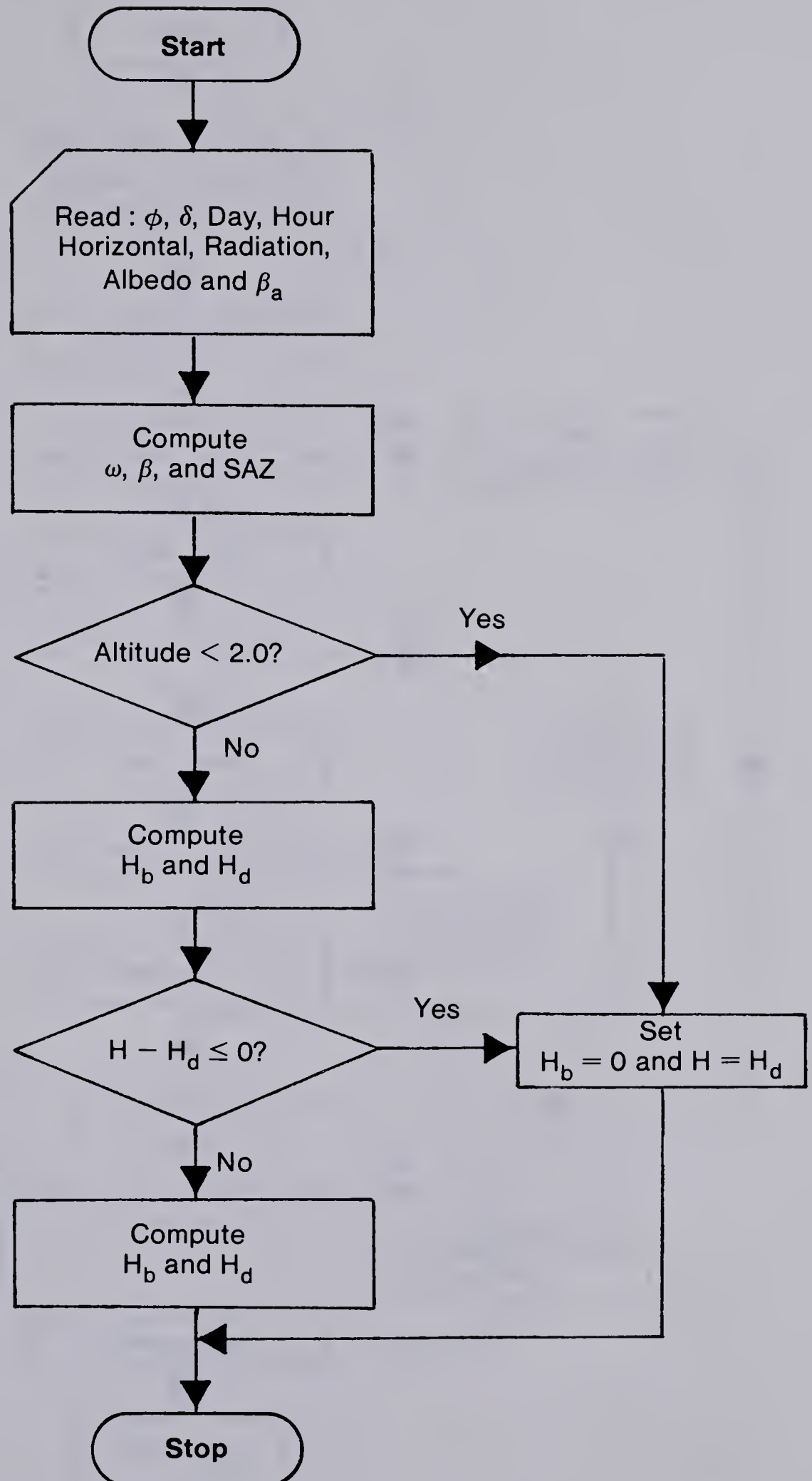


Figure 5.3 Flow chart for subroutine HBMDIF

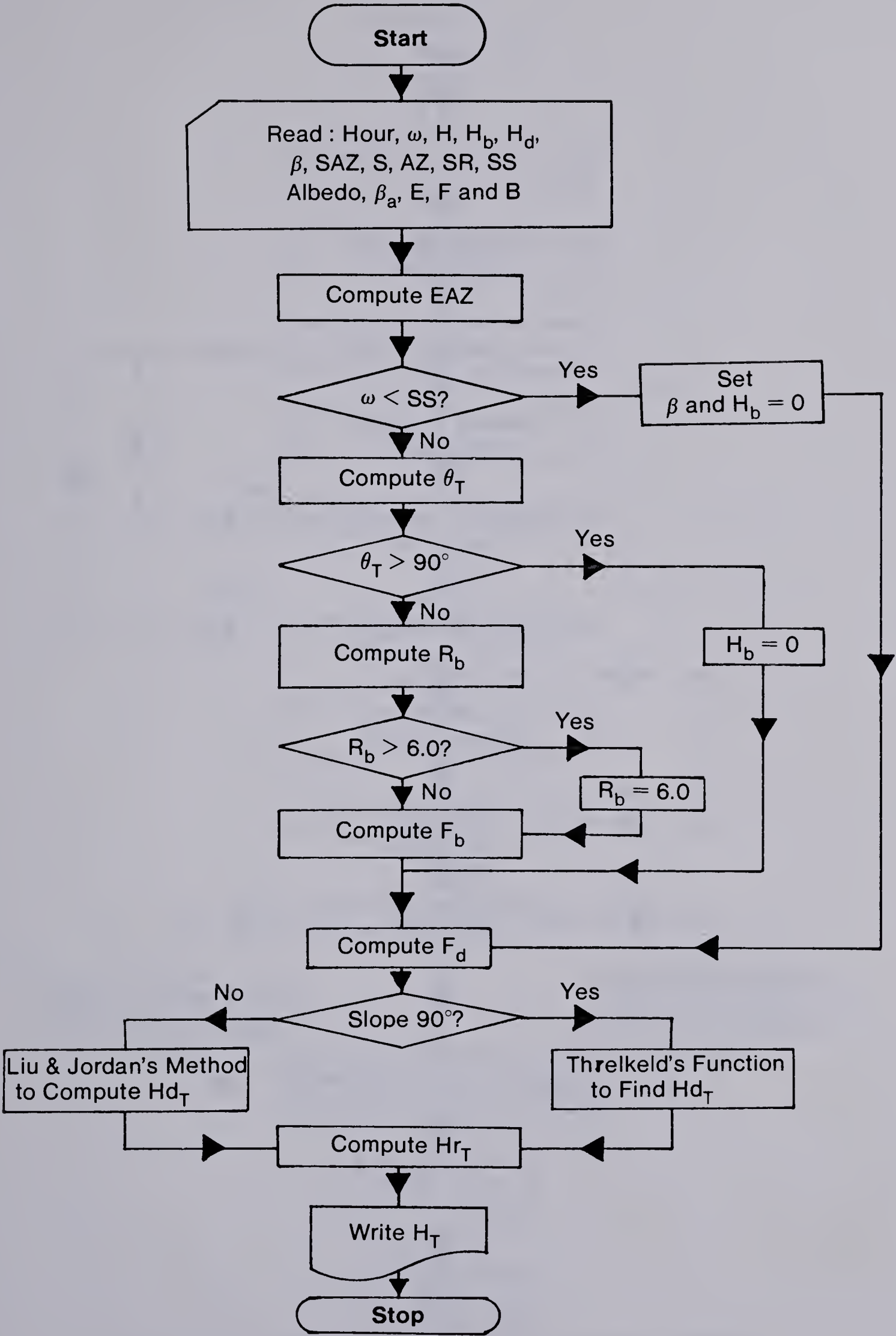


Figure 5.4 Flow chart for subroutine HTILT

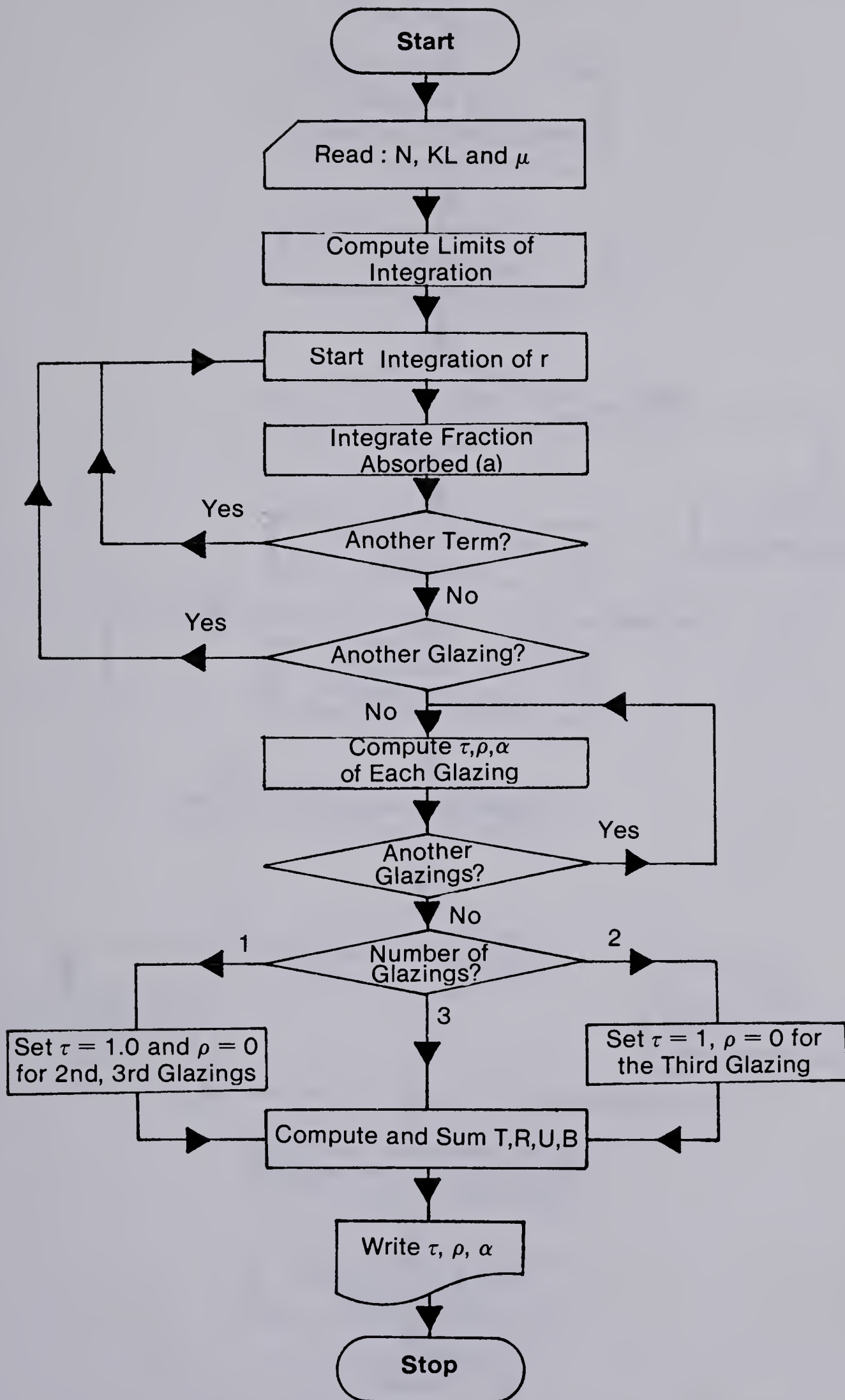


Figure 5.5 Flow chart for subroutine GPRDIF

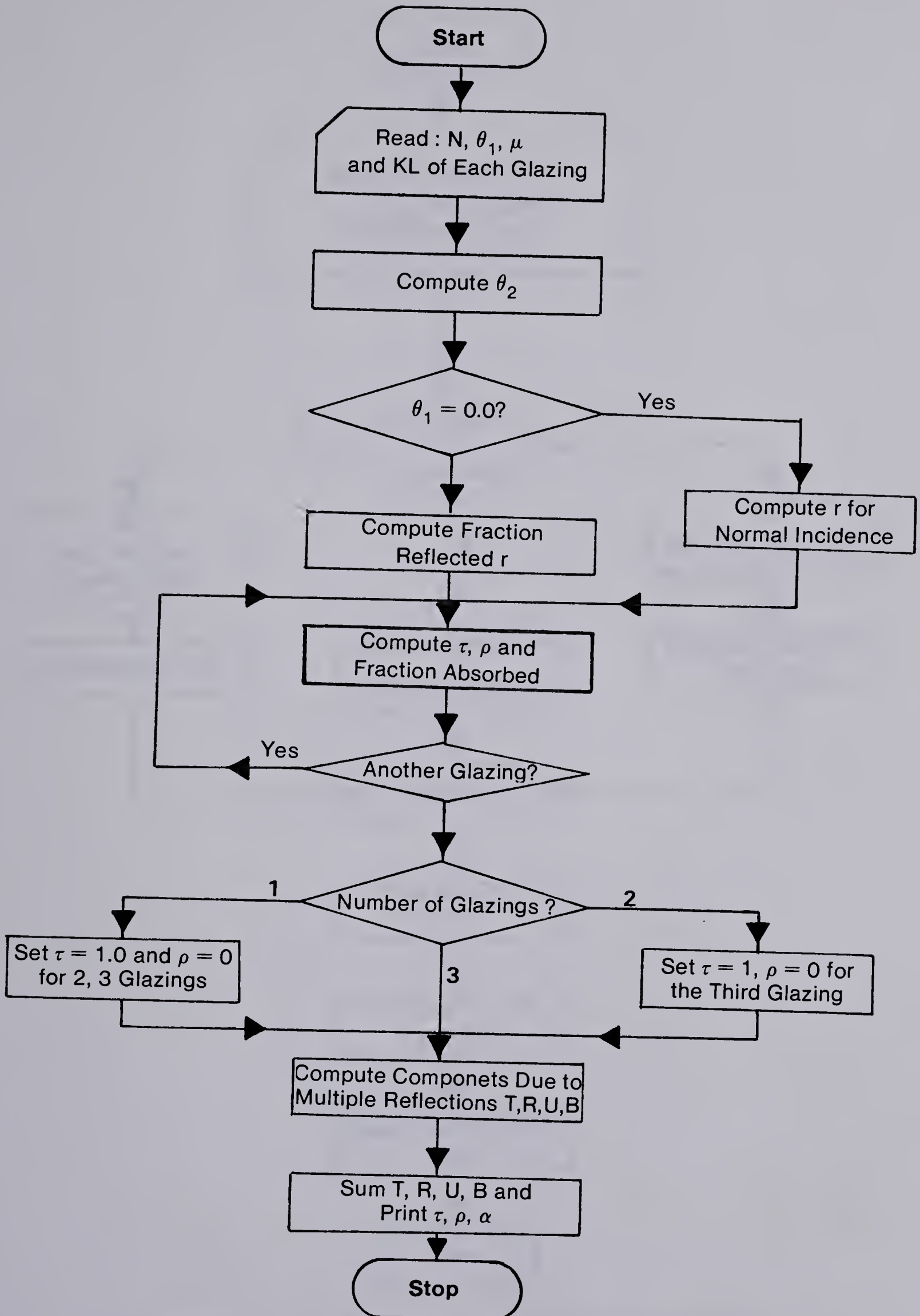


Figure 5.6 Flow chart for subroutine GPRDIR

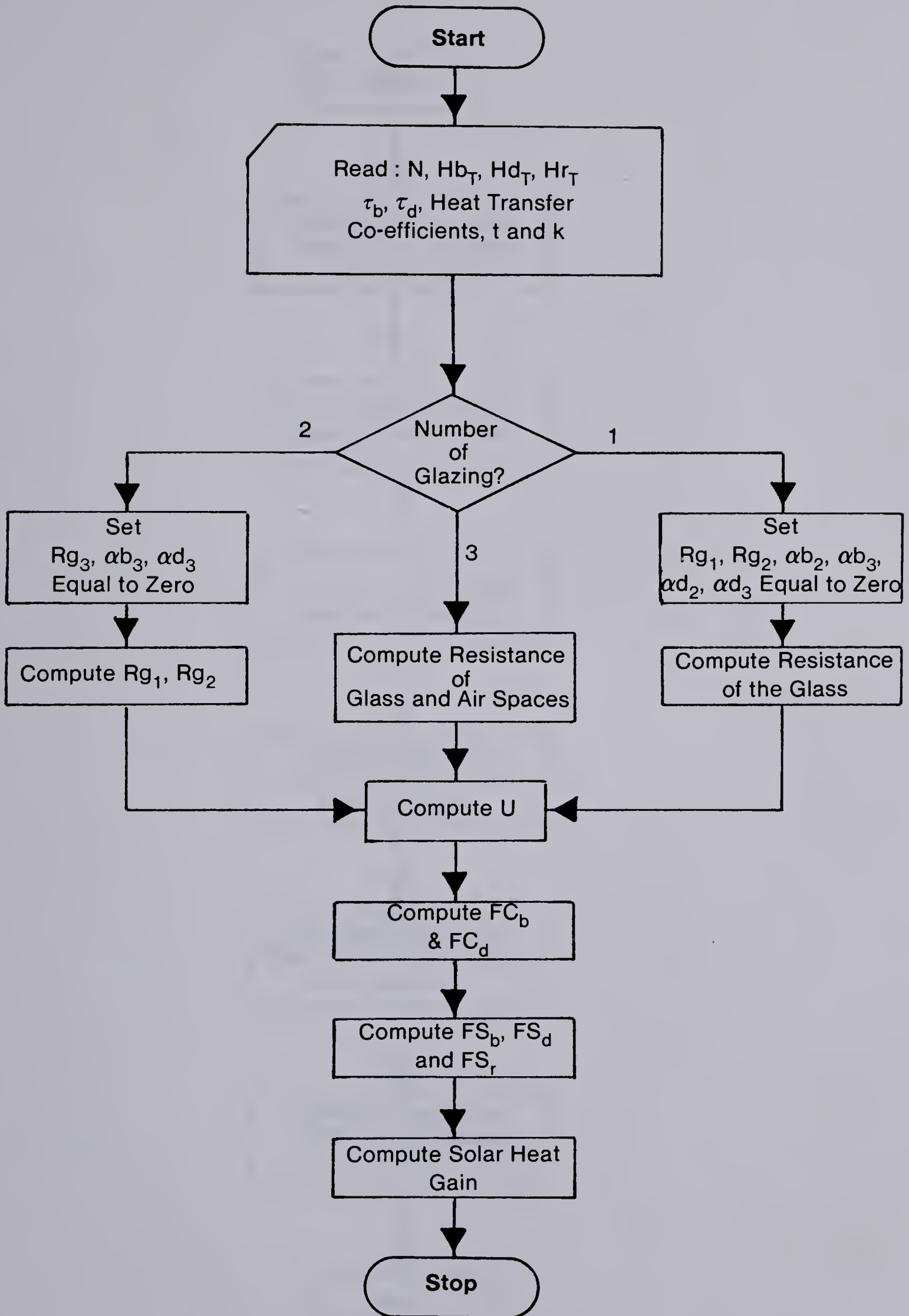


Figure 5.7 Flow chart for subroutine SOLHGF

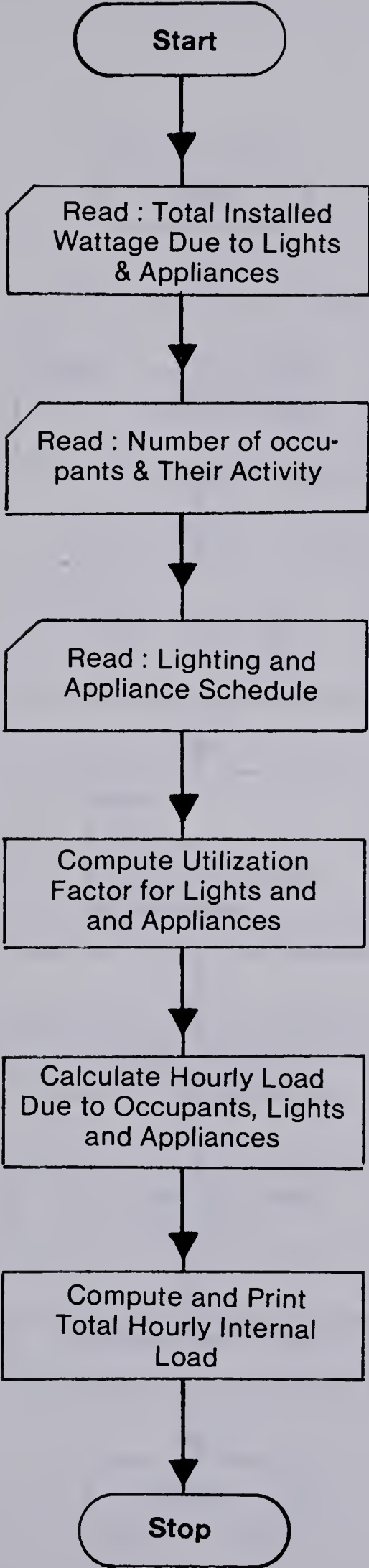


Figure 5.8 Flow chart for subroutine QINTER

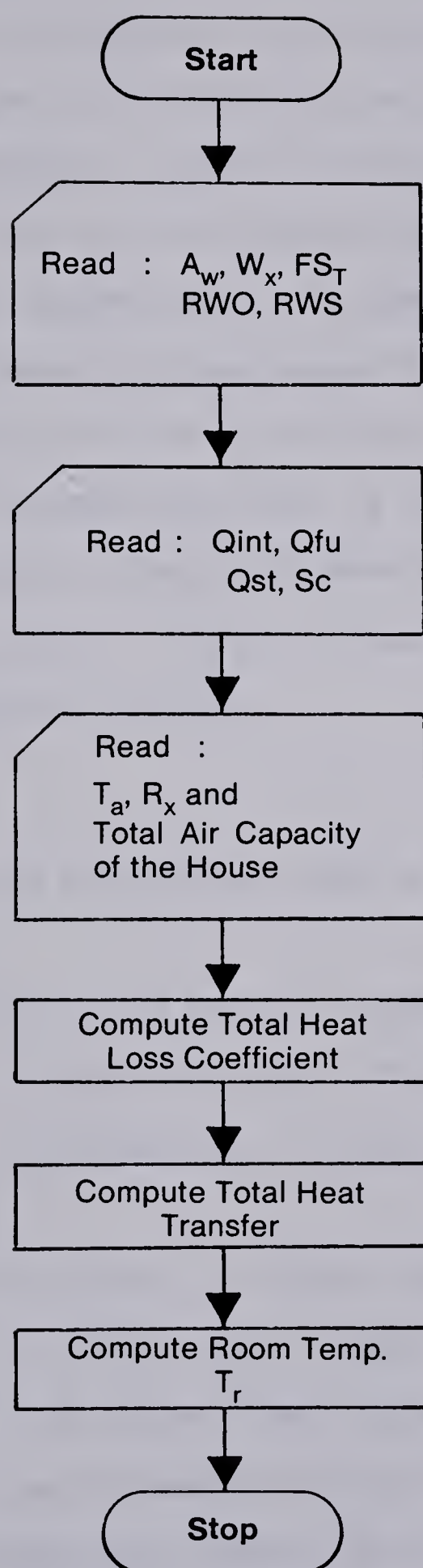


Figure 5.9 Flow chart for subroutine ENRGL

6. SIMULATION RESULTS AND DISCUSSION

6.1 Introduction

The motivation behind the development of the present thermal model was to be able to predict the functional relationship between a number of variables that go into the calculation of the auxiliary heat requirement of a house. The direct gain window model discussed in section 3.0 forms an important element of the present thermal model. Therefore a short discussion on the results of the direct gain window model are first presented. This is followed by the more comprehensive results like the dynamics of the thermal mass in the house, the general design curves, and the economics of the passive design features.

6.2 Transmittance of Window Glass as a Function of Angle of Incidence

In the direct gain passive systems, the design of window element is most critical. Obviously, a great deal of sophistication is necessary in modelling the direct gain window element.

In the calculations of solar heat gain, the transmissivity of glass due to beam as well as diffuse radiation has to be determined accurately. Therefore in the present model the transmissivity of the clear glass was calculated at each hour angle. As an illustration the transmissivity of clear glass as a function of angle of

incidence was plotted in figure 6.1. The transmissivity of clear glass was assumed to be a function of angle of incident beam radiation, the absorption coefficient of the glass, and the thickness of the glass. The transmissivity of clear glass was assumed to be constant over the solar spectrum. Also, the effects of longwave radiation, dust, and the temperature were neglected.

It is interesting to note that the transmissivity of heat absorbing glass is 22% less than that of a triple glass. The effectiveness of heat absorbing glass in reducing the summer solar gain is therefore evident. However, this is not a desirable feature for winter months.

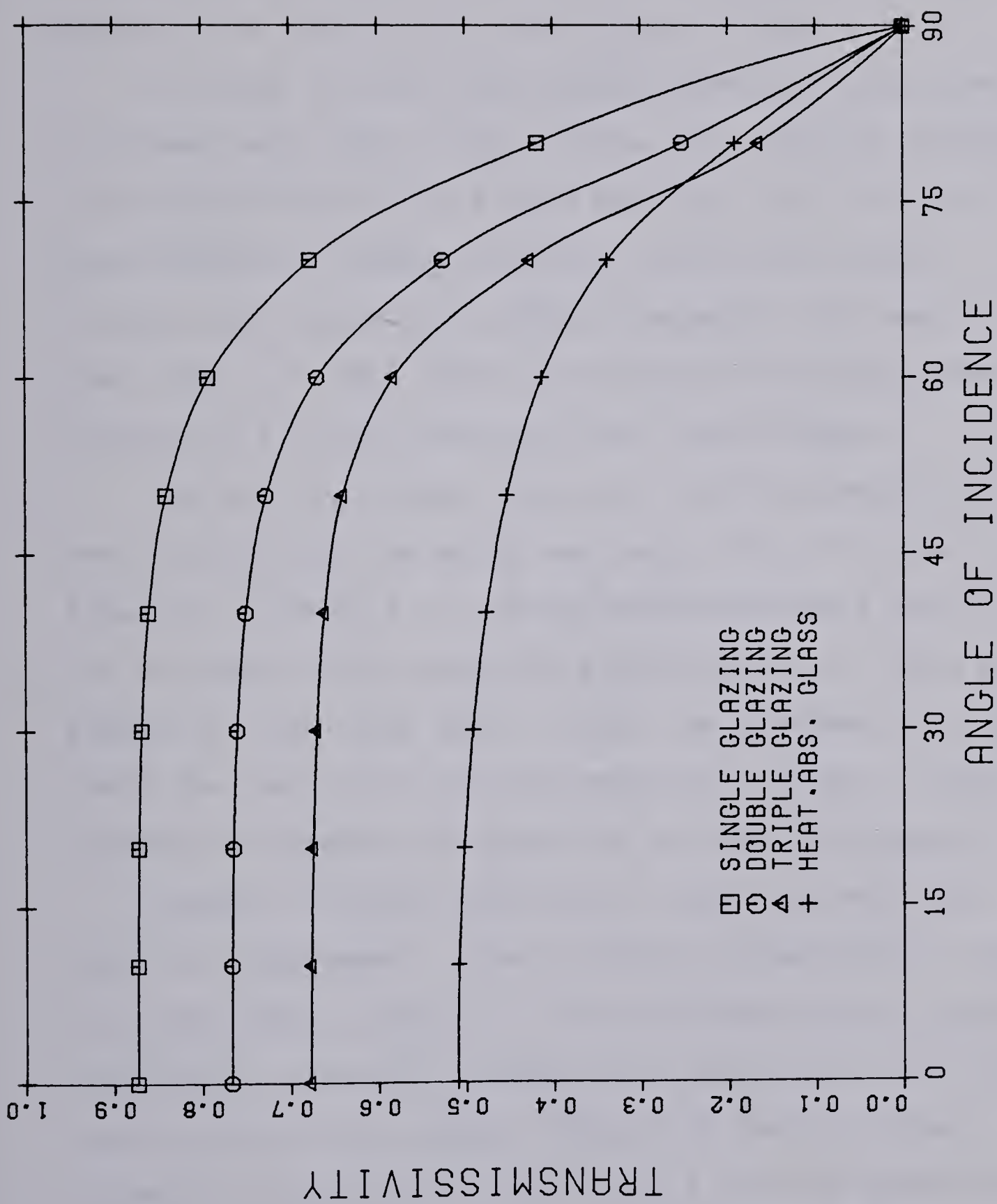


Figure 6.1 Transmittance of window glass as a function of angle of incidence.

6.3 Effect of Solid Overhang on the Summer Solar Gain

The problem of minimizing the summer solar gain yet not decreasing the winter solar gain can be studied by proper design of an overhang on clear glass window.

In order to study the effectiveness of solid overhang two cases were considered. In the first case an overhang with dimensions of $F=2.5$ feet and $E=1.0$ feet (figure 3.5) was studied on a double glazing clear glass window. In the second case the overhang dimensions were increased to $F=5.0$ feet and $E=2.5$ feet. The two designs of overhang were also studied on a triple glazing clear glass window.

The monthly average solar gain during January and July were plotted for the above two cases. This is shown in figures 6.2 and 6.3. It can be observed from figure 6.2 that the decrease in the solar heat gain due to a triple glazing window is relatively small. Also, the overhang does not shade the low winter sun but works to a greater advantage in shading the summer sun radiation as shown in figure 6.3.

However, the satisfaction of these two entirely opposite requirements from a single window element cannot be fully realised in practice. This problem can be somewhat elevated by choosing a window area appropriate for the heating load of the house. The set of design curves presented in section 6.7 will assist in this selection.

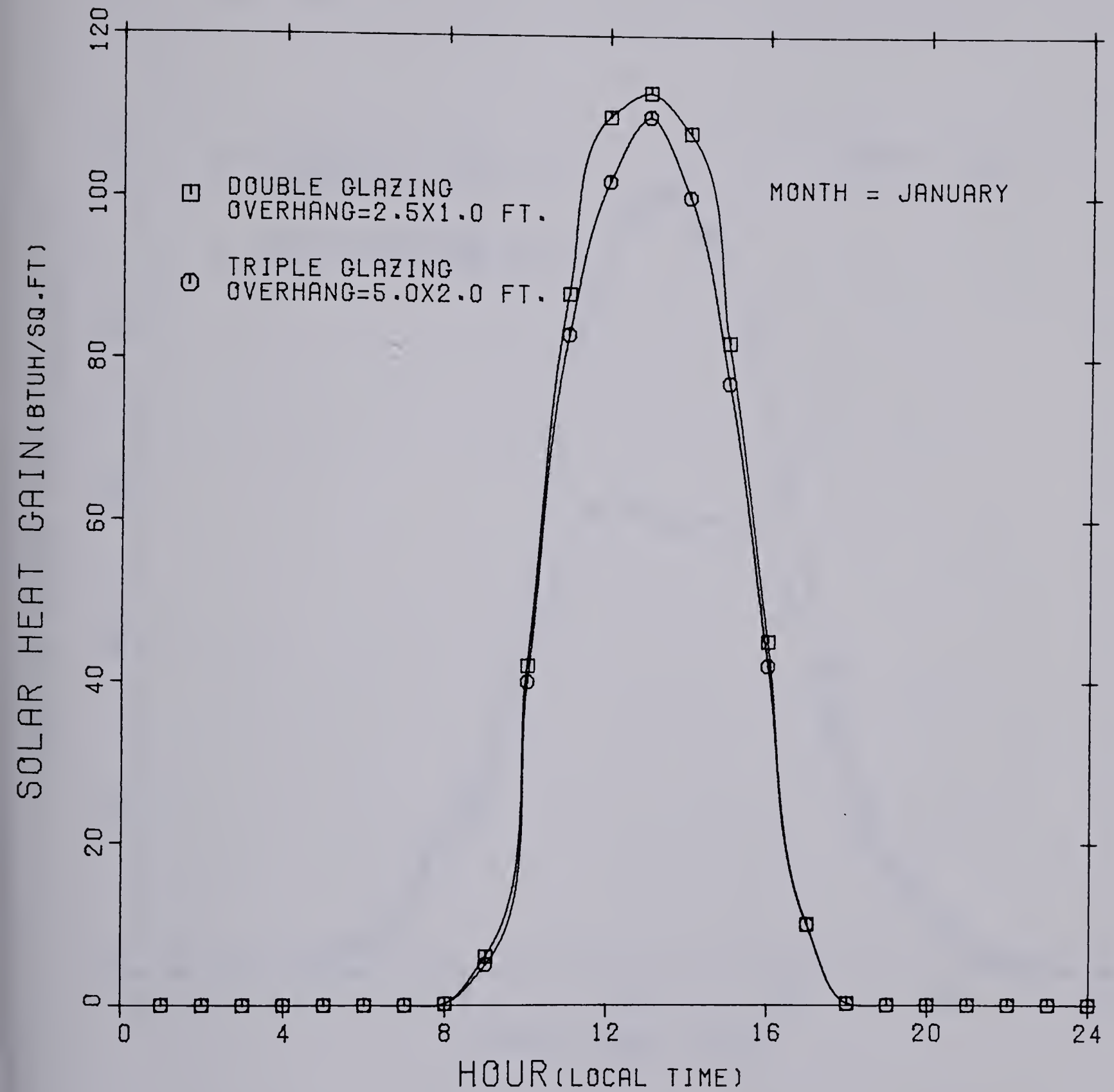


Figure 6.2 Typical solar heat gain through a double and triple glass window for the month of January.

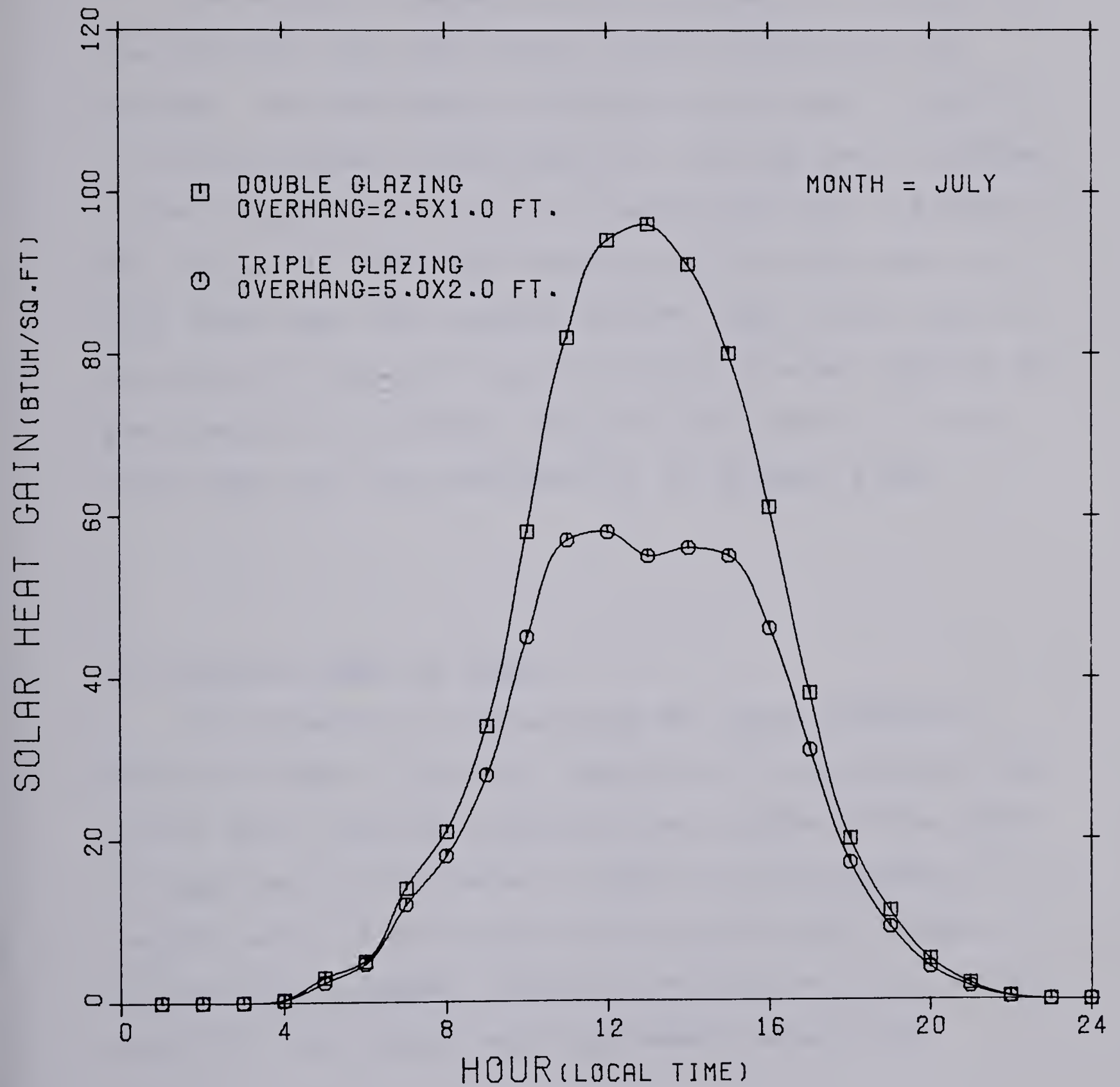


Figure 6.3 Effectiveness of a solid overhang in reducing the summer solar gain

6.4 Optimal Thickness of Mass Wall

The effect of increasing the thickness of mass wall on the auxiliary heat requirement of R42-25-25 house was studied. The house design parameters are listed in table 1. It can be observed from figure 6.4 that the ideal thickness of the thermal mass for diurnal energy storage is either in the form of 2.5 inch thick surfacings or in the form of 5 inch thick mass wall exposed on both sides to the room air. Thickness of mass wall beyond 5 inches does not improve the performance of the house. Based on this result a 5 inch thick mass wall was considered in the present study.

6.5 Optimum Number of Nodes

The dynamics of thermal mass wall were studied on R42-25-25 house. Figure 6.5 shows that the accuracy of the yearly heat requirement calculations depends on the number of nodal points considered in modelling the dynamics of the masonry wall. It can be seen that selection of 4 nodes in a 2.5 inch thick masonry surfacing involves an error of less than 1% in the yearly heat requirement calculations.

Table 1. Design Specifications of Houses Modelled.

Design	Window			Walls			Ceiling			Basement		Air change rate/hr	Heat loss coefficient BTU /F ⁰ -Hour
	R-Value Shutters	Area Sft		R-Value	Area Sft		R-Value	Area Sft		R-Value	Area Sft		
R14- 7-15	No shutters	151		7	1460		14	1337		15	2136	0.50	628
R25-15-25	8	151		15	1460		25	1337		25	2136	0.50	418
R42-25-25	14	151		25	1460		42	1337		25	2136	0.25	267
R70-40-40	26	151		40	1460		70	1337		40	2136	0.10	145

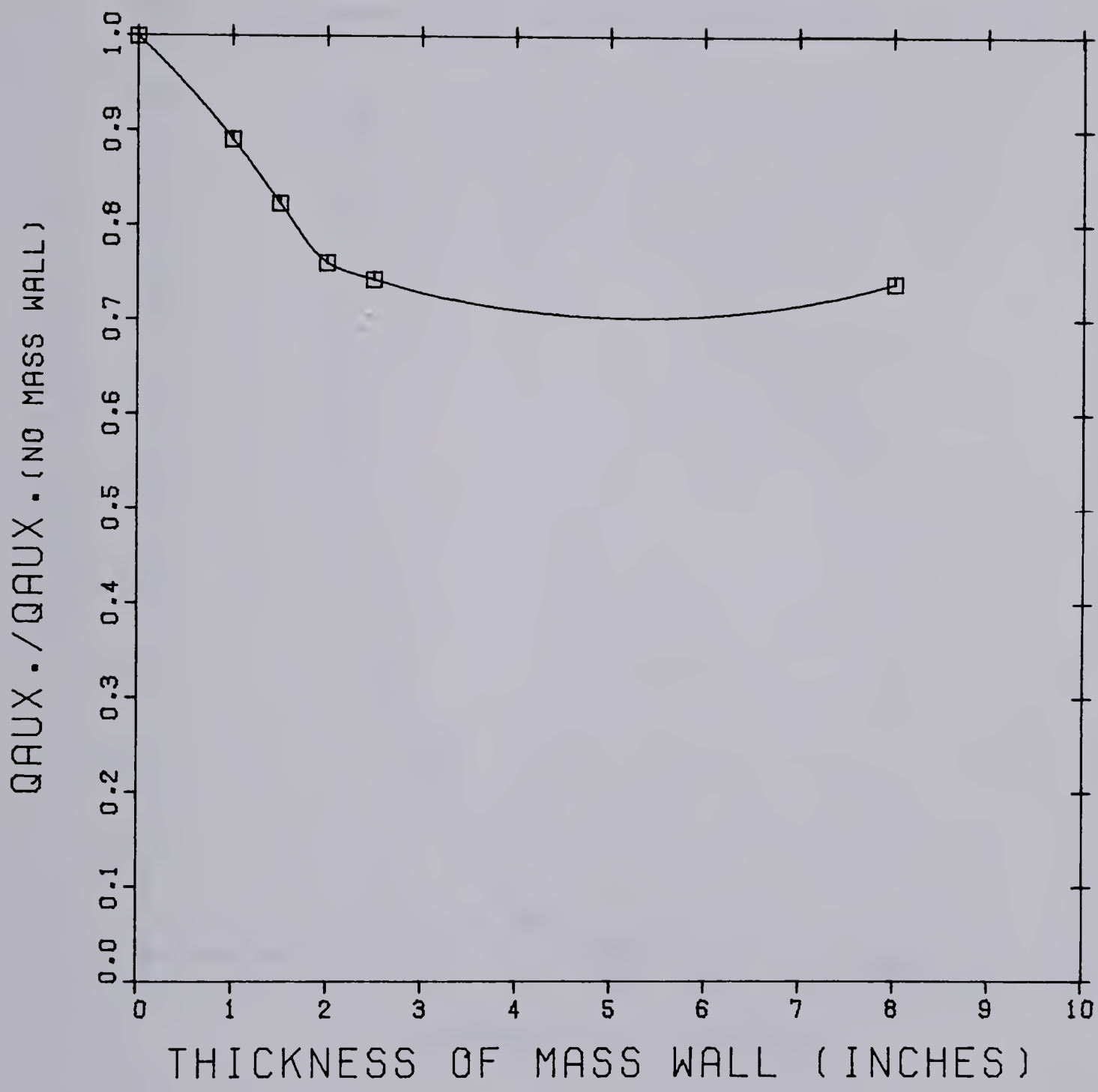


Figure 6.4 Effect of increasing the thickness of the mass wall on the yearly heat requirement.

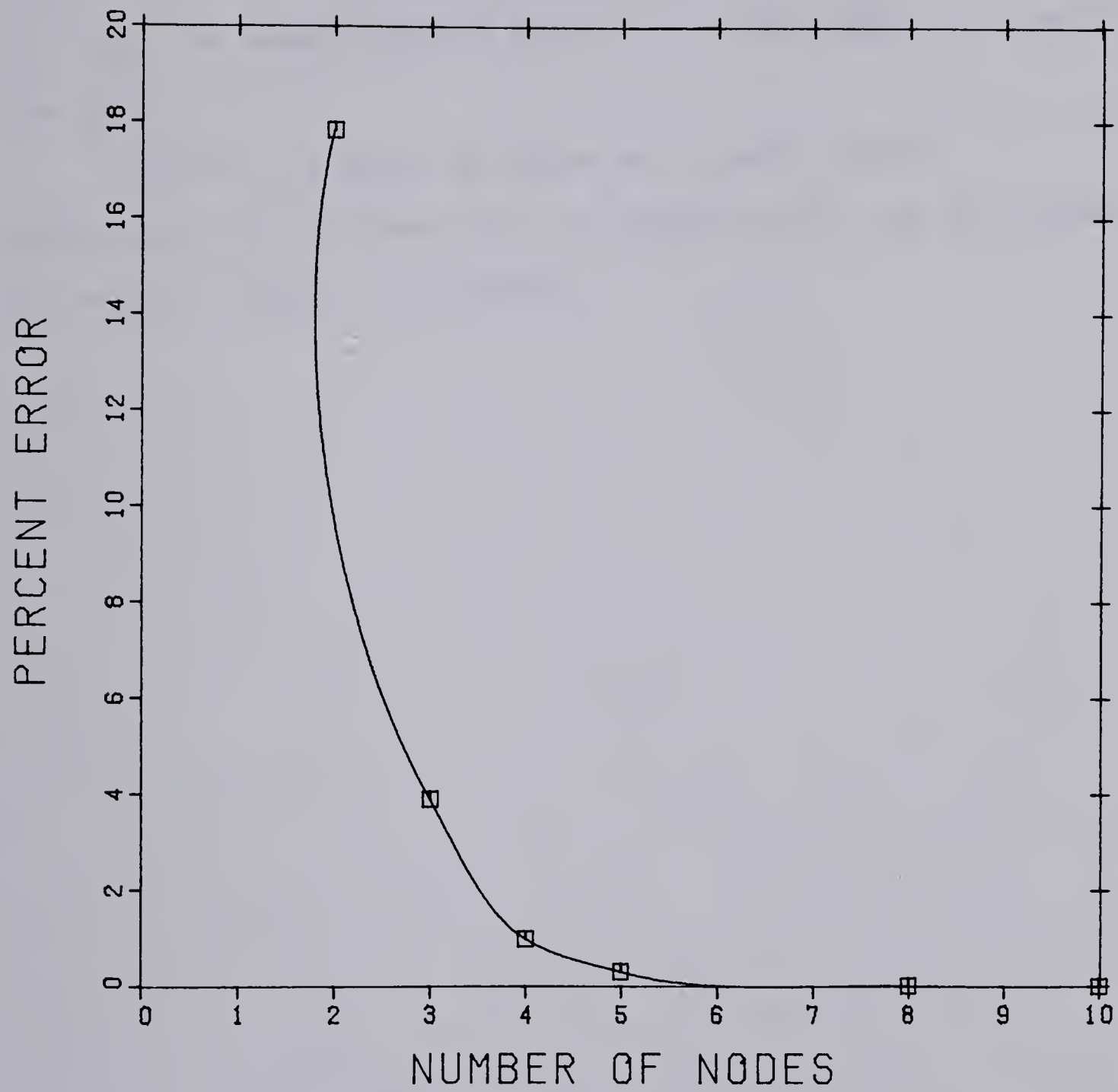


Figure 6.5 Effect of nodal points on the yearly heat requirement calculations.

This error is based on the heat requirement calculations obtained using double the number of nodes in the same thickness of mass wall. An increase in the number of nodes beyond 5 does not greatly improve the accuracy of the calculations. This result suggests that the optimum number of nodes in modelling the dynamics of the mass wall should be about 5.

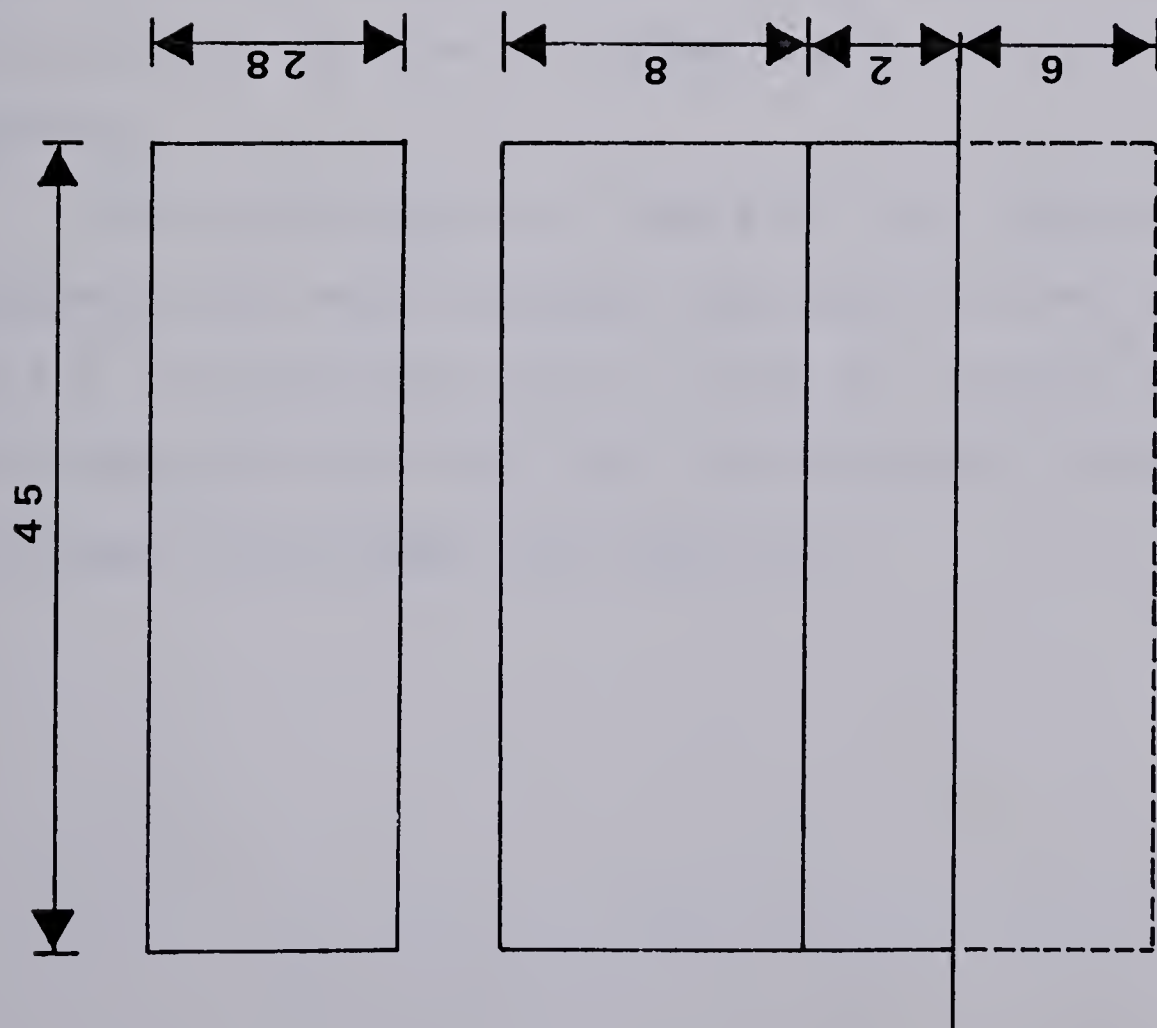
figures 6.4 and 6.5 serve as a useful guide in selecting the thickness of the masonry wall and the number of nodes in modelling studies.

6.6 Design Curves for the Houses Modelled

Four different designs with identical overall dimensions, figure 6.6, but different insulation levels, table 1, were considered for the present study. It is believed that the wide variations in the insulation levels of the houses represent the majority of the contemporary house insulation practices.

As shown in table 1 the houses were identified by a number e.g. R14-7-15 for the first house. This designation indicates the insulation level of the house, that is 14 represents the resistance value of the ceiling, 7 that of the walls, and 15 that of below grade basement walls and floor. Table 1 gives the details of the houses such as area of the walls, ceiling, basement (below grade walls plus basement floor), their resistance values, the air change rates, and the heat loss coefficients. The heat loss coefficients were calculated considering a 12% window area (based on above grade floor area). A simple method of calculating the heat loss coefficient of a house is given in appendix A-2. The present model assumes a reasonable internal load schedule, figure 2.3, for a family of 3.35 (two adults plus two children).

Design R14-7-15 was chosen as a reference design to compare the performance of other three designs.



Dimensions are in feet

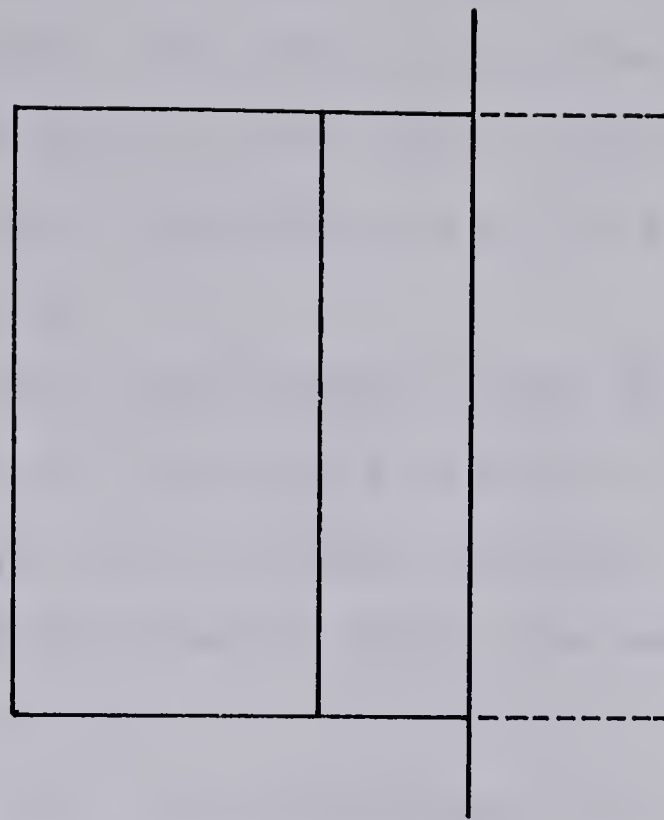


Figure 6.6 Design dimensions of the house

The auxiliary heat requirement was calculated for increased south facing window area (as a percent of above grade floor area) and the heat capacity in the house. Figure 6.7 shows the effect of increasing the window area on the heat requirement of the house.

The relative heating requirement of the four houses is evident from figure 6.7. The results indicate the importance of the insulation level of the houses. Considering for the moment no windows and no internal loads, the heat required for the R70-40-40 enclosure is 0.22 of the R14-7-15 enclosure. In such a well insulated house the internal load can supply much of the heating requirement so that the heating requirement with internal load is 0.04 of the R14-7-15 design. Further reduction can be obtained by using south facing windows. Eventually, the actual heating requirement could be made essentially zero with such a design.

The curves shown in figure 6.7 were obtained by assuming the manual shutter routine described in section 2.2.2. It should be realised that an increase in the window area beyond 18% of the floor area results in excessive overheating as shown in figure 6.8.

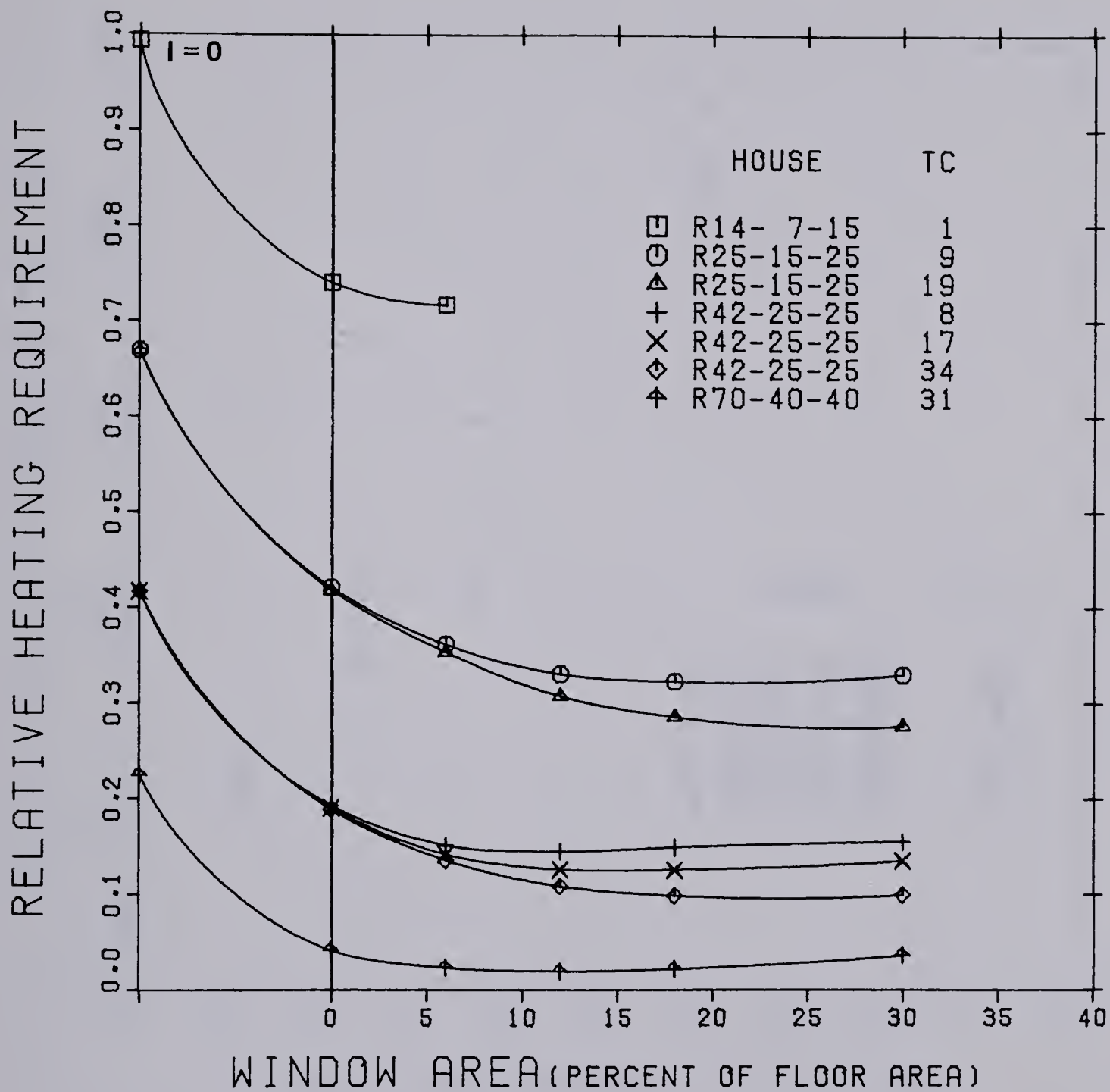


Figure 6.7 Effect of south facing window area, the thermal mass and the insulation level on the yearly heat requirement of a house.

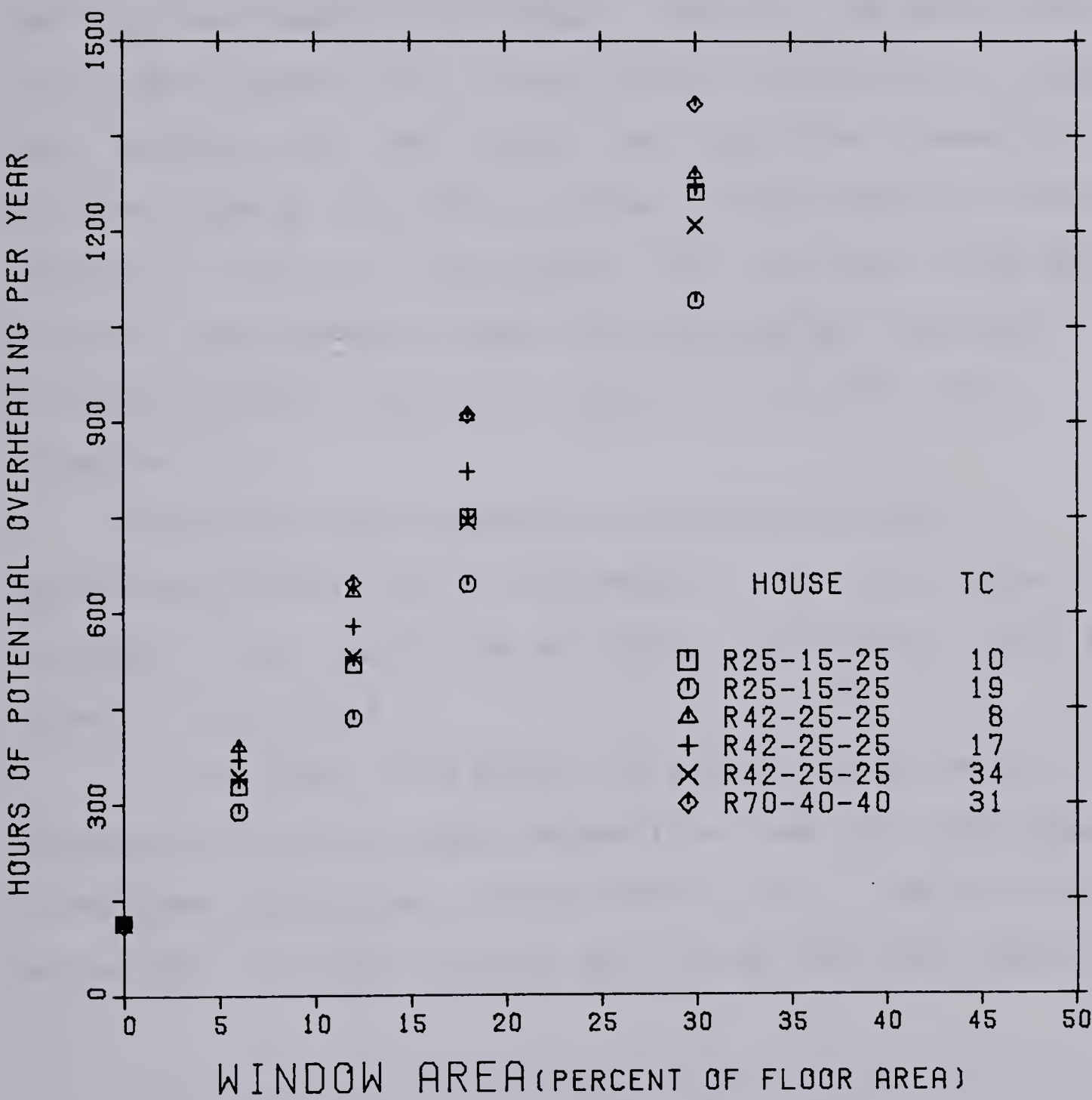


Figure 6.8 Hours of potential overheating as a function of south facing window area.

6.7 The General Design Curves

The curves shown in figure 6.7 give an indication of the impact of various specific design decisions on the heating requirement of the house. However, one would like to have a more general way of estimating the effects of thermal mass, window area, and internal heat gain for a house of arbitrary design. For this purpose a normalization of the results in figure 6.7 was sought that would make them more generally applicable to any arbitrary design subjected to different weather data and a different internal load schedule.

To provide some guidance in selection of the appropriate normalization parameters it is instructive to consider a very simplified version of the thermal model as shown in figure 6.9

In this simplified model the entire thermal mass is assumed to be at the room temperature, and the room receives three time varying heat inputs $SHG(t)$, $I(t)$, and the furnace output Q_{fu} . The heat balance describing this model would be

$$C \, dT_r / dt = I + SHG + Q_{fu} - U (T_r - T_{\infty}) \quad 6.7.1$$

To extract the appropriate normalization parameters from this equation each term or group of terms will be compared in some way with the heat loss rate $U (T_r - T_{\infty})$.

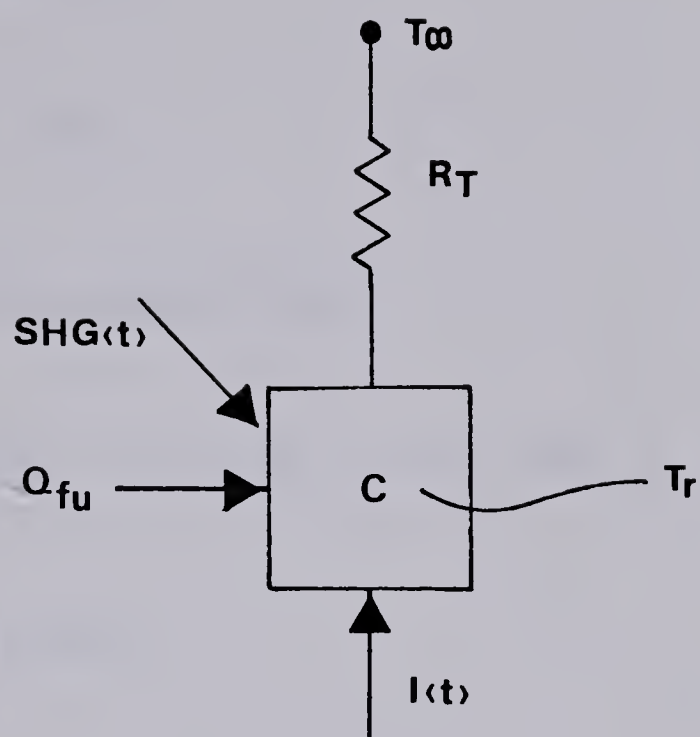


Figure 6.9 A schematic illustration of the energy exchanges through the resistive and capacitive elements of the house.

First, the total heat energy that can be stored in the thermal mass is $C (T_{\max} - T_{\min})$. This value should be compared with the typical rate of heat loss during the heating season which is

$$U \text{ HDHr} / \text{HHr}$$

Where HDHr (Heating degree hours)

$$= \int_{1 \text{ year}} (T_{\min} - T_{\infty}) dt \quad (T_{\infty} < T_{\min}) \quad 6.7.2$$

And HHr (Heating hours)

$$= \int_{1 \text{ year}} dt \quad (T_{\infty} < T_{\min}) \quad 6.7.3$$

The ratio HDHr / HHr is just the mean temperature difference $(T_{\min} - T_{\infty})$ during the heating season. The ratio of the amount of heat storage to the mean rate of heat loss is a storage time constant,

$$\tau = \frac{C (T_{\max} - T_{\min})}{U \text{ HDHr} / \text{HHr}} \quad 6.7.4$$

Where $C = \rho c V$

This is the first important parameter of a house design and it gives a quantitative assesment of the effect of the

thermal mass of the house. Appendix A-3 describes a numerical example of calculating the time constant of a house.

The three heat inputs, I , SHG, and Q_{fu} , to the house should also be compared to the heat loss rate of the house. These three inputs can be combined and expressed as only two parameters if some thought is given to the matter. Consider the internal loads. The internal loads can be thought of as consisting of a constant component (I_c) that occurs during the day or at night, plus a fluctuating component (I_f) that peaks during the day or in the evening. That is

$$I = I_c + I_f$$

During the heating season the constant component, I_c directly replaces part of the furnace heat requirement Q_{fu} and thus it is appropriate to combine these two components. The fluctuating component can be thought of as acting in a very similar way to the solar heat gain SHG during the day time and therefore it is appropriate to combine (I_f) with SHG. In both cases it is the integral over the heating season that is important. The two dimensionless parameters that result are the

Solar and Internal Gain (SIG) factor

$$\frac{ISHGF \times \text{Window area} + I_f \times HHr}{U \times HDHr} \quad 6.7.5$$

Where

$$ISHGF = \int_{1\text{Year}} SHGF \, dt \quad (T_{\infty} < T_{min})$$

and the Annual Heating Load Reduction (AHLR) factor

$$\frac{\int_{1\text{Year}} Q_{fu} + I_c \times HHr}{U \times HDHr} \quad 6.7.6$$

The SIG factor thus gives a quantitative assesment of the annual space heating available from solar and the fluctuating internal loads for transacting the heat losses. The AHLR factor is the output parameter which describes how much furnace or auxiliary heating is required in the house. The annual heating requirement Q_{fu} , is related to the value one would obtain from a static calculation neglecting the solar gain, $U \times HDHr$, through this latter factor.

Generally, the time constant of the house has been an index to predict the performance of the houses. However, the new factors, SIG and AHLR along with the time constant of the house fully describe the storage efficiency of a house in transacting the various heat losses and the heat gains.

There are three meteorological parameters which appear in these expressions. These are the Integrated Solar Heat Gain (ISHG) factor, the heating degree hour index (HDHr), and the number of heating hours (HHr). The latter two are usually more or less known for a given location (for Edmonton HDHr = 137,000°C-hr and HHr = 8042). The first term, the ISHG, is a new parameter which must be calculated from meteorological data. It describes the annual useful solar heat gain that may be obtained per square foot of window area. For a vertical, south facing, double glazed window in Edmonton ISHG = 182,000 Btu/ft².

Employing the above analysis the effect of increasing the SIG factor on the AHLR factor was studied. The results of figure 6.10 show that the different levels of the house insulation are properly normalized. Several curves have been drawn through the data to indicate the general dependence of AHLR factor on the SIG factor for different values of time constant (TC). One would expect that for a house with large time constant the heating requirement would approach zero, AHLR=0, for SIG=1.0. The data shows that as the time constant is increased this value is approached. For a time constant of 32 hour which is considered to be the maximum possible value obtainable in a passive house design the AHLR is 0.55. A more practical passive house design might have a time constant of 8 hour which would suggest a heat saving of about 25 percent (AHLR = 0.75).

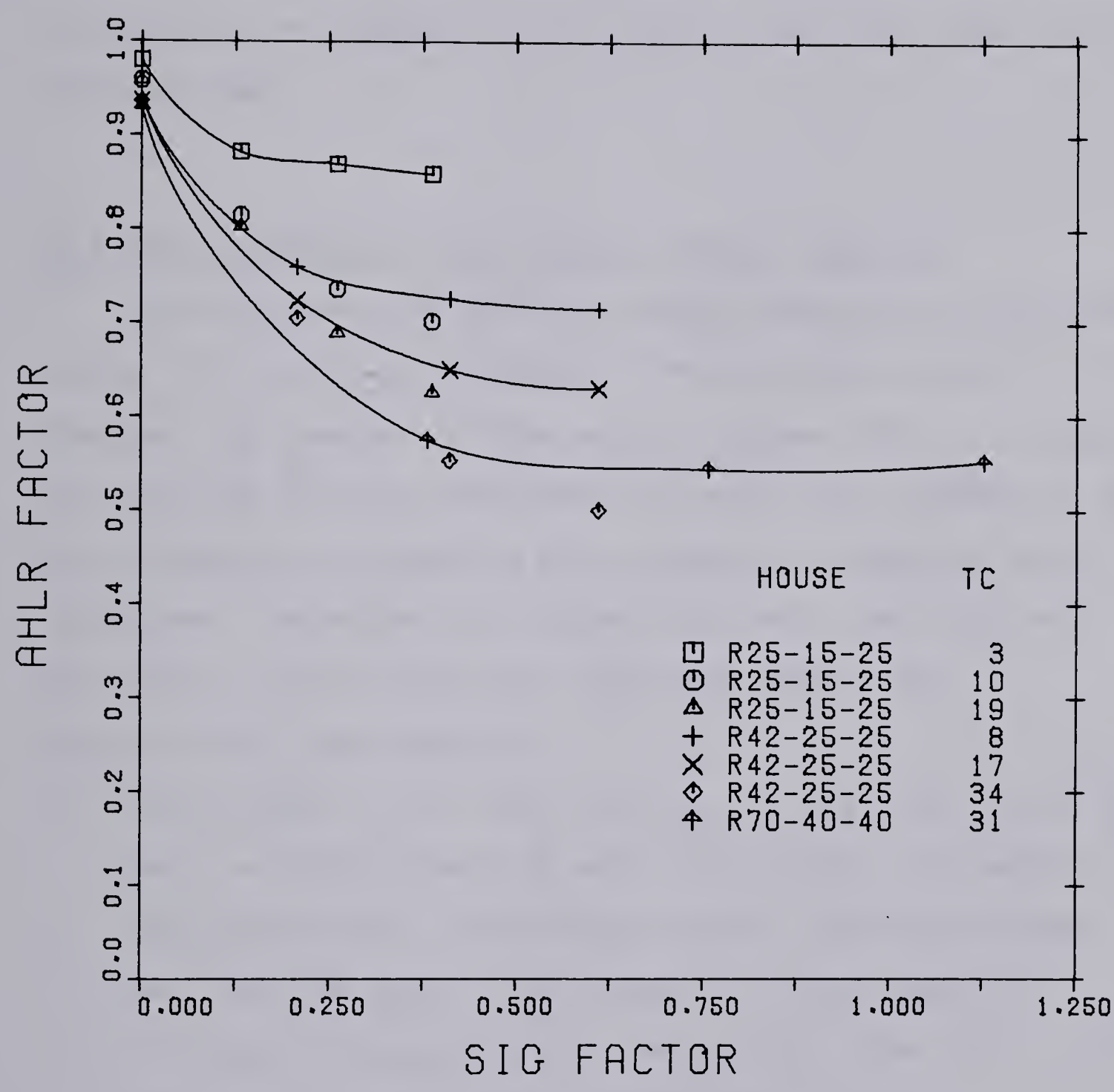


Figure 6.10 The general design curves.

For each time constant there is a broad minimum in the AHLR as a function of SIG. This implies that there is a broad minimum technical optimum window area for a given time constant. If the time constant can be increased the window area can be increased as well with a resulting reduction in heating load.

6.8 The Economics of the Passive Design Features

The economics of passive design features can be studied using life cycle cost analysis. The procedure essentially remains the same as for the active systems (43). It should be realized that the following analysis are intended to show the procedure of studying the economics of passive design features. Therefore the numbers arrived at may not have particular significance but the ideas behind the calculations are important.

1. An estimate of the additional costs associated with the passive design features were calculated. The features considered were the shutter system, the thermal mass wall and the costs associated with improvement in R-values of the walls and the ceiling. The life of the above features was considered to be 20 years.
2. Over a period of 20 years, the anticipated costs due to repayment of money borrowed, interest, insurance, operation, maintenance and additional property taxes were estimated.
3. Considering a market discount rate (ie. rate of return

on the best alternative investment), of 12%, an estimate on how much would have to be invested now to meet the anticipated costs was made.

4. The sum of the investments gives the present worth of the passive design.
5. The savings due to the passive design features and a non passive house were compared on the present worth basis.

Employing the above procedure, the following three possibilities were examined.

1. The savings due to an improvement in the R-values of the enclosure elements.
2. The savings due to the installation of a shutter system.
and
3. The savings due to the installation of a thermal mass wall.

Figure 6.11 shows the economics of increasing the insulation level of a house. The R14-7-15 house was chosen as a reference design. The extra cost involved in increasing the insulation level from R14-7-15 house to R25-15-25 house was obtained from reference (44). Similarly an estimate of extra cost for increasing the insulation level of R14-7-15 house to R42-25-25 and R70-40-40 was also obtained from the same source. These cost estimates are shown in table 2 under column "Estimate 2". Estimates 1 and 3 were arbitrarily chosen as lower and higher estimates with respect to estimate 2.

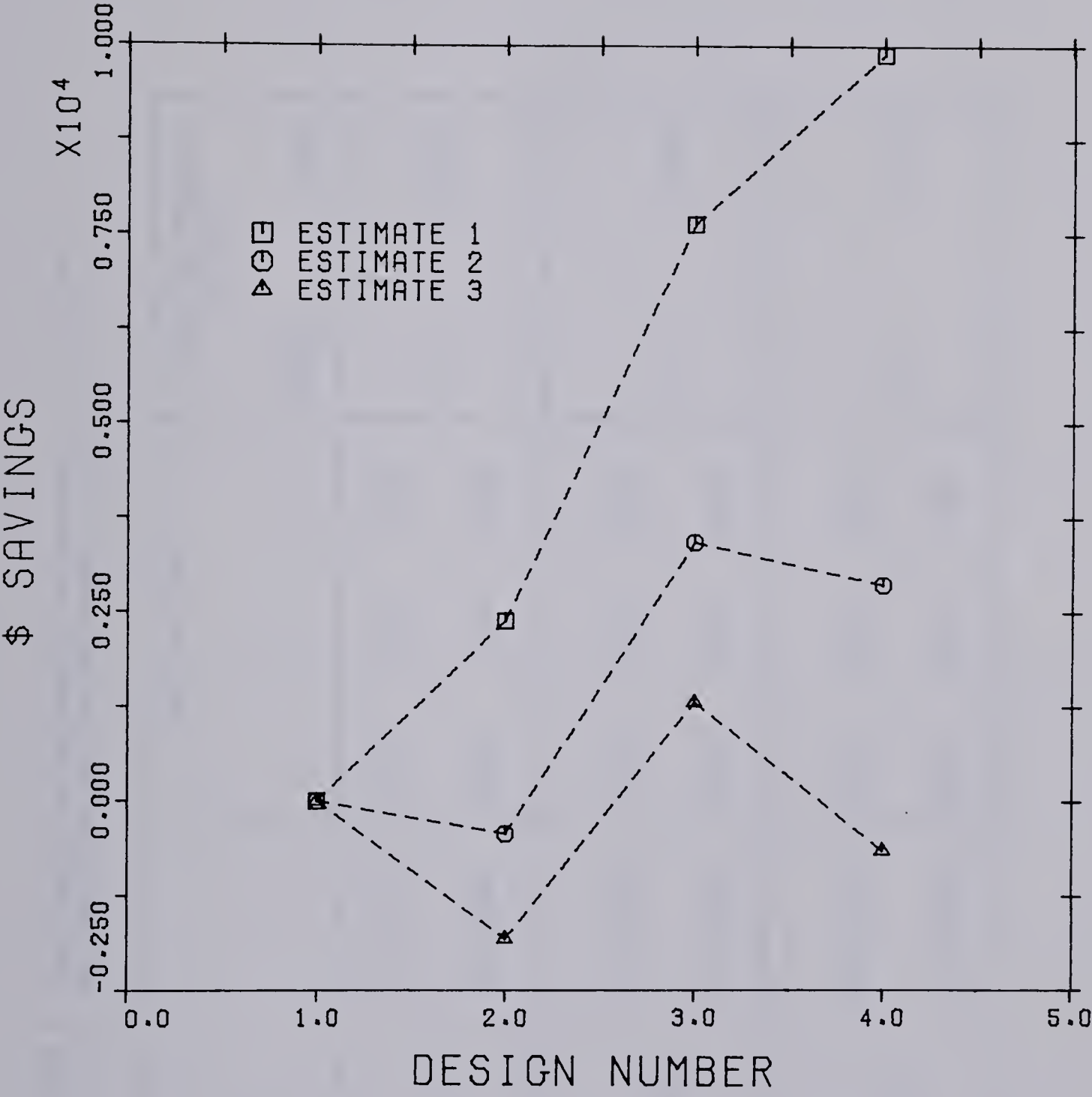


Figure 6.11 The economics of the insulation level of a house

Table 2. Approximate cost estimates, the savings, as a function of insulation level of the house.

Design	Cost estimates (c\$)			Auxiliary Heating (10 ⁶ BTU)	
	1	2	3	Before	After
R25-15-25	Extra Cost	1000	2000	2500	
	\$ Savings	2382	-428	-1819	147 98.79
R42-25-25	Extra Cost	1500	3000	3750	
	\$ Savings	7635	3419	1311	147 61.56
R70-40-40	Extra Cost	2500	5000	6250	
	\$ Savings	9888	2861	-651	147 33.25

At each cost estimate, the additional investment towards insulation was compared with the cumulative fuel savings over a period of 20 years. In the above calculations the gas cost was assumed to be \$1.70 per MBTU.

For convenience the four house designs of table 1 were identified as follows.

House	Design Number
R14- 7-15	1
R25-15-25	2
R42-25-25	3
R70-40-40	4

The abscissa in figure 6.11 represents the above houses by their design numbers. It can be seen that as the cost of adding the insulation goes up the optimum point shifts towards insulation level corresponding to design 3.

The economics of installing a shutter system were studied on a R42-25-25 house with a time constant of 17 hour. Table 3 gives three cost estimates for installing a shutter system. Estimate 1 was obtained from reference (44). Estimates 2 and 3 were arbitrarily chosen. The window area as a percent of above grade floor area was increased from 6% to 18%. The cumulative fuel savings were obtained by summing the difference between heating the R42-25-25 house with and without the shutter system. The above analysis were carried out at two gas costs as shown in figure 6.12.

Table 3. Assumed cost estimates and the calculated savings
as a function of window shutter area

Design R42-25-25 Window Area	Cost estimates (c\$)				Auxiliary Heating (10 ⁶ BTU)	
	1	2	3		Before	After
	\$10/sft	\$5/sft	\$2.5/sft			
6%	Extra Cost	756	378	189	25.62	20.98
	\$ Savings	-3521 (-5769)	-2419 (-4668)	-1868 (-4117)		
12%	Extra Cost	1512	756	378	26.66	18.63
	\$ Savings	-3592 (-2203)	-1389 (0.0)	-287 (1101)		
18%	Extra Cost	2268	1134	567	29.60	18.58
	\$ Savings	-5325 (-3135)	-2020 (169)	-368 (1821)		

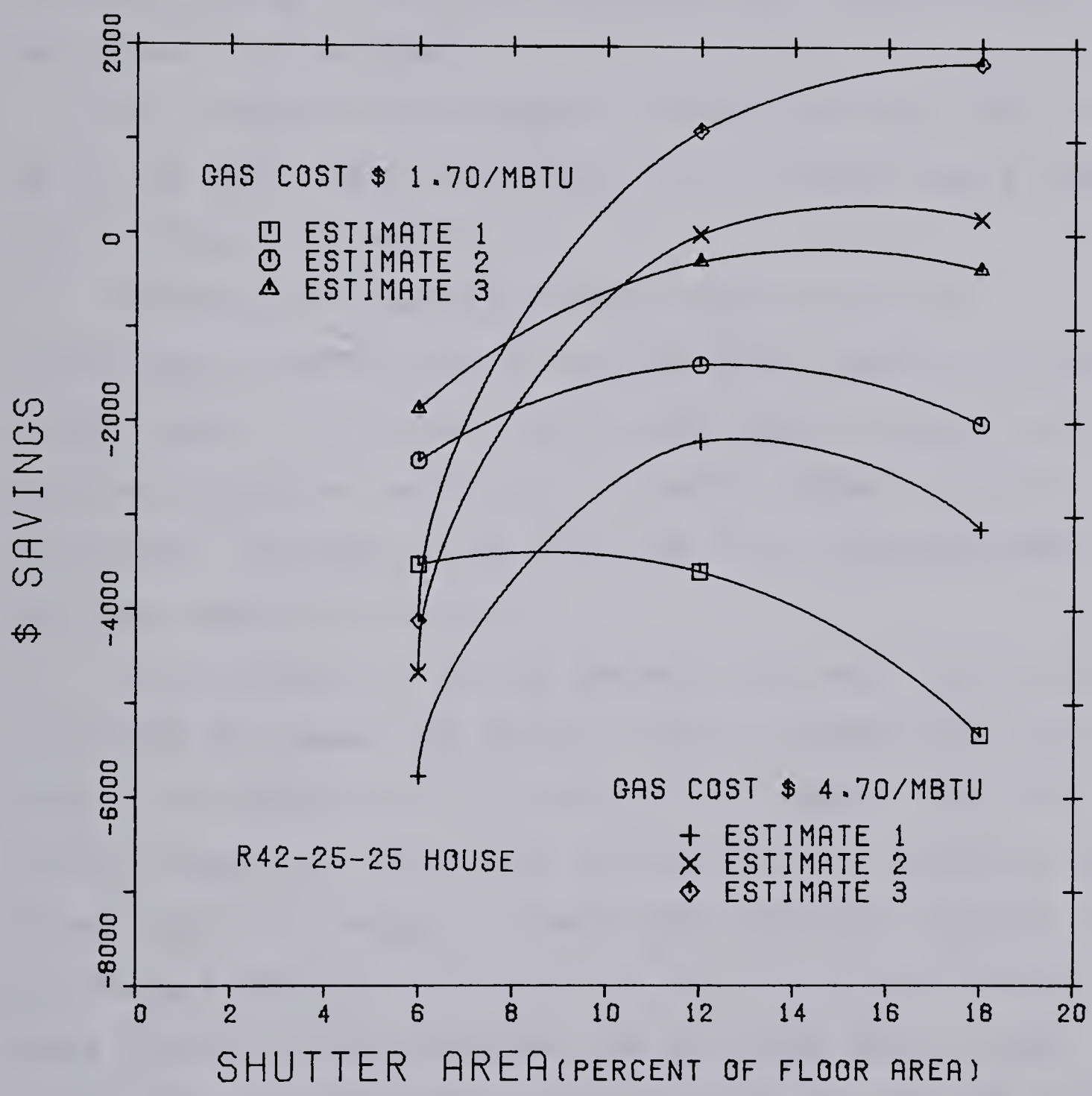


Figure 6.12 The economics of shutter system.

The first and second gas costs were assumed to be \$1.70/MBTU and \$4.70/MBTU respectively. The \$ savings corresponding to two gas costs are shown in table 3. The numbers shown in paranthesis in table 3 correspond to the second gas cost, differentiating it from the first gas cost savings which are not shown in paranthesis.

It is evident from figure 6.12 that at a gas cost of \$4.70 per MBTU and a shutter cost of \$ 2.5 per square foot, net savings would result.

Employing the above procedure the economics of installing a shutter system on other house designs can be investigated. It is expected that the shutter system would be more economical on low time constant houses (such as R25-15-25) because of the fact that their storage capacity will be comparatively small.

The economics of adding thermal mass were investigated on R42-25-25 house. The present cost of installation of a 5 inch thick masonry wall is around \$ 45 /square foot (44). Table 4 shows two additional cost estimates. Estimate 2 and 3 were kept low enough to investigate the most economic cost of thermal mass wall. The area of the distributed thermal mass (DM) wall was increased from 0.5 times above grade floor (F) area, (DM=1/2F in table 4) to twice the above grade floor area (DM=2F). In each case the time constant of the house was calculated. The cummulative savings were plotted as a function of time constant of the house.

Table 4. Assumed cost estimates and the calculated savings,
as a function of thermal mass area

Design	Cost estimates (c\$)			Auxiliary Heating (10 ⁶ BTU)	
	1	2	3	Before	After
R25-15-25	\$45/sft \$4.5/stf \$1/sft				
DM = 1/2F	Extra Cost	7087	708	157	
	\$ Savings	-19718 (-19376)	-1791 (-1449)	-242 (100)	25.93 21.42
DM = 1F	Extra Cost	14174	1417	315	
	\$ Savings	-39137 (-37942)	-3283 (-2087)	-187 (1010)	25.93 18.63
DM = 2F	Extra Cost	28348	2834	730	
	\$ Savings	-78513 (-76531)	-6805 (-4832)	-889 (1092)	25.93 16.05

The analysis were carried out at two gas costs as shown in figure 6.13. The numbers in paranthesis in table 4 correspond to the second gas cost of \$ 4.70 / 10^6 BTU whereas the other numbers correspond to the first gas cost of \$1.70/ 10^6 BTU.

It is clear that savings due to the installation of thermal mass would only be possible at a cost as low as \$ 1 per square foot. In such an event the optimum time constant of the house and therefore the area of mass wall can be selected from figure 6.13.

The above analysis are essentially intended to show the procedure of studying the economics of passive house designs. The three cost estimates were selected to account for a wide range of uncertainties. It is believed that somewhere between the maximum and the minimum estimates the actual figures should lie. Therefore the trends shown in figures 6.11 through 6.13 would be applicable to a majority of the situations.

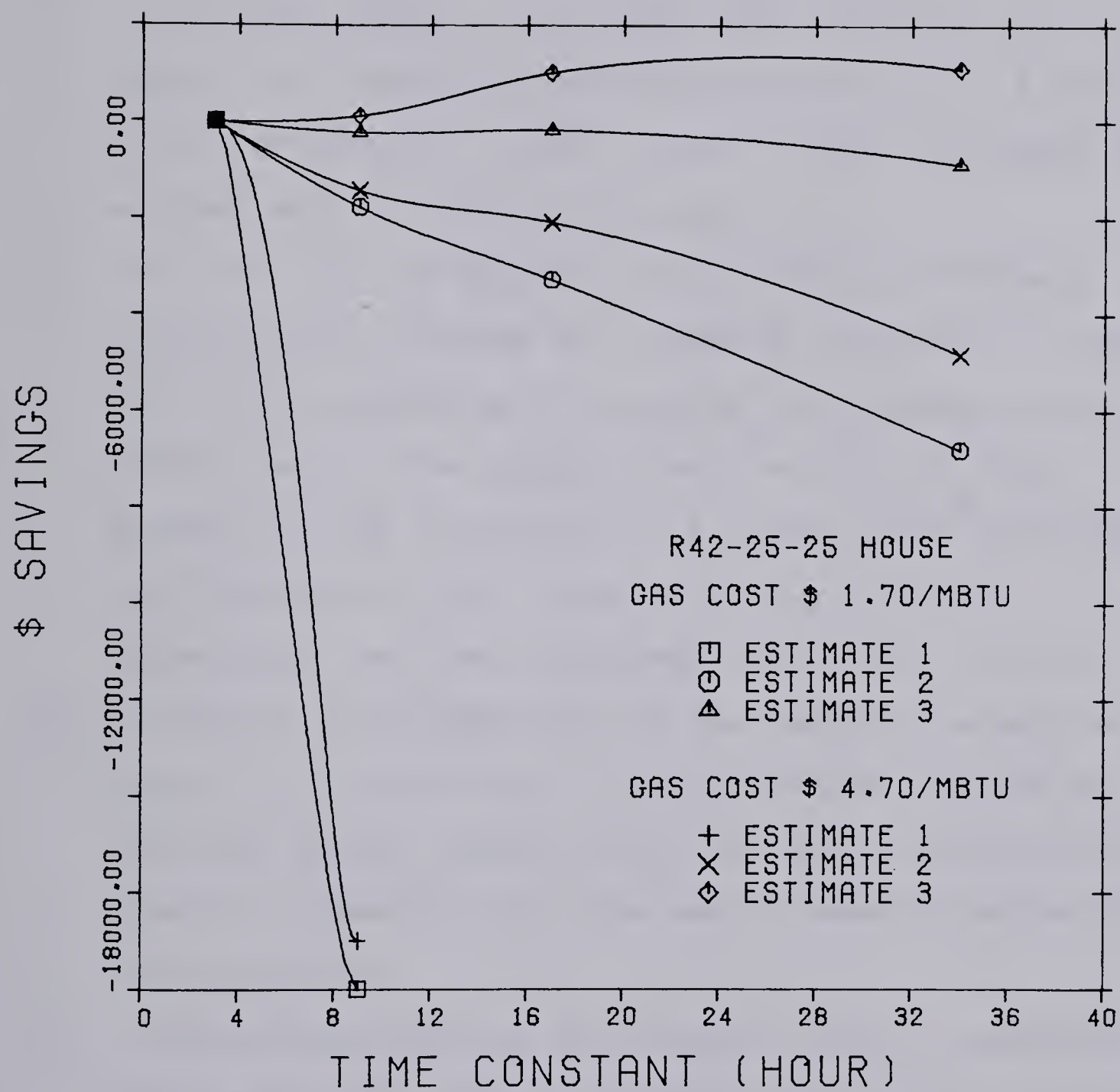


Figure 6.13 The economics of thermal mass wall

7. CONCLUSIONS AND RECOMMENDATIONS

7.1 Conclusions

Some of the important conclusions drawn from this study are as follows:

1. For diurnal energy storage the ideal thickness of a masonry wall should be either in the form of 2.5 inch thick surfacing or in the form of 5 inch thick mass wall exposed on both sides to room air.
2. For stability and accuracy of the finite difference calculations a minimum of 4 nodes or preferably 5 nodes have to be considered in studying the dynamics of the masonry wall. This suggests that in a 5 inch thick masonry wall or alternatively 2.5 inch thick surfacings the thickness of each layer should be $1/2$ inch. Accordingly the time step works out to be 3 minutes.
3. An important consideration in the design of a passive house is sizing the south facing windows. The SIG and the AHLR factors together with the general design curves given in figure 6.10 are the useful means of achieving this objective.
4. A comparative study on four houses (table 1) employing life cycle cost analysis suggests that the most economic insulation level of a house would be comparable to that of R42-25-25 design.
5. In order for the shutter system to be economical on a R42-25-25 house (time constant 17 hour), the

installation cost has to be around \$2.5/square foot.

6. In order for the thermal mass wall to be economical a cost reduction factor of about 30 has to be achieved over its present installation cost.

7.2 Recommendations

1. The two areas requiring further consideration are the modelling techniques for infiltration and the basement heat loss calculations.
2. The accuracy of the predictions made by the present thermal model has to be verified by carrying out experimental studies.
3. The economic analysis and the wood frame construction practices suggest that alternative storage methods have to be examined to replace the heavier and more expensive masonry walls. One possibility is to study the energy storage using eutectic mixtures.
4. An extension of this study would be to look at the thermal model from both heating as well as cooling point of view using passive concepts.

REFERENCES

1. Konard, A., and Larsen, T.A., "ENCORE - CANADA, Computer Program for the Study of Energy Consumption of Residential Buildings in Canada", National Research Council, Division of Building Research, NRCC 17663, 1978.
2. Zulfikar, O.C., and et al., "Dynamic Response of Conventional Residential Construction to Solar Radiation through the Windows during the Heating Season", Consultants Computation Bureau, Cumali Associates, Oakland, California, 1979.
3. Davies, M.G., "A Thermal Model for a Solar Heated Building", Building Science, special supplement, Pergamon Press, pp 67-75, 1975.
4. Balcomb, J.D., and et al., "Passive Solar Heating of Buildings", Symposium Papers, Energy From The Sun, 1978, Institute of Gas Technology, Illinois, PP.123-155.
5. Mazria, E., Wessling, F.C., "An Analytical Model for Passive Solar Heated Buildings", Proc. 1977, Annual Meeting, American Section of ISES, PP. 11.10 - 11.14.
6. "DOE-2 Energy Analysis Program", Volumes I, II, and III, Lawrence Berkeley Laboratory, CA., 1979.
7. Dumont, R.S., Besant, R.W., Green, G.H., "Passive Solar Heating in Residences, An Analysis for the Southern Canadian Prairie Climate", Proc. Solar Energy Update Conference, SESC, Edmonton, 1977.
8. Jones, R.E., and Tymura, J., "Passive Solar Heating

Design for Canada", Proc. Solar Energy Update Conference, SESC, Edmonton, 1977.

9. Balcomb, J.D., and MacFarland, R.D., "A Simple Technique of Estimating the Performance of Passive Solar Heating Systems", Proc. of ISES, 1978, Denver, Volume 2.2, PP. 89 - 96.
10. Wheeling, T., and et al., "Performance of Passive Test Units During 1978 - 1979 Heating Season", Proc. of ISES, 1979, Vol. 2, PP. 1589 - 1593.
11. Dumont, R.S. and Besant, R.W., et al. "Passive Solar Heating Results from Two Saskatchewan Residences", Proc. Annual Meeting, SESC, London, Ontario, 1978.
12. Chen, B., et al. "Preliminary Winter Comparison Results of Four Passive Test Cells in Omaha, Nebraska", Proc. of ISES, 1979, Vol. 2, PP. 1583 - 1587.
13. Palmiter, L., and et al., "Measured and Modeled Passive Performance in Montana", Proc. of ISES, 1978, Vol. 2.2, PP. 59 - 63.
14. Jones, R.E., "Results from Passive Solar Test Room Investigations in Cold Climate", Proc. of ISES, 1978, Vol. 2.2, PP. 53 - 58.
15. Gilpin, R.R., "The Use of South Facing Windows for Solar Heating in a Northern Climate", Solar Energy Update 1977, Edmonton, Alberta, Canada.
16. Yellot, J.I., "Calculation of Solar Heat Gain Through Single Glass", Solar Energy, Vol. 7, No. 4, 1963, PP. 167 - 175.

17. Parmelee, G.V., and et al., "Solar and Total Heat Gain Through Double Flat Glass", ASHVE Trans., Vol.54, 1948, PP. 407 - 428.
18. Stephenson, D.G., "Equations for Solar Heat Gain Through Windows", Solar Energy, Vol.9, No.2, 1965, PP. 81 - 86.
19. Stephenson, D.G., "Tables of Solar Altitude, Azimuth, Intensity and Heat Gain Factors for Latitudes from 43 to 55 degrees North", National Research Council, Division of Building Research, NRC 9528, 1967.
20. ASHRAE 1977., Hand Book and Product Directory, Fundamentals, American Society of Heating, Refrigerating and Air Conditioning Engineers, New York.
21. Hsieh, C.K., and Su, K.C., "Thermal Radiative Properties of Glass From 0.32 to 206 Micro Meter", Solar Energy, Vol.22, PP. 37 - 43.
22. Duffie, J.A., and Beckman, W.A., Solar Energy Thermal Processes, 1974, John Wiley and Sons, New York.
23. Parmelee, G.V., "The Transmission of Solar Radiation through Flat Glass under Summer Conditions", ASHVE Transactions, Vol. 51, 1945, PP. 317 - 350.
24. Mitalas, G.P., and Stephenson, D.G., "Absorption and Transmission of Thermal Radiation by Single and Double Glazed Windows", National Research Council, NRC 7104, 1962.
25. Siegel, R., "Net Radiation Method for Transmittance Through Partially Transparent Plates", Solar Energy, Vol.15, 1973, PP. 273.

26. Wijesundera, N.E., "A Net Radiation Method for the Transmittance and Absorptivity of a Series of Parallel Regions", Solar Energy, Vol.17, 1975, PP. 75 - 77.
27. Puri, V.M., "Transmittance of Diffuse Solar Radiation Through a Series of Parallel Regions", Solar Energy, Vol.22, 1979, PP. 183 - 185.
28. Liu, B.Y.H. and Jordan, R.C., "The Interrelationship and Characteristic Distribution of Direct, Diffuse and Total Solar Radiation", Solar Energy, Vol. 4, pp 1-19, 1960.
29. Parmelee, G.V., "Irradiation of Vertical and Horizontal Surfaces by Diffuse Solar Radiation from Cloudless Skies", ASHVE Trans., Vol.60, 1954, PP. 341 - 358.
30. Threlkeld, J.L., "Solar Irradiation of Surfaces on Clear Days", Transactions ASHRAE Vol. 69, p 24, 1963.
31. Puri, V.M., "A Stochastic Insolation Model For Tilted Surfaces", Dessertation, Ph.D., University of Delaware, 1976.
32. Ruth, D.W., and Chant, R.E., "The Relationship of Diffuse radiation to Total Radiation in Canada", Solar Energy, Vol.18, 1976, PP. 153 - 154.
33. Pereira, M.C., and Rabl, A., "The average Radiation of Solar Radiation Correlations Between Diffuse and Hemispherical and Between Daily and Hourly Insolation Values", Solar Energy, Vol.22, 1979, PP. 155 - 164.
34. Hay, J.E., "Tabulation and Analysis of Solar Radiation Data for Alberta" Research Council of Alberta, Information Series 79, 1977.

35. Wesely, M., and Lipschutz, C., "A Method for Hourly Averages of Diffuse and Direct Solar Radiation Under a Layer of Scattered Clouds", Solar Energy, Vol.18, 1976, PP. 467 - 473.
36. Nicholls, R.L., and Child, T.N., "Solar Radiation Charts", Solar Energy, Vol.22, 1979, PP. 91 - 97.
37. Cole, R.J., "The Longwave Radiation Incident Upon Inclined Surfaces", Solar Energy, Vol.22, 1978, PP. 459 -462.
38. Dave, J.V., "Isotropic Distribution Approximation in Solar Energy Estimations", Solar Energy, Vol.22, 1978, PP. 15 - 19.
39. Utzinger, D.M., and Klein, S.A., "A Method of Estimating Monthly Average Solar Radiation on Shaded Receivers", Solar Energy, Vol.23, 1979, PP. 369 - 378.
40. Gilpin, R.R. and Chan, W.H., "Computer Simulation of Passive Solar Heating", Departmental Report Number 16, Department of Mechanical Engineering, The University of Alberta, 1979.
41. Boileau, G.G., and Latta, J.K., "Calculation of Basement Heat Losses", NRC 10477, 1968, Division of Building Research, Ottawa, Canada.
42. Dale, J.D., and et al., "Adaptable Modules for Air Infiltration Studies in Home Heating", Proc., International Seminar on Air Infiltration and Ventilation, Building Research Establishment, Watford, U.K., April, 1980.

43. Duffie, J.A., and Beckman, W.A., "Design of Active Solar Heating Systems", Energy from the Sun, Institute of Gas Technology, Chicago, Illinois, pp 183-208, 1978.
44. NUWEST Development Corp. Ltd., Edmonton, Personal Communication, May, 1980.
45. Threlkeld, J.L., Thermal Environmental Engineering, Prentice Hall, New York, 1962.
46. Smith, G.W., Engineering Economy, Analysis of Capital Expenditures, The Iowa State University Press, Ames, Iowa, 1968.
47. Myers, R.F., Analytical Methods in Conduction Heat Transfer, McGraw-Hill Book Company, New York, 1971.

APPENDIX A-1
Conversion Table

<u>Quantity</u>	<u>English units</u>	<u>SI Units</u>
Length	1 Ft	0.3048 m
Area	1 FT ²	0.0929 m ²
Volume	1 FT ³	0.0283 m ³
Mass	1 Lb	0.4535 Kg
Density	1 Lb/Ft ³	16.018 Kg/m ³
Specific Heat	1 Btu/Lb-F ⁰	4.1868 KJ/Kg-C ⁰
Insolation	1 Btu/Sq.ft-Hr	0.088 KJ/m ² -Hr
Heat Transfer	1 Btu/Sq.ft-Hr-F ⁰	5.678 W/m ² -C ⁰
Coefficient		
Thermal	1 F ⁰ -Hr-Sq.ft/Btu	0.1761m ² -C ⁰ /W
Resistance		
Heat	1 Btu	1.055 KJ
	1 MBtu	1.055 GJ
Energy	1 Btu/Hr	0.293 Watt
Heat Loss	1 Btu/Hr-F ⁰	0.5274 W/C ⁰
Coefficient		
Heat Capacity	1 Btu/F ⁰	1.9 KJ/C ⁰

APPENDIX A-2

Calculation of Heat Loss Coefficient (U) of House

Considering R42-25-25 house

From table 1

$$A_{wa} = 1209 \text{ Sq.ft}$$

$$R_{wa} = 25 \text{ } ^\circ\text{F-Hr-Sq.ft/Btu}$$

$$A_{bg} = 2136 \text{ Sq.ft}$$

$$R_{bg} = 25 \text{ } ^\circ\text{F-Hr-Sq.ft/Btu}$$

$$A_c = 1337 \text{ Sq.ft}$$

$$R_c = 42 \text{ } ^\circ\text{F-Hr-Sq.ft/Btu}$$

$$A_{wi} = 151 \text{ Sq.ft}$$

$$R_{wi} = 14 \text{ } ^\circ\text{F-Hr-Sq.ft/Btu}$$

$$R = 0.25 \text{ (dimensionless)}$$

The heat capacity of air can be taken as 0.018 Btu/ $^\circ\text{F}$

Total volume of house (above as well as below grade) was estimated to be 20160 Ft^3 .

Neglecting the ground temperature effects and assuming resistance value of shutter in closed position, the heat loss coefficient was obtained as follows

$$= \frac{A_{wa}}{R_{wa}} + \frac{A_{bg}}{R_{bg}} + \frac{A_c}{R_c} + \frac{A_{wi}}{R_{wi}} + \rho_c V R$$

$$= \frac{1209}{25} + \frac{2136}{25} + \frac{1337}{42} + \frac{151}{14} + 0.018 (20160) (0.25)$$

$$= 267 \text{ Btu}/^\circ\text{F-Hr}$$

APPENDIX A-3

Calculation of Time Constant of House

Considering R42-25-25 house

From table 1 the heat loss coefficient $U = 267 \text{ Btu/F}^\circ\text{-Hr}$

Let the house has 5 inch thick mass wall of total surface area equal to 630 sq.ft

Heat capacity of the mass wall is equal to

$$\begin{aligned}
 &= \rho c V \\
 &120 (0.24) (5/12) (630) \\
 &= 7560 \text{ Btu/F}^\circ
 \end{aligned}$$

From equation 6.7.4 the time constant of a house is equal to

$$\tau = \frac{C (T_{\max} - T_{\min})}{U \text{ HDHr/HHr}}$$

For Edmonton

$$\text{HDHr} = 10286 (24)$$

$$\text{HHr} = 8042$$

$$\text{With } T_{\max} - T_{\min} = 10^\circ$$

$$= \frac{7560 (10) (8042)}{267 (10286) (24)}$$

$$\text{Therefore } \tau = 9.2 \text{ Hour}$$

APPENDIX A-4

Sample Computer Run

THIS PROGRAM UTILIZES THE HOURLY RADIATION DATA OF MAJOR CANADIAN CITIES AND ANALYZES THE BEHAVIOUR OF HOUSE EMPLOYING PASSIVE SOLAR HEATING THROUGH CLEAR AND OR HEAT ABSORBING GLASS WINDOWS. THE COMPUTER MODEL CAN SIMULATE THE DYNAMIC RESPONSE OF THE HOUSE TO TEMPORAL VARIATIONS IN RADIATION FLUXES AND AIR TEMPERATURES.

TO USE THE PROGRAM ANSWER THE QUESTIONS.
DO YOU NEED INSTRUCTIONS(Y OR N){

N
ENTER CITY CALL NUMBER
11

TYPE IN SECTION CALL NUMBER (E.G. C20 ETC.)

C10
ENTER NUMBER OF RESISTIVE AND STORAGE ENCLOSURE
ELEMENTS:(EG.8,2,)

7,1,

ENTER TYPE OF STORAGE WALL:(ELEMENT NUMBER,TYPE)
(EG. 9,1,: REPEAT FOR EACH STORAGE WALL)

- 1 STORAGE WALL EXPOSED TO ROOM AIR
- 2 STORAGE WALL RECEIVING TRANSMITTED RADIATION FROM THE GLASS AND EXPOSED TO ROOM AIR

8,1,

C10 (ENCLOSURE ELEMENTS):ENTER ELEMENT NUMBER,
VARIABLE CODE,AND THE NEW VALUE. EG.4,2,156.0

C20

ENTER TOTAL NUMBER OF CLEAR GLASS WINDOWS

1,

ENTER CODE FOR SHUTTER OPERATION: EG.,

- 0 NO SHUTTERS
- 1 AUTOMATIC SHUTTER OPERATION
- 2 SHUTTER OPENED AT SUNRISE AND CLOSED AT SUNSET EXCEPT OPEN 24 HRS DURING SUMMER MONTHS(MAY-SEP)

2

C20 (CLEAR GLASS WINDOWS):ENTER WINDOW NUMBER
VARIABLE CODE,AND THE NEW VALUE. EG.3,6,3.5

1,1,2.0

C20 (CLEAR GLASS WINDOWS):ENTER WINDOW NUMBER
VARIABLE CODE,AND THE NEW VALUE. EG.3,6,3.5

1,2,151.0

C20 (CLEAR GLASS WINDOWS):ENTER WINDOW NUMBER
VARIABLE CODE,AND THE NEW VALUE. EG.3,6,3.5

1,4,2.0

C20 (CLEAR GLASS WINDOWS):ENTER WINDOW NUMBER
VARIABLE CODE,AND THE NEW VALUE. EG.3,6,3.5
C30

ENTER TOTAL NUMBER OF HEAT ABSORBING GLASS WINDOWS
0

TYPE IN SECTION CALL NUMBER (E.G. C20 ETC.)
R

EDMONTON LAT= 53.50

HOUSE DESIGN PARAMETERS

R70-40-40
HOUSE ORIENTATION ANGLE= 0.0
FLOOR AREA= 1260.00
HOUSE VOLUME= 20160.00
NUMBER OF PEOPLE LIVING IN THE HOUSE= 3.35

ENCLOSURE ELEMENTS

ELE NUMB	TYPE	AREA	R-VALUE
1	1.00	450.00	40.00
2	2.00	324.00	40.00
3	3.00	280.00	40.00
4	4.00	280.00	40.00
5	5.00	876.00	40.00
6	5.00	1337.00	70.00
7	7.00	1260.00	40.00
8	6.00	630.00	6804.00 (HEAT CAPACITY)

ELE TYPE DESCRIPTION

- 1 NORTH FACING WALL
- 2 SOUTH FACING WALL
- 3 EAST FACING WALL
- 4 WEST FACING WALL
- 5 CEILING
- 5 SUB-GRADE WALLS
- 6 STORAGE WALLS
- 7 BASEMENT FLOOR

CLEAR GLASS WINDOWS

WIN NUMB	TYPE	AREA SQ.FT	SLOPE DEG.	GLAZINGS (NUMB)	OVERHANG FT	R-VALUE SHUT.OPEN	R-VALUE SHUT.CLOSED
1	2.00	151.00	90.00	2.00	2.5X1.0	1.90	26.00

WIN TYPE DESCRIPTION

- 1 NORTH FACING WINDOW
- 2 SOUTH FACING WINDOW
- 3 EAST FACING WINDOW
- 4 WEST FACING WINDOW

MONTH= 1

TOTAL NUMBER OF DEGREE DAYS DURING THE MONTH= 2101.02

HOUR	ROOM TEMP (F)	AIR TEMP (F)	AIR CHNGS PER HR	SHUTTER OPENING FRACTION	SOLAR HEAT (BTU)	NET GAIN WINDOWS (BTU)	HEAT STORED (BTU)	AUX. HEATING (BTU)
1	65.00	-2.94	0.10	0.0	0.0	-65.76	-532.55	5788.65
2	65.00	-3.19	0.10	0.0	0.0	-65.89	-438.97	6929.87
3	65.00	-3.32	0.10	0.0	0.0	-66.07	-362.17	7032.32
4	65.00	-3.58	0.10	0.0	0.0	-66.26	-308.60	7108.84
5	65.00	-3.71	0.10	0.0	0.0	-66.45	-263.38	7177.07
6	65.10	-3.97	0.10	0.0	0.0	-66.66	-184.35	3995.80
7	65.17	-4.48	0.10	0.0	0.0	-67.16	-32.36	1242.24
8	65.19	-5.19	0.10	0.0	0.0	-67.79	-42.57	1298.10
9	65.00	-5.39	0.10	0.77	783.16	-3392.24	-265.71	7695.76
10	65.98	-5.29	0.10	1.00	6289.90	681.98	278.18	6910.39
11	68.11	-4.74	0.18	1.00	13223.16	7504.72	2186.88	1592.90
12	67.85	-3.65	0.25	1.00	16562.36	10835.36	1874.52	572.83
13	69.22	-2.32	0.25	1.00	17904.61	12239.98	1999.54	795.95
14	69.29	-1.06	0.18	1.00	16278.22	10658.51	2216.86	1176.07
15	68.74	-0.48	0.10	1.00	12409.52	6859.78	1481.31	1994.42
16	65.72	-0.13	0.10	1.00	6746.46	1383.14	-1265.47	3770.65
17	65.50	0.19	0.10	0.03	126.15	-114.84	-1720.80	1985.10
18	65.76	-0.58	0.10	0.0	0.0	-63.75	-556.43	322.59
19	65.38	-1.32	0.10	0.0	0.0	-64.37	-825.82	1013.76
20	65.34	-1.68	0.10	0.0	0.0	-64.71	-770.87	1935.69
21	65.32	-2.03	0.10	0.0	0.0	-65.04	-625.50	1946.84
22	65.28	-2.97	0.10	0.0	0.0	-65.65	-559.39	2083.00
23	65.23	-3.00	0.10	0.0	0.0	-66.05	-524.85	2487.43
24	65.12	-3.29	0.10	0.0	0.0	-66.13	-529.41	3476.65

TYPICAL DAILY TOTAL : 90323.44 45668.45 228.09 80332.63

NUMBER OF HOURS OF OVER HEATING DURING THE MONTH= 0(0)

MONTH= 2

B30289